

# **3D Box Positioning and Orientation System**

*Tiago Pinto Barreira*

**Master Dissertation**

FEUP Supervisor: Prof. Manuel Romano dos Santos Pinto Barbosa

FEUP Supervisor: Prof. Teresa Margarida Guerra Pereira Duarte

Company Supervisor: Eng. Nuno Miguel Gonçalves Reis



**Master in Mechanical Engineering**

July 2022

*(Blank Page)*

*“O que dá o verdadeiro sentido  
ao encontro é a busca, e é  
preciso andar muito para  
se alcançar o que está perto”  
José Saramago*

*(Blank Page)*



## Abstract

The dissertation here presented describes and explains the study and development of a module that separates, positions and guides medicinal boxes in an autonomous way. This module will be integrated in a main structure of an automated storage of this type of products in local pharmacies.

Thus, in a first phase several concepts are described in order to contextualize the problem. Subsequently, various automated solutions that assist the human being in this type of daily functions are presented in order to understand the current point of this industry, being then presented the mode of operation of the main system for which the current model was developed in order to be integrated. Finally, in this part there are presented the solutions that already exist in the market for a similar purpose of the module that was intended to be developed.

Afterwards, the entire evolutionary process until the final concept is presented, from the various alternatives studied until arriving at a final concept that was then submitted to a testing phase. It was also explained how this real prototype was produced as well as all the details studied during this experimental phase and its conclusions.

Based on the results with the real prototype, the final idea was fully developed, where the concepts studied using the prototype were detailed designed. In this phase the whole design mode was described, including the information from the suppliers that were contacted were also mentioned, was made the need calculations that validate the choices of certain components, as well as the detailed drawings of all the components developed for the project in question.

Finally, a conclusion is made where a reflection about all the work developed throughout the dissertation as well as an analysis of the objectives accomplished. In addition to all this, possible future steps to be developed in order to create an operational model ready to be commercialised are also described.

**Keywords:** Automated warehouses, logistic process, sorter machines, medical pill boxes separation, positioning, automation.

*(Blank Page)*

## Resumo

### Sistema de Posicionamento e Orientação de Caixas em 3D

A presente dissertação tem como objetivo o estudo e desenvolvimento de um módulo que separa, posiciona e orienta caixas de medicamentos de forma autónoma. Este módulo será integrado numa estrutura principal que faz o armazenamento deste tipo de produtos em farmácias locais.

Assim sendo, numa primeira fase são descritos vários conceitos de forma a contextualizar o assunto em causa. Posteriormente, são apresentadas diversas soluções automatizadas que auxiliam o ser humano em funções diárias neste tipo de tarefas, de modo a perceber o estado atual desta indústria, sendo de seguida apresentado o modo de funcionamento do módulo principal no qual será integrado o modelo a desenvolver. Por fim, nesta parte serão analisadas as soluções que já estão disponíveis no mercado com funções semelhantes às do módulo que se pretende desenvolver.

Posteriormente é apresentado todo o processo evolutivo do conceito final, desde as várias alternativas estudadas até se chegar a um conceito final que será submetido depois a uma fase de testes. Após esta ser feita, também será explicada a forma de como foi produzido esse protótipo real bem como todos os detalhes estudados durante esta fase experimental e as suas conclusões.

Com base nos resultados obtidos com a realização do protótipo físico, será desenvolvida a ideia final onde os conceitos estudados com o protótipo foram projetados com o detalhe necessário. Nesta fase é descrito todo o modo de criação, os fornecedores contactados, cálculos para as escolhas de certos componentes, bem como desenhos de definição de todos os componentes desenvolvidos para o projeto em questão.

Por fim, são apresentadas as conclusões onde se faz uma reflexão sobre todo o trabalho desenvolvido, bem como a análise dos objetivos cumpridos. Para além disso, também são apresentados possíveis passos a desenvolver no futuro para se completar o desenvolvimento de um modelo operacional e pronto a ser comercializado.

**Palavras-chave:** Armazéns automáticos, processo logístico, máquinas de separação, separação de caixas de comprimidos, posicionamento, automação.

*(Blank Page)*

## Acknowledgements

With the completion of this dissertation project I could not fail to thank some people who, directly or indirectly, helped me in the realization of this work throughout the semester.

First of all, I would like to thank Professors Manuel Romano Barbosa and Teresa Duarte for their availability to clarify any doubts and in the preparation of this report and the ideas exchanged and advice given throughout the semester.

I also want to thank the whole SIER Group members for the welcome and help given at any moment and for the professionalism shown at any time. A special thanks to Engineer Miguel Reis for the way he received me in the company since the first day and for the help provided throughout the internship.

I would also like to express my gratitude to my course colleagues who have always encouraged me to give my best in any project and have always advised me throughout these years both on a personal and professional level.

To Juliana Melo for all the patience, care and love shown throughout this challenging project, without her it wouldn't have been the same and for that a big thank you.

Last but not least I thank my family, especially my parents, Armando and Lucília, and my younger brother Miguel, who have always helped me to achieve my goals, for always being there to support me when necessary and advise me at the right times.

*(Blank Page)*

## Contents

1	Introduction.....	1
1.1	Project framework and motivation.....	1
1.2	Objectives of the project .....	2
1.3	Method followed in the project.....	4
1.4	Dissertation structure .....	5
2	State of the art.....	7
2.1	Logistic processes and automated warehouses .....	7
2.2	Automated storage systems for local pharmacies .....	11
2.3	Sorters in the pharmacy industry .....	12
3	Project development .....	19
3.1	Problem specifications .....	19
3.2	Conceptual ideas .....	21
3.3	Testing phase .....	24
4	Development of the final concept.....	35
4.1	Materials selection .....	35
4.2	Conveyor components .....	36
4.3	Verification of components resistance.....	62
5	Power transmission system and automation system.....	69
5.1	Force analysis on the belt conveyors .....	69
5.2	First conveyor .....	72
5.3	Second and third conveyors .....	80
5.4	Module automatization .....	84
6	Module assembly and Bill of Materials.....	91
6.1	Module assembly .....	91
6.2	Bill of Materials (BoM) and cost estimation .....	95
7	Conclusions and future work .....	97
	References .....	99
	Appendix A – Technical Drawings .....	101
	Appendix B – Products Datasheets .....	131
	Appendix C - Bill of Materials .....	141

## Figures

Figure 1.1 - Gantt Chart.....	4
Figure 2.1 - Generic logistic process .....	8
Figure 2.2 – ASRS System.....	9
Figure 2.3 – Carousel System.....	9
Figure 2.4 - Swisslog mini load ASRS.....	10
Figure 2.5 - Swisslog AGV system .....	10
Figure 2.6 - Omnicell storage warehouse.....	11
Figure 2.7 - Sorting machines producers.....	12
Figure 2.8 - ROWA Pro Log .....	13
Figure 2.9 - Fill in Box .....	16
Figure 3.1 - Available space .....	19
Figure 3.2 - First concept.....	21
Figure 3.3 - Second concept .....	21
Figure 3.4 - Third concept.....	22
Figure 3.5 - Fourth concept .....	22
Figure 3.6 - Fifth concept .....	23
Figure 3.7 - Final conceptual solution.....	24
Figure 3.8 - Development phase of the physical prototype construction .....	24
Figure 3.9 - Transmission mechanisms (left – driving pulley and right – driven pulley).....	25
Figure 3.10 - Conveyor system .....	26
Figure 3.11 - Barrier assembly mechanism .....	26
Figure 3.12 - Barrier real models.....	27
Figure 3.13 - First concept testing model.....	27
Figure 3.14 - Tests with 5mm thickness barrier .....	28
Figure 3.15 – Curve maquette .....	29
Figure 3.16 - Testing with the curve model.....	29
Figure 3.17 - Knife Edge 3D model concept.....	30
Figure 3.18 - Correct and Incorrect chicane alternatives.....	30
Figure 3.19 - Third concept testing model .....	30
Figure 3.20 – MDF ramp model.....	31
Figure 3.21 - Third concept testing experiments with the gap problem solved .....	31
Figure 3.22 - Third concept testing experiments .....	32
Figure 3.23 - Ramp for the positioning process .....	32
Figure 3.24 - Positioning system in operation.....	33



Figure 3.25 - Testing phase final prototype.....	33
Figure 4.1 – First conveyor dimensions .....	36
Figure 4.2 - Bearings couplings.....	40
Figure 4.3 - Conveyor guide supporters .....	41
Figure 4.4 - Driving shaft support .....	41
Figure 4.5 - Motor support .....	42
Figure 4.6 - Spacer .....	42
Figure 4.7 - Tensioner .....	43
Figure 4.8 - Tensioner mechanism .....	44
Figure 4.9 – Driving shaft assembly.....	44
Figure 4.10 - Motor assembly .....	45
Figure 4.11 - Driven shaft assembly.....	45
Figure 4.12 – Belt support.....	46
Figure 4.13 - First conveyor fully assembled.....	49
Figure 4.14 – Right side support sheet 2D planification .....	50
Figure 4.15 – Left side support sheet 2D planification .....	50
Figure 4.16 – Cover 2D planification.....	51
Figure 4.17 - Barrier folding principle .....	52
Figure 4.18 – Barrier exploded assembly view .....	53
Figure 4.19 – Barrier spacer .....	53
Figure 4.20 – Mounting the barrier spacing .....	53
Figure 4.21 – First conveyor ready to be mounted on the principal structure.....	53
Figure 4.22 – Second and third conveyors dimensions.....	54
Figure 4.23 - Knife edge conveyor example .....	55
Figure 4.24 - MISUMI coupled bearing.....	57
Figure 4.25 - Second conveyor assemble .....	57
Figure 4.26 - Spacer (250 mm).....	58
Figure 4.27 – 2D planification of the left support sheet for the second and third conveyor....	59
Figure 4.28 - Chicane dimensions .....	60
Figure 4.29 - 2D planification of the chicane.....	61
Figure 4.30 - Ramp 2D planification.....	61
Figure 4.31 - Second and third conveyor full assembly .....	62
Figure 4.32 - Distribution of Von Mises stresses in the tensioner .....	63
Figure 4.33 - Deformation of the tensioner .....	63
Figure 4.34 - Distribution of Von Mises stresses in the driving shaft support.....	64
Figure 4.35 - Deformation in the driving shaft support.....	64
Figure 4.36 - Distribution of Von Mises stresses in the motor and driving shaft support .....	65

Figure 4.37 - Deformation in the motor and driving shaft support .....	65
Figure 4.38 - Distribution of Von Mises stresses in the right support of the first conveyor ....	66
Figure 4.39 - Deformation in the right support of the first conveyor .....	66
Figure 4.40 - Distribution of Von Mises stresses in the left support of the first conveyor .....	67
Figure 4.41 Deformation in the left support of the first conveyor .....	67
Figure 4.42 - Distribution of Von Mises stresses in the right support of the second conveyor	67
Figure 4.43 - Deformation in the right support of the second conveyor .....	67
Figure 4.44 - Distribution of Von Mises stresses in the left support of the second conveyor .	68
Figure 4.45 - Deformation in the left support of the second conveyor .....	68
Figure 5.1 - Generic conveyor diagram.....	69
Figure 5.2 - Pulley diagram .....	71
Figure 5.3 - Barrier diagram where ( <i>L is the length of the barrier [193 mm]</i> ),.....	73
Figure 5.4 - First conveyor motor characteristic curve .....	79
Figure 5.5 - Second conveyor motor characteristic curve .....	83
Figure 5.6 - Sensors position in a generic diagram .....	84
Figure 5.7 - Controller CX 9020 .....	85
Figure 5.8 - Terminal EL 7041 .....	86
Figure 5.9 - EL 1014 .....	87
Figure 5.10 - Mean Well Power Supply .....	88
Figure 5.11 - VS3 <i>Banner</i> photoelectric sensor .....	88
Figure 6.1 - Main support structure measurements .....	91
Figure 6.2 – External components support accessory .....	92
Figure 6.3 - Conveyors assembly in the main structure .....	92
Figure 6.4 - Positioning ramp measurements .....	93
Figure 6.5 - Support for the positioning ramp .....	93
Figure 6.6 - Positioning wall .....	93
Figure 6.7 - Positioning module assembly .....	94
Figure 6.8 - Final assembly module 1 .....	94
Figure 6.9 - Final assembly module 2 .....	94

## Tables

Table 2.1 – Specifications of ROWA sorter machines.....	14
Table 2.2 - <i>Gollmann</i> sorter machine specifications .....	15
Table 2.3 - <i>Alpha</i> Specifications.....	16
Table 2.4 -Fill in Box Specifications.....	17
Table 3.1 - Range of box dimensions (in mm).....	20
Table 3.2 - Barrier Mass variation (kg) .....	27
Table 4.1 - Selected aluminium alloys specifications .....	36
Table 4.2 - P9/Z specifications .....	37
Table 4.3 - Driving and driven pulley specifications .....	39
Table 4.4 - Bearing assembly components specifications .....	40
Table 4.5 - Driven shaft support.....	41
Table 4.6 - Motor support specifications.....	42
Table 4.7 – Spacer (450 mm) specifications .....	42
Table 4.8 - Tensioner specifications.....	43
Table 4.9 - Big and small pulleys specifications .....	47
Table 4.10 - Transmission belt specifications .....	48
Table 4.11 - First conveyor motor specifications .....	48
Table 4.12 – Al 5754 and first conveyor supports specifications .....	51
Table 4.13 – Barrier measurements.....	52
Table 4.14 - P9/A specifications.....	54
Table 4.15 - Driving roller specifications.....	56
Table 4.16 - Driven roller specifications .....	56
Table 4.17 - <i>MISUMI</i> coupled bearing specifications .....	57
Table 4.18 - Spacer (250 mm) specifications .....	58
Table 4.19 - Second and third conveyor motor specifications .....	58
Table 4.20 - Transmission system pulleys .....	59
Table 4.21 - Transmission belt .....	59
Table 4.22 - Second conveyor support specifications .....	60
Table 4.23 – Ramp specifications.....	61
Table 4.24 - Maximum values obtained for the tensioner.....	63
Table 4.25 - Maximum values obtained for the driving shaft support .....	64
Table 4.26 - Maximum values obtained for the motor and driving shaft support.....	65
Table 4.27 - Maximum values obtained for the right support of the first conveyor .....	66
Table 4.28 - Maximum values obtained for the left support of the first conveyor.....	67
Table 4.29 - Maximum values obtained for the right support of the second conveyor.....	68

Table 4.30 - Maximum values obtained for the left support of the second conveyor .....	68
Table 5.1 - First conveyor specifications.....	72
Table 5.2 - Motor needed specifications .....	77
Table 5.3 – Moments of inertia applied to the object axis .....	78
Table 5.4 - Moments of inertia applied to the motor axis .....	78
Table 5.5 - Second and third conveyor specifications.....	80
Table 5.6 – Moving the load needed specifications .....	80
Table 5.7 - Conveyor shaft obtained results .....	81
Table 5.8 - Second pulley obtained results.....	81
Table 5.9 - First pulley obtained results .....	81
Table 5.10 - Second conveyor motor needed specifications .....	81
Table 5.11 – Moments of inertia applied to the object axis .....	82
Table 5.12 - Moments of inertia applied to the motor axis .....	82
Table 5.13 - Second and third conveyor motor specifications .....	82
Table 5.14 - Controller CX 9020 specifications.....	85
Table 5.15 - Terminal EL 7041 specifications .....	86
Table 5.16 - EL 1014 specifications.....	87
Table 5.17 - Power Supply specifications .....	88
Table 6.1 – External components support accessory specifications.....	92
Table 6.2 - Positioning ramp specifications .....	93
Table 6.3 - Support for the positioning ramp specifications .....	93
Table 6.4 - Positioning wall specifications.....	93
Table 6.5 – Total estimated costs .....	95

## Abbreviations

<b>3D</b>	Three Dimensions
<b>AGV</b>	Automated Guided Vehicle
<b>ASRS</b>	Automated Storage and Retrieval System
<b>BoM</b>	Bill of Materials
<b>CAD</b>	Computer-Aid Design
<b>CAM</b>	Computer-Aid Manufacturing
<b>CIM</b>	Computer-Integrated Manufacturing
<b>CNC</b>	Computer Numerical Control
<b>CSSD</b>	Central Sterile Service Department
<b>HMI</b>	Human-Machine Interface
<b>Max</b>	Maximum
<b>MDF</b>	Medium-Density Fibreboard
<b>Min</b>	Minimum
<b>OCR</b>	Optical Character Recognition
<b>Packs</b>	Packages
<b>PLA</b>	Polylactic Acid
<b>PVC</b>	Polyvinyl Chloride
<b>WCS</b>	Warehouse Control System
<b>WMS</b>	Warehouse Management System

*(Blank Page)*

# 1 Introduction

The first chapter of this work is mainly dedicated to the introduction and contextualization of the problem. It is subdivided into four sections where in the first part it is presented the motivation to accept the challenge of doing this project and explaining some general basic concepts that help to better understand what it was approached with the development of this work.

Afterwards, it is going to be presented the partner company where the work was carried out, their mission, and their future goals. The last two topics are dedicated to explaining how the work was done by presenting the used method to reach all the goals for this project and then the structure of this report.

## 1.1 Project framework and motivation

This project comes in the scope of the realisation of the master's thesis within the Mechanical Engineering master's degree, specialization in Materials and Technological Processes, where in partnership with the company *ENGINIS* it is intended to develop a complementary module for an automated storage system to be used in local pharmacies. This module will be located at the beginning of the system, working as a receiving station, to make the process of manual loading of pharmaceutical products, of different sizes, more expedite.

Nowadays, in the micro-logistic business, there are numerous solutions on the market with technologies that allow recognition and handling of objects as small as individual pills up to bigger objects such as boxes and containers. However, solutions that allow automatic separation and recognition of different sizes of pillboxes are still hard to find, with a few alternatives starting to appear on the market. These alternatives still have an enormous margin for development and growth which motivates *ENGINIS* to develop an in-house solution which became the main focus of this work.

Of special interest in the development of this project is the opportunity and the need to combine different areas of expertise, from mechanical design and materials selection, associated with the supporting structure and separation mechanisms, to the selection of actuators and dividing systems, and the integration with the main robotised storage system.

The *ENGINIS* company, founded in 2008 [1], is dedicated to the development of computer, electronic and mechanical integration systems. In this context, the brand Unik Robotics was created, which is associated with robotic automation and other intelligent and logistics optimisation systems. The company structure and associated brands have been organized within the SIER Group, that is on the market for over 25 years and has the goal to provide their customers all services and the necessary system to help them simplify everyday tasks.

In order to optimise the micro-logistics processes of the pharmaceutical industry, the *ENGINIS* company has developed a robotised system for an automatic storage and retrieval of medical boxes that makes the associated handling operations of pharmaceutical products more efficient. This main module, entirely developed internally by the company, stores and checks the products in stock, thus preventing any unwanted stock-outs, as well as taking care to check the validity of all stored products, something of extreme importance to the area in question. It also separates and delivers orders completely autonomously, so that there are no human errors in the sales service for this type of products.

Additionally, the company is constantly creating upgrades to this system in order to solidify its position in the pharmaceutical market. An automatic receiving station is being created in which the products are placed manually inside a special shelf and then the rest of the system takes care of the identification and storage of the product. Another project that has been developing is an independent module that collects and sends the orders, at a much faster rate than the system already in place.

At this stage, the need arises to develop a new module that will complement the existing robotised system, making the introduction of the products into the warehouse completely automatic, without having to manually separate the boxes as happens with the charging system presented above, giving also to the company a more robust and complete solutions to offer to the market.

## **1.2 Objectives of the project**

With the technological advances we have been witnessing, it is increasingly common to get used with the idea of integration of robotic mechanisms into our daily lives in order to simplify our routines. Following this trend and being a safe bet for the future, all areas of the industry are trying to adapt themselves to these circumstances.

In addition, with the emergence of the pandemic another market model has emerged where online shopping has been in high demand. To meet all these needs, it is crucial to have a well-organised corporate system. Therefore, the logistics processes have been attracting more and more attention from people in the most diverse market areas.

Nowadays, it is possible to see large and extremely well organised logistics halls capable of organising components of all kinds of geometries and dimensions. However, micro logistics is one of the areas with less focus due to its high degree of difficulty, where the available space is very confined, making the task of putting together different mandatory components very complicated. It is on this premise that the need to develop a machine that will serve as a complement, not only to the employees, but also to other systems already fully developed and operational arises.



Focusing essentially on the pharmaceutical industry, the company's main area of focus, efficient pill box storage becomes a very valuable addition to pharmacies, giving them maximum assurance of knowing what types of medicines they have in stock, how many they have, as well as their expiration date, allowing them to have a better idea of what they have in stock.

However, the way to introduce all the products in the current used solution is still manual, being the process of product identification and separation entirely carried out by the operator. With this work, the goal is to remove this function of dividing boxes from the operator, with a completely autonomous machine doing it. The employee will only have the job of receiving the boxes from the supplier and dumping them all in a completely random way into the machine. The subsequent phases of the process are carried out by the robot.

This module will have two different mandatory stages, the separation process, and the identification process, where a scanning system will have to detect the precise information about each box. The goal for the current work it is only focused on the first stage, where we have to ensure that there is only one box at a time before the identification process.

Furthermore, it was also requested that the controller of this module, with the main functions of controlling the actuators, works independently from the main storage controller system, but with the capability to communicate that the box is ready to be collected and proceed to the identification stage. There were also some restrictions in terms of space, as well as the size of boxes that the module can carry.

In summary, the main objectives of this work are to design a solution for sorting amounts of unordered medicine boxes, manually loaded, integrated in an existing robotized system for storage and retrieval operations, including:

- The study and analysis of concept mechanisms for separation of the medicine boxes;
- The creation of a physical prototype to test and validate the selected solutions;
- The design of a supporting structure, mechanisms and respective actuators;
- Identification of the elements of the control system that allow integration with the main controller of the existing robotized system.

### 1.3 Method followed in the project

The project started with the creation of a Gantt chart, Figure 1.1, in order to define the main tasks and set dates to meet the objectives. This way, it was possible to have a better organisation of time and have a better perception of the direction the work was taking. Next, it was carried out research about the state of the art to understand which solutions exist on the market for the machine model that was intended to be designed, and a more general search was also made on how the pharmaceutical industry has adapted to new technologies, following the trend associated with the Industry 4.0.

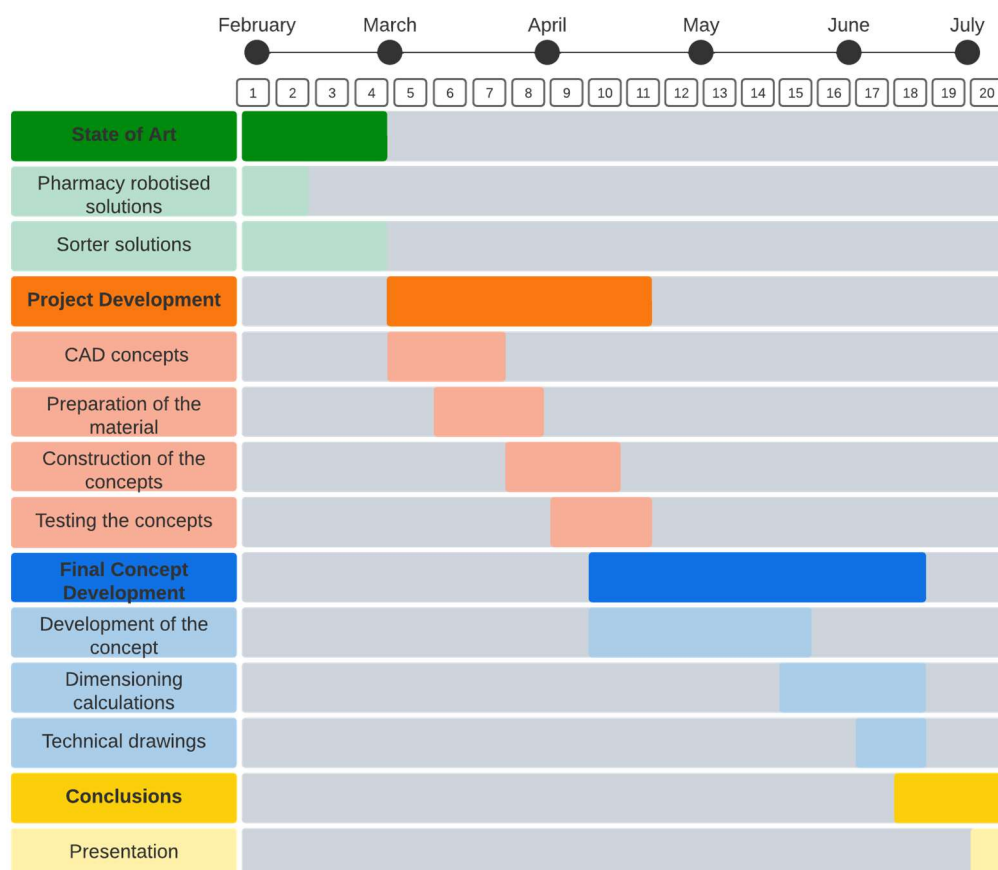


Figure 1.1 - Gantt Chart

Subsequently, all the information gathered from the investigation and analysis of solutions existing in the market, combined with a detailed analysis of the requirements established for the system to be developed, provided the grounds on which the development and design of the proposed solution was based. After thinking of some ideas to implement in the project, the company provided CAD tools, in this case the software used was [FUSION 360], and modelling of concepts started being made. Later, an assembly of a prototype that took part in the testing phase was assembled and some experiments were made in order to refine certain aspects for the final concept.

After testing and proving that the concepts were functional, it was necessary to develop a final design that complied with all the requirements. To achieve this final concept, many suppliers were contacted so as to decide which materials / components should be used. To verify the performance of the model, calculations were carried out to prove so, and also a structural simulation was done with the help of *Abaqus* software.

## 1.4 Dissertation structure

The dissertation is organised into seven chapters. Following this introduction chapter, the second one focuses on the identification and analysis of the automated solutions available on the market for handling, storage and retrieving of medicines in the pharmaceutical businesses.

The third chapter was divided into three phases. In the first one, all the imposed restrictions of this project are identified, a second part where the conceptual ideas are presented, and a third and final phase with all the testing and explanations of the final selected concept.

The fourth chapter mainly focuses on the detailed construction of each of the conveyors, where all the chosen standard elements are presented, as well as the components that were designed for this work in question where it was made a structural study to validate their correct functioning.

The fifth chapter presents the mathematical model that validates the entire power transmission system, where the calculations performed for the selection of components such as motors, pulleys and belt are shown. Finally, the control system of the entire module is also mentioned, where the main elements are presented, as well as the operating principle.

The sixth chapter is dedicated to explaining the assembly process of the whole set, as well as the list of materials needed to build this model.

Finally, the seventh chapter presents the conclusions and recommended future work to be added on.

*(Blank Page)*

## 2 State of the art

Automated solutions for materials handling and storage are, as expected, highly dependent on the specific characteristics of the materials, components or items to be processed. However, there are also common aspects across the various businesses and industry applications when dealing with material's flow operations. In this chapter, an initial overview was made to characterize a Logistic Process and an Automated Warehouse, as well as the advantages of automated solutions for supporting the flow of materials, with an emphasis on the pharmaceutical industry.

Next, an analysis was made of the existing solutions that can be directly related with input sorting stations for pharmacy automated storages, in order to identify the current level of automation available for these systems. Finally, a characterisation of the system to be developed considering the commercially available solutions, analysed previously, is presented, in order to clarify the requirements of the system to be developed and get a sense of how to create an alternative and workable solution.

### 2.1 Logistic processes and automated warehouses

“Logistic” is a discipline which has been increasingly brought into our daily lives because of the good results that brings, as it improves the quality of the business processes and enables a company to have a quick reaction to the market and the costumers demands [2].

However, the concept of “Logistic” has been changing through the years, being in the early days more related with the military field, where the aim was to try to move battle-specific equipment and people around in an agile and discreet way. Over the decades the word has been re-adapted to any circumstance and today is more commonly used in the context of moving commercial goods within the supply chain [3].

To add to that, “Logistics” can be seen as an overseeing of the flow of information, material and energy and many other parameters. The core of logistics also implies the correct amount of resources to varies bodies of a company being delivered at the right time but also at a good quality and reasonable price point. To ensure this, it is necessary to guarantee a clear flow of information throughout levels, either at planning level or execution level. A representation of the various functions that are affected by logistics and its relationship with the material follow and information flow can be seen in Figure 2.1.

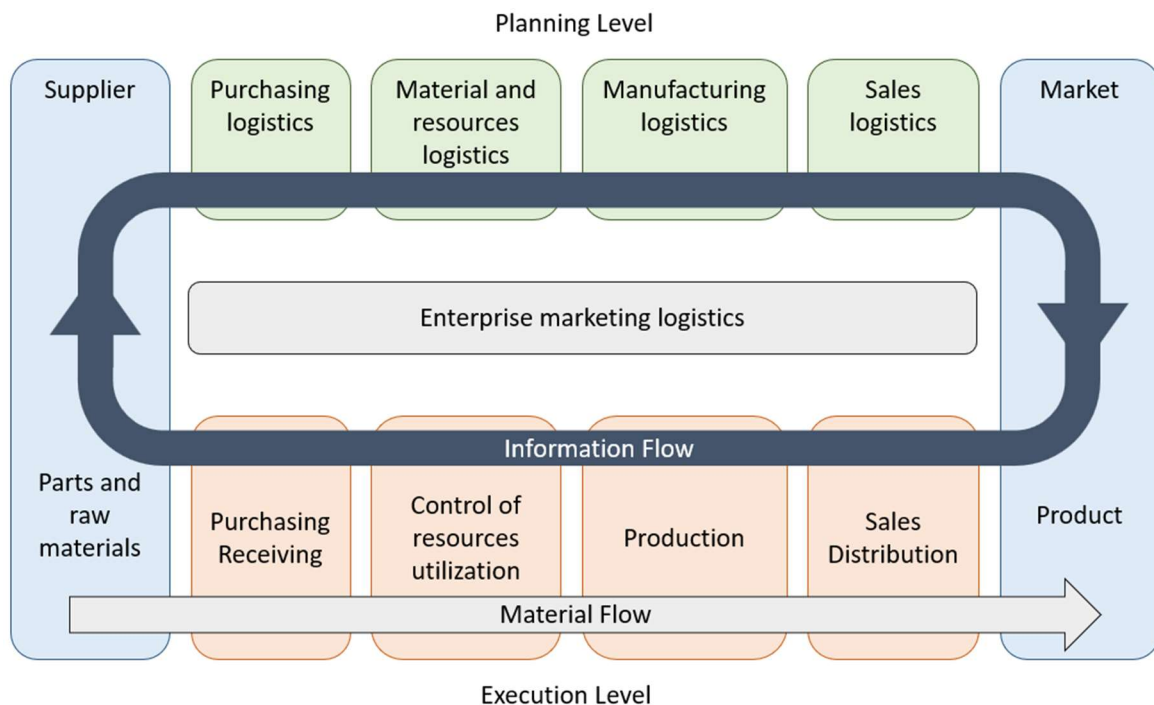


Figure 2.1 - Generic logistic process [4]

In general, there are multiple solutions and levels of automation for transportation and storage of materials or goods, ranging from basic and centralised mechanically actuated systems to currently highly automated solutions which incorporate various types of sensors and actuators controlled by powerful computer systems, managing to build impressive automated warehouses.

In either case, a software application that allows a detailed control over the load movements is normally involved. This software applications can be categorised as a Warehouse Management Systems (WMS), that control, coordinate and optimise the movements, process and operation of the whole assembly and a Warehouse Control Systems (WCS), that orchestrate the flow of activity within a warehouse coordinating the materials handling systems and equipments [5].

This type of warehouses can be characterized by different levels of automation and multiple physical configurations. A common classification is to distinguish between ASRS (Automated Storage and Retrieval System) and a Carousel system.

An ASRS system, Figure 2.2, also called in-aisle cranes, replace the conventional manual-based system of storing objects. Where the locations are fixed and a robotic device, or a retrieval machine, moves in the horizontal and vertical directions in the full extension of the corridor to access the desire location [6].

In the Carousel type system, Figure 2.3, the operation principle is the opposite, where the storing location is moving instead of having a retrieval machine to travel. Usually, the system is composed by shelves that are rotating in circular cycles. In either the cases, the design and the performance of such models have their own specifications and advantages, however, nowadays it is more common to use an ASRS solution [6].



Figure 2.2 – ASRS System [7]



Figure 2.3 – Carousel System [8]

Therefore, in order to make adaptation to Industry 4.0 increasingly smoother, there are more and more companies adopting this type of logistics solutions for their businesses, as they can communicate in real time with the entire warehouse and know all types of informations, such as the quantity available in stock of a certain product, the exact location of an order or predict the delivery time of that order. Furthermore, by adopting these systems, there is greater time optimisation, allowing a faster and more efficient response for the demands.

#### - Some examples of automated warehouses

Focusing now on the search for real solutions applied to the warehouse automation industry, many diversified solutions were found. One of the main companies in this robotise area is *Swisslog* [9], that presents two different solutions for the products storage. For the relevance of this work, it was focus on the solution to store small items that presents as main advantages the fact that it can be adapted to various industries, due to its good spatial optimisation, customizable and scalable modules that can be easily adapted depending on the needs of their costumers [9].

In Figure 2.4 it is possible to see an example of a large automated warehouse produced by the company. Although this solution is made on a very large scale, it is easy to see that *Swisslog* is able to offer solutions for all kinds of products, since as we can see from the picture these warehouses are assembled by modules, being able to increase or decrease the size of the warehouse according to needs, becoming a strong company in the robotisation area.



Figure 2.4 - Swisslog mini load ASRS [9]

Focusing on the solutions developed for the pharmaceutical industry, *Swisslog* is able to offer automated warehouses that allow companies in this area to comply with strict government regulations imposed on them, as well as the best practices offered by the industry, since it has internal software that allows real-time tracking of all products in motion in the warehouse, the SynQ. An example of this is the warehouse they developed in Switzerland in partnership with a pharmaceutical company, Hoffmann-La Roche AG, where they managed to build a storage point with low temperature refrigeration capacity to store the products in a safe way [10].

Furthermore, *Swisslog* also presents an alternative for the transportation of loads from point A to point B. “The mobile solution of the future” [11], or also called an AGV (Automated Guided Vehicle) system is a technology that the company has been working on for over than 45 years and tend to be a more flexible technology than the fixed installations presented previously.



Figure 2.5 - Swisslog AGV system [11]

Although the solution presented by *Swisslog* is entirely dedicated to transporting goods for storage, there are also other manufacturers, such as *Robotic Automation* an Australian company [12], implementing this concept in hospitals, allowing the automatic transport of:

- Meals from kitchen to wards and the way back when the patient has finished his meal;
- Sterile Supplies between CSSD (Central Sterile Services Department) and Surgical Theatre;
- Drugs between all the points they are needed inside an hospital [13];



Additionally, there are companies that present types of solutions already specifically planned for the storage of pharmaceutical products, as well as the processing of prescriptions and prescriptions in digital format, separating orders according to medical orders. Companies like DEMATIC [14] and KNAPP [15] present these solutions for large hospital scales, providing a solution able to give a quick response, according to the needs at the moment.

## 2.2 Automated storage systems for local pharmacies

Focusing now on automated storage solutions, specially developed to be applied in local pharmacies, it is possible to find some alternatives, including the one from *ENGINIS*. This type of concept is well defined by the industry, being characterized as a robot through all the manufacturers, since they have the ability to operate autonomously and adapt themselves, depending on the product that they have to move, manipulate or transport. Furthermore, these mechanisms also implement algorithms that allows them to make the best decision possible according to the necessities [16].

Starting by describing the storage space, these warehouses normally have fixed shelf modules forming an aisle through which a mechanism (robot), that makes the whole system work, moves in the middle, similar to an ASRS systems, as it was seen previously.

The robot ends up being the main component, since all the tasks turn around its performance. Taking the example of the machine developed by *ENGINIS* and considering its current state of development, the process starts with the manual separation and identification of products coming from the supplier. Subsequently, these products are placed on a specific point of the conveyor and from there on no human intervention in the system is needed, apart from emergency situations.

After placing the boxes on the conveyor, the highly technological robot, Figure 2.6, grabs the product with a pair of tweezers and finds the best place to deposit it, considering not only the frequency of output of this type of product, but also its expiration date or even the shortest route to be taken by the machine. When it is necessary to fetch the product, the process is identical, with the same component catching the desired product and depositing it in a predefined place.



Figure 2.6 - Omnicell storage warehouse [17]

In addition, this machine has other features, for example, in times when it is not necessary to perform any of the previous operations, the machine will optimize the warehouse occupation. In other words, the robot will reorder the position of the products according to the criteria previously defined by the programmer, making it even more a system with an unusual capacity for autonomy and optimization, something that in conventional warehouses is almost impossible to do.

As it can be seen, this is a very evolved and complex system, however there is still a large margin for progress, and it is on the basis of this concept that the *ENGINIS* company intends to complement this system by introducing new modules with distinct actions.

The module that will be developed throughout this work will be located in the receiving station of the system. This module aims to reduce the human action in the separation and identification of the product, so that the operator only has to deposit the products in bulk into the module. This way, the module will have two distinct phases, the separation phase and the identification phase, however, the objectives of the current work only contemplate the first phase of division and positioning of the boxes.

## 2.3 Sorters in the pharmacy industry

Some companies in the automation and robotics area have already been developing automatic division and identification systems, for the pharmacy industry. A brief presentation is made of these brands in order to understand their approach for the problem and if there is any type of standardisation of processes and solutions adopted. Furthermore, with this analysis it is also important to understand what kind of limitations these models have. Limitations such as the rate of operation, or the size of the products that these modules can identify.

Figure 2.7 shows the four selected companies and respective for which information was available online.

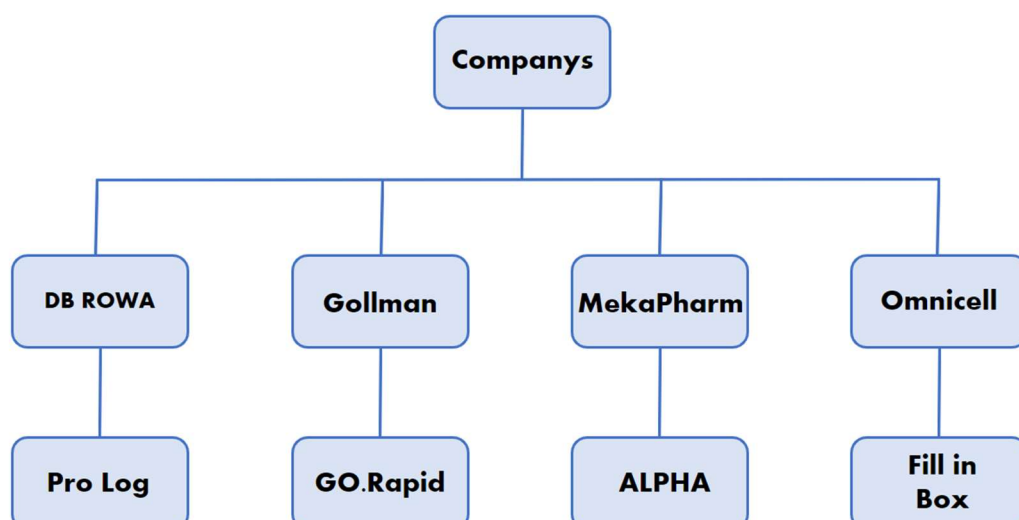


Figure 2.7 - Sorting machines producers

Before presenting each of the solutions found online in particular, it is interesting to note that all the models work as complements to a main storage system, and in some cases can be placed inside or outside the main module. In addition, all systems choose to place conveyor systems to move the loads internally, however the way these are positioned differ depending on the models. Finally, it is also important to note that all the models analysed have incorporated a feature that identifies the boxes. However, for this work, this function is not relevant.

## - DB ROWA

Based in Kelberg, Germany, *Rowa Automatisierungssysteme GmbH*, or simply *ROWA* [18] is a brand that is on the market with solutions for automated handling and identification of products for stocking warehouses in pharmacies and hospitals. The company has been developing several machines that prove to be important tools in assisting the basic functions of employees. For the relevance of this work, it was analysed the *ROWA Pro Log*, a system that is described by the company as a "Fully automatic input", Figure 2.8.



Figure 2.8 - ROWA Pro Log [18]

The *ROWA Pro Log* is an external module that is connected to the main storage system, also developed by ROWA, and becomes a tool that ROWA claims to have the following advantages:

- Reduction of manual workload to a minimum;
- Automatic expiration date recognition (OCR);
- Time saving due, for example, the overnight inputting;
- Available as an external and integrated system [18].

The separation system adopted by the company consists basically of a horizontal conveyor where the boxes are loaded. Afterwards, the boxes are moved up by a conveyor belt with horizontal ribs which are then left in a closed environment that has an up and down used to prepare the boxes for the positioning process.

This positioning system is based on an optical camera and suction mechanism of each box. With the boxes in the closed environment an optical camera incorporated with a proper software detects and identifies each individual box and its exact position. Having identified the objects correct placement, a suction mechanism is used to pick up one box at a time and place it in the desired end position, ready to go into the next step.

Regarding the specifications provided by the company, some interesting data allows to have a better idea of the operability of the machine. It should be noted that the company produces two types of sorters, the *ROWA Pro Log*, which is an external device to the system, and the *ROWA iPro Log*, which is an internal complement to the main system, thus having different specifications. It is also important to mention that the company offers a range of dimensions of the first conveyor, which allows to further increase the number of possibilities to choose from and the splitting capacity. For a better understanding, the data can be seen in the following summary table:

Table 2.1 – Specifications of ROWA sorter machines [18]

		DB ROWA	
		ROWA Pro Log	ROWA iPro Log
Module size	Width [m]	1.68 m	2.44 m
	Depth [m]	0.53 m	0.35 m
	Height [m]	1.62 m	1.54 m
Stocking capacity [packs/h]		120 packs/h	
Box limitations	Min. packs. dimensions [mm]	35 x 15 x 15 mm	
	Max. packs. dimensions [mm]	230 x 145 x 140 mm	
	Weight [g]	5 – 800 g	

#### - Gollmann

Another German company also renowned in this industry is *Gollmann Kommissioniersysteme GmbH*, based in Halle, being distinguished in 2014 and 2015 as the best pharmacy partner[19]. The company also offers multi-functional solutions with most of them being an internal complement to their main robot.

Focusing on their sorter solution, the separation process is mainly done by two consecutive conveyor belts with small inclines and little falls. Afterwards the boxes are taken to an upper floor by a vertical lifter and are left on a third conveyor belt before being positioned. The positioning process is identical to the *ROWA* approach, where an optical camera combined with a suction system and a respective vision software detects and position the boxes, making them ready for the next phase.

As this is an internal module to be implanted inside the main system, there was little information available, since most of the data available were related to their main system. The specifications that were collect can be seen in Table 2.2.

Table 2.2 - *Gollmann* sorter machine specifications [19]

		<b>Gollman</b>
<b>Module size</b>	<b>Width [m]</b>	-
	<b>Depth [m]</b>	-
	<b>Height [m]</b>	-
<b>Stocking capacity [packs/h]</b>		150 – 180
<b>Box limitations</b>	<b>Min. packs. dimensions [mm]</b>	40 x 22 x 15
	<b>Max. packs. dimensions [mm]</b>	200 x 120 x 80
	<b>Weight</b>	200 ml – bottle 600 g – box

#### - **Alpha Mekapharm**

*Mekapharm*, a widely known French company founded in 1999 also designs, manufacture, install and do the maintenance of technological solutions for the storage and preparations of individual orders in the fields of pharmacy industry. The company produces four different types of machines specifically targeted for the storage of pharmaceutical products [20]:

- **OMEGA** - a storage system combined with a multi-picking option makes this robot the fastest robot on the market in terms of moving the boxes and preparing the costumers orders;
- **APOTEKA** - a speed box that helps to improve the speed, capacity and modularity of the automated system;
- **OPTIMA** - this solution incorporates the two previous ones, making the module a very useful automated option in terms of efficiency;
- **ALPHA** - separates and identifies every single box in an autonomous way becoming a very important complement for the previous alternatives that the company provides.

The *ALPHA* machine is directly related with the purpose of this work. Like the other producers, the sorting system starts with a horizontal conveyor belt where the boxes are inputted. In this conveyor there are barriers that delimit the boxes in height. Afterwards, these go onto a spiral ramp that manages to place them in a specific point after the fall, thus helping to initiate their positioning.

The positioning system is a mechanical solution where it combines perpendicular movements to the conveyor movements, with halls and sensors to make the box always positioned at the right spot. This approach ends up being a much simpler alternative, however it takes up much more space than the others. In terms of specifications of this machine, the information available is displayed in Table 2.3.

Table 2.3 - *Alpha* Specifications [20]

		<b>ALPHA</b>
<b>Module size</b>	<b>Width [m]</b>	1.01
	<b>Depth [m]</b>	0.9
	<b>Height [m]</b>	1.485
<b>Stocking capacity [packs/h]</b>		360
<b>Box limitations</b>	<b>Min. Packs. Dimensions [mm]</b>	Width > 7
	<b>Max. Packs. Dimensions [mm]</b>	Width < 175
	<b>Weight [g]</b>	600

### - Omnicell

The last company that was selected to analyse solutions for this type of problem is the American brand, *Omnicell* [21]. They offer a huge variety of systems in the medicine fields, but we will only focus on the Fill in Box system they developed, Figure 2.9.



Figure 2.9 - Fill in Box [21]

This machine works as an external complement of Mach 4, the storage and picking robot that the company produces. With a very simplistic design and an effective way of work, this machine has some benefits that the company describes as [21]:

- Reduce time spent searching for medications;
- Improving patients' safety by reducing dispensing errors;
- Improving inventory control and savings;
- Increase dispensary output capacity 24/7;
- Optimise use of space in the pharmacy;
- Reduce patient waiting time.

The splitting system of this machine is also very similar to the other competitors, where the first conveyor belt combined with vertical barriers divide the boxes in height, followed by a free fall and after a combination of two conveyors that are inclined belts to separate the boxes on the other axes.

For the positioning system, the company came up with a different approach as they make the boxes fall down a ramp with a certain inclination which forces them to follow a certain path, then they are taken to a shorter belt, whereby means of a mechanical clamp they are positioned in the correct position. In Table 2.4 is represented the specific information about the Fill in Box module.

Table 2.4 -Fill in Box Specifications [21]

		Fill in Box
Module size	Width [m]	1.5
	Depth [m]	0.5
	Height [m]	1.25
Stocking capacity [packs/h]		250
Box limitations	Min. Packs. Dimensions [mm]	-
	Max. Packs. Dimensions [mm]	
	Weight [g]	

To sum up, it can be seen that there are some solutions on the market with different ways to solve the same problem. From what was noticed, *Gollmann* has an overkill solution for the sorting process, has it incorporated a rotary vertical lifter which can bring more failure points. In terms of positioning and boxes detection, it ends up being a well-developed solution, alongside the *ROWA* system, which is very similar.

Overall, the sorting systems developed by *ROWA*, *Mekapharm* and *Omnicell* are not very perceptible but from the information available on internet all of them seem to make their job perfectly. For the positioning system, the *Mekapharm* solution is simpler, but it has the problem of spatial occupation, so the *Omnicell* solution ends up being the best option as it seems to be the most minimalist and effective way of performing the function for which it was made.

*(Blank Page)*



### 3 Project development

This third chapter is going to mainly focus on the explanation of the development of alternative design concepts, where it is also going to be presented some more specific constraints that should be taken into considerations throughout the process.

In order to simplify the creation of a conceptual model, it was decided to divide the process in two phases. First, on how to split the boxes to ensure that from the moment they were loaded in together until the end of this stage, it is guaranteed that only one box arrives at a time. Then, the second phase, which is the positioning process, where it should be guaranteed that the box always ends up in that precise position.

In these two stages, the concepts that were developed are going to be explained in further detail. Most of the concepts were put aside and the explanations for these decisions are also given in this section. The other ideas were submitted to a testing phase where the concept was implemented, and some more detailed conclusions about the viability of that idea were made.

#### 3.1 Problem specifications

##### - Volume available

As this was a complement for an already existing storage system there are restrictions derived from the design of the existing structure. The main system is supported on 40 x 40 mm square-shaped aluminium profiles, divided into modules of equal dimensions, 1000 x 500 x 2800 mm. In Figure 3.1, it is presented three of those modules that are used in the main storage system. For this project, the area that is available is highlighted in that same figure, with the following dimensions 2040 x 500 x 1500 mm.

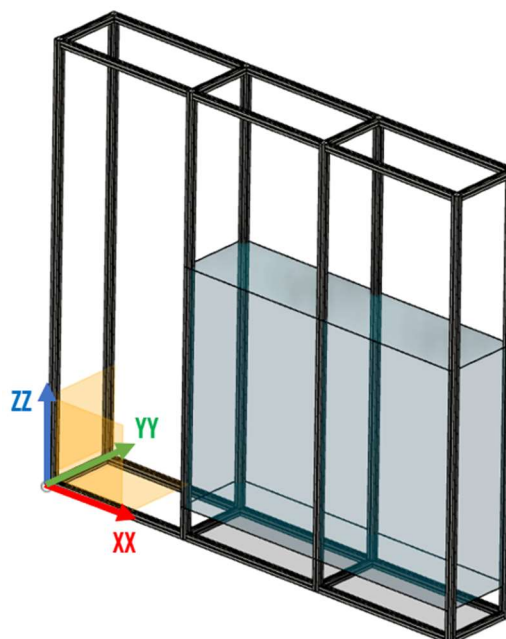


Figure 3.1 - Available space

### - Pill box size variations

There are numerous combinations of pillbox sizes and shapes and the variations between the dimensions is very wide. For this work, it was specified the range values that are presented in the following table. In terms of weight per box, no value limiting the range was given. Being arbitrated a 3 kg of total mass for the medical boxes to be introduced inside the module in the beginning. Furthermore, it was not defined a minimum flow rate for the materials as it is still a prototyping phase.

Table 3.1 - Range of box dimensions (in mm)

	<b>Smaller</b>	<b>Bigger</b>
<b>Length</b>	15	150
<b>Width</b>	15	150
<b>Depth</b>	45	250

### - Maximum height

The point at which the pillboxes are inserted into the module must be suitable for a person of average height. For standardization purposes, it was decided to use a value that fits in with the standard values, considering that the boxes should not be deposited inside the module at a height higher than 1500 mm.

In addition to this, it is also recommended to prevent the boxes from falling off a considerable height in order to not damage them. Therefore, a test phase was carried out and it was concluded that the maximum height for a fall is topped of at 400 mm.

### - Other restrictions

In terms of construction processes, it was advisable to avoid welding processes and fixed connections, it was also recommended to always try to find solutions that can be carried out internally in the company, in order to minimise the cost of production of certain components, being also preferable to avoid pneumatic mechanisms as much as possible because of their high cost and complex maintenance.

Finally, and in order to ensure a greater standardization of the components used for the construction of other equipment, some suppliers were recommended which have been working with the company for some time and their catalogues were consulted to find compatible solutions for the project's needs.

### 3.2 Conceptual ideas

After collecting all the needed information to have a general idea about what it was pretended to obtain, it was time to start the development of conceptual ideas. It was used a 3D CAD software, in this case 'FUSION 360', to provide a better perception of what was developed, and thus, be able to formulate a consistent opinion of each of the concepts, before creating a real prototype for the testing phase.

#### - First two concepts

Starting with the division process, it was followed a strategy of focusing on each of the three coordinate axes  $[x, y, z]$  in separate ways, in order to ensure that the boxes are efficiently split. As it can be seen from Figure 3.2 and Figure 3.3, the first two concepts developed were similar, but the positioning of the belts were in different directions.

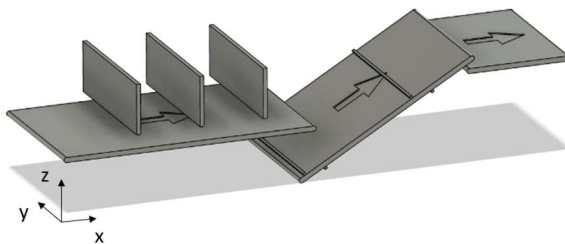


Figure 3.2 - First concept

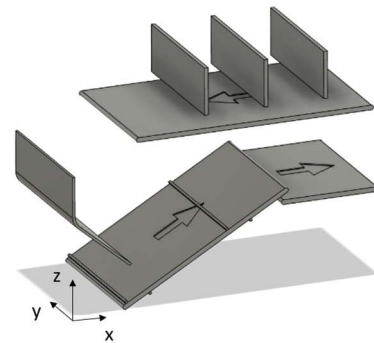


Figure 3.3 - Second concept

Starting by focusing on the  $ZZ$  axes, the easiest way to knock down the boxes seemed to be by creating physical barriers. The barriers could be fixed to a rotating axis, so with the movement of the belt and the force came from the weight of the boxes, they will create a rotating movement that lift the barriers, and consequently pushes the boxes that are on top of the others to fall or move backwards.

Afterwards, the boxes would go into an inclined conveyor that would take them to a higher level. It should be noted that the belt of the conveyor would have horizontal ribs that would allow the boxes to be aligned along the  $YY$  axis. The positioning along the  $XX$  axis would be made by actuating clamps to ensure correct positioning.

This idea seemed to be very minimalist for the requirements, and one possibility to have an additional control in the box separation is by making them fall, due to the gravitational force into a lower level (Figure 3.2). These two ideas combined came up not being the most efficient solutions, as it would not guarantee the effective separation of the boxes, especially along the  $XX$  and  $YY$  axes. Furthermore, in the second example, in order to place the second belt with the necessary slope, it is necessary to use a considerable space under the first conveyor, which would cause a bigger drop for the boxes, something mandatory in order to not damage the boxes.

### - Third concept

Since the idea that was used on the first two examples for separating the boxes in the ZZ axes was seen as the most effective, easier and less costly alternative, it was decided to maintain this concept in every new idea, searching only for new alternatives that guaranty the correct division in the XX and YY axes.

In Figure 3.4 it is presented the third concept. After the first conveyor, it was introduced a ramp that has inclination that forces the boxes going into a specific point. Then the boxes would go to two conveyors in series with distinct accelerations to separate them along to the YY axis, and finally there was a curved wall that would make the boxes separate on the XX axis. On the side they would have another conveyor to assist the separation movement. By creating this curve, it was expected that the boxes line up in front of each other and move on to the side conveyor and proceed to the correct positioning. This was one of the ideas that were constructed, and the results obtained were not as expected, and it was decided to leave this option aside.

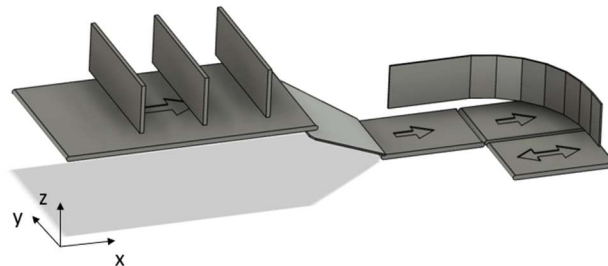


Figure 3.4 - Third concept

### - Fourth concept

Another alternative, derived from the previous concept, is illustrated in Figure 3.5. After the first stage the boxes would fall, damped on a ramp leading to two conveyors in series, but with perpendicular movement directions. The C2 conveyor, after the drop, would roll in the positive direction of the XX axis, while the second, C3, would roll perpendicular. With this combination of perpendicular moving directions, it was expected that the boxes become rearranged in space so that only one box hit the edge of the barrier at a time. With this barrier it was expected that the boxes would be lined up before going to the positioning phase.

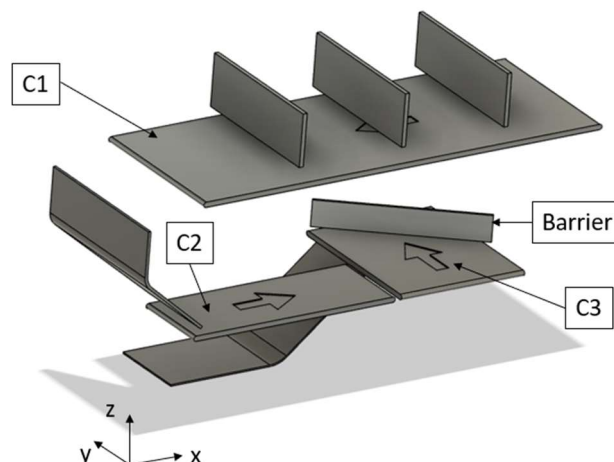


Figure 3.5 - Fourth concept

This idea was not followed further, not only because it is a very elaborate concept, with so many different belt movements, but also due to space limitations which would not make it possible to put conveyors large enough to rotate the bigger boxes. Furthermore, it would not be guaranteed that only one box is at the end of the last conveyor, neither if the wall will make the correct alignment of the boxes ensuring that there are no boxes next to each other, so we put aside this concept.

#### - Fifth concept

The last concept that was developed in this phase is represented in Figure 3.6. After the first conveyor, C1, the boxes will have a small fall into a lower level, where it will be implemented a ramp to avoid a free fall that damages them. In this lower level, there will be two conveyors, C2 and C3, in series but with different velocities, so we could distance the boxes on the XX axis. For the YY axes, it will be implemented a chicane, so we force the boxes going into that way, avoiding a dead zone in the path, with this system it is then expected that at the end of the chicanes, there are no boxes side by side.

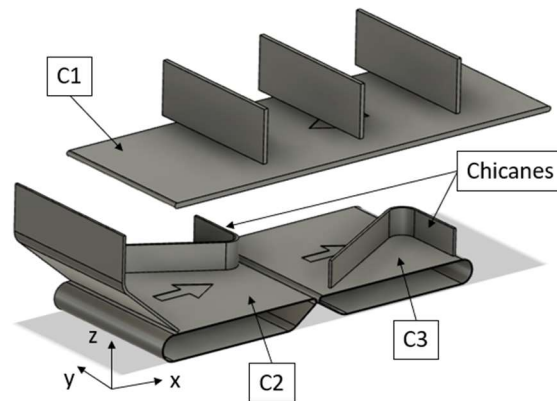


Figure 3.6 - Fifth concept

#### - Positioning System

Afterwards, it was time to focus on the development of the positioning system. In the beginning, it was thought about using an optical detection system where, through the combination of a camera with spatial recognition and a dedicated software, it would be possible to determine the exact position of the boxes. However, this idea was put aside, due to the fact that it would bring higher costs and complexity to the development process.

In addition, a mechanical system with two clamps that would compress against each other and align the box in the middle was also considered, but as previously mentioned, systems involving pneumatic actuators should be avoided.

Having said this, a mechanically simpler but at the same time functional solution was thought and it was concluded that a metallic sheet with small bends may result. This metallic sheet would have an inclination that allowed the boxes to fall by gravity, and, with this, the boxes should go down in the middle of the ramp and at the end there would be a wall that lined up in the other direction.

This solution will be placed after the last conveyor as shown in Figure 3.7. It was also constructed to see if it is reliable solutions and get the expected results. Furthermore, it is important to assemble the ramp, as this will give a better idea of the most appropriate bending angles that this last plate must have so the boxes could flow smoothly.

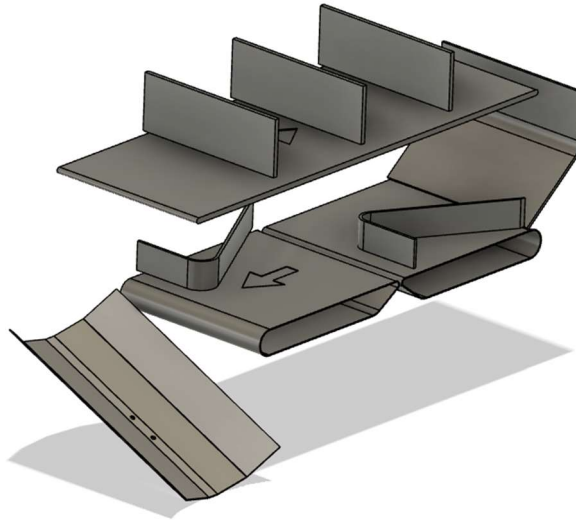


Figure 3.7 - Final conceptual solution

### 3.3 Testing phase

This section is dedicated to describing the physical implementation of the developed concepts previously presented. With this implementation, it was possible to get a sense of whether the ideas are doable, the pros and cons of each alternative as well as possible refinements that could be made in order to get a more reliable concept. For building the ideas, it was necessary to start the process from beginning until reaching the final physical model. To do this it was needed to create the CAD models, see the manufacturing processes and materials available for the components production, generate the CAM models, when needed, produce them, and then finally assemble all the components, Figure 3.8.

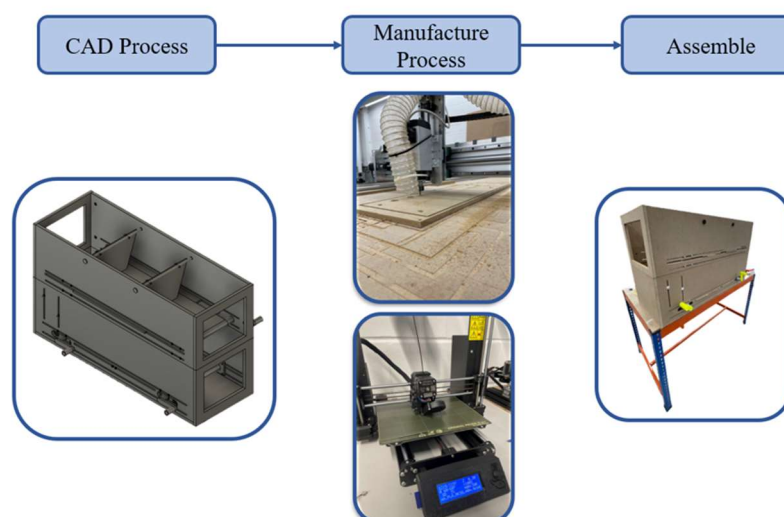


Figure 3.8 - Development phase of the physical prototype construction

As the goal for this stage was to implement the ideas as fast as we could, with the lowest possible cost, the first step was to see what was available on the warehouse so that was only needed to buy what was strictly necessary and avoid the waste of time in the shipping of the products. For that reason, the main component that was founded were the conveyor belts, and it was from their dimensions that the ideas began to develop.

#### - Overall structure to build the module

For creating the structure, it was used MDF boards, which is a wood-based material that can be easily manufactured according to the configurations desired. It is only necessary to create the CAM models and cut the boards according to the dimensions and shapes pretended in the milling machine, which was also available in the company. Additionally, components such as the sleeve bearings, which are parts that are subject to high wear, since they were in contact to the rotational axis of the barriers, were made in PLA, Polylactic Acid, by a 3D printer which for the purpose suits perfectly the requirements. Besides it is a cheap and quick way to produce these components.

The belt was driven manually as this is the simplest mechanism and it allows to control the movement more easily. On the other part of the shaft, there is a mechanism with a bearing that allows the assembly to rotate freely. The driven pulley has exactly the same mechanism on each side of the shaft, Figure 3.9. The assemble components for a single conveyor is illustrated in Figure 3.10. In addition, the shaft was made from circular PVC pipes, this alternative ended up working well, having been necessary to sand the surface of the profile in order to create more friction between the belt and the shaft so the movement could be transmitted.

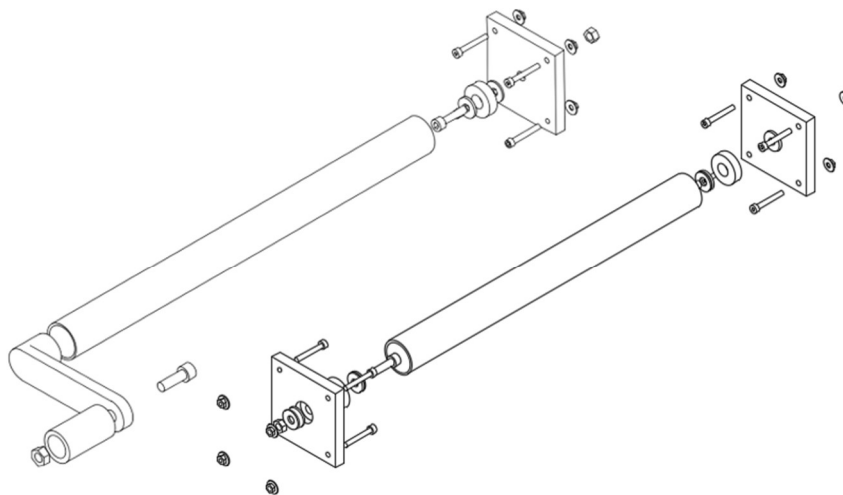


Figure 3.9 - Transmission mechanisms (left – driving pulley and right – driven pulley)

In Figure 3.10, the pulleys were screwed to slots created in the MDF sideboard. These slots allow the shafts to move linearly so the distances between them can be adapted, depending on the size of the belt used. In addition, these cuts are also important to ensure that the belt is stretched enough to be able to guarantee the transmission of the movement from the shaft to the belt. This is only a provisional solution, as it does not guarantee the dimensional precision needed to put into the final design, but for the purposes of this testing phase, the mechanism worked.

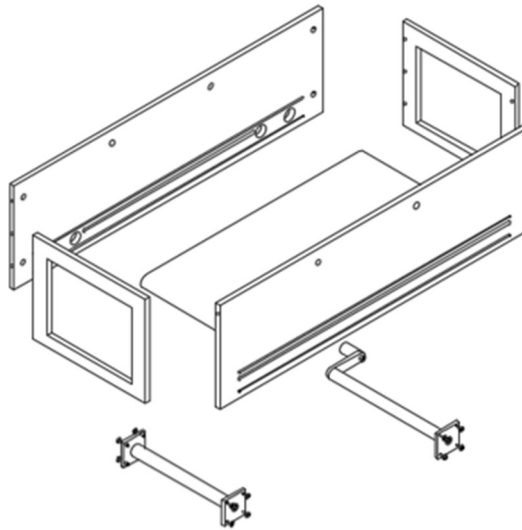


Figure 3.10 - Conveyor system

#### - Barrier's test

Starting with the concept that spread the boxes along the ZZ axis, it was necessary to create barriers that rotated around an axis. To do this, the barriers were bolted to an axis that rotate on bushings printed in PLA, as it was mentioned previously. These bushings were pressed into the MDF and prevent the barrier from moving longitudinally. Figure 3.11 shows how the components are assembled.

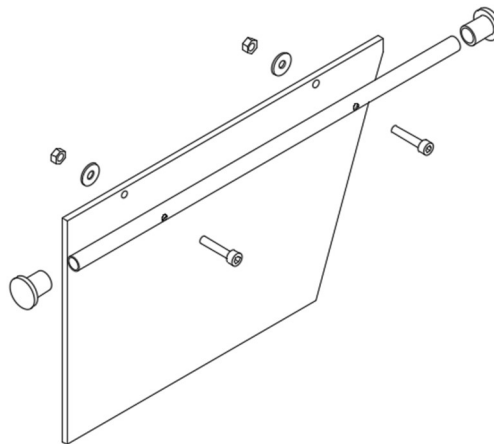


Figure 3.11 - Barrier assembly mechanism

The aim of this test was to find out the best barrier configuration in order to reduce the number of boxes on height in the most efficient way. To achieve this, the best solution was to change the mass of the barriers and see what happens throughout the tests. Therefore, tests were carried out with three barriers with different thicknesses (16mm, 10mm and 5mm), Figure 3.12, and their masses are illustrated in Table 3.2. In addition, the sum of the masses of the rotary axis and standard accessories such as bolts, bushes and nuts are also represented.



Table 3.2 - Barrier Mass variation (kg)

Thickness [mm]	1 <sup>st</sup> Barrier	2 <sup>nd</sup> Barrier
5	0.27	0.26
10	0.42	0.44
16	0.61	0.62
Rotary axis + Accessories	0.06	



Figure 3.12 - Barrier real models

As it can be seen from the table, the mass of the first and the second barriers does not vary significantly, approximately 2 to 5%, which is beneficial, as it allows to have barriers of the same thickness and with very close mass values for the experiment. However, when the thickness is changed, it is noticed that the mass varies almost proportionally, with some slight differences due to the fact that the geometries are not completely equal, in order to make the connection to the rotary axis viable.

Other details to consider were the distance between the bottom of the barrier and the belt, which has to be at least equal to the smallest width of the boxes (it was chosen 15 mm, since it is the lowest height of the boxes), as well as the spacing between the barriers, so that the boxes do not overload the system, which in this case was 350 mm. Furthermore, the belt should also have some small notches in order to push the boxes into the barriers. At this phase, those details were made with hot glue, but in the final concept the supplier of this product has a proper way to create these details. In Figure 3.13 it is illustrated the construction of the first conveyor.



Figure 3.13 - First concept testing model

After running a few attempts with every barrier thickness and with different box sizes, it was possible to conclude some unexpected aspects. The barriers with 16 mm and 10 mm ended up having similar results as both of them split the boxes in every situation, although in some cases the small boxes had some difficulty to move forward with the 16 mm thickness barrier.

The barriers with 5mm of thickness, Figure 3.14, only had better results when they were running with boxes with lower weight. When this last barrier was tested with boxes of different sizes, it was concluded that when a heavier box goes in front the barrier will move easily and if then is a set of smaller boxes at the back, this barrier will do nothing to these smaller boxes as it does not have enough inertia to return quickly back to the initial position and send the smaller boxes down. For this reason, it was excluded this thickness to make the barriers.

In addition to that, other different barrier thicknesses combinations were used which came up having some improvements but nothing extraordinary. So, for the point of simplification and standardisation of the process, the two barriers will have the same thickness, which is 10 mm.

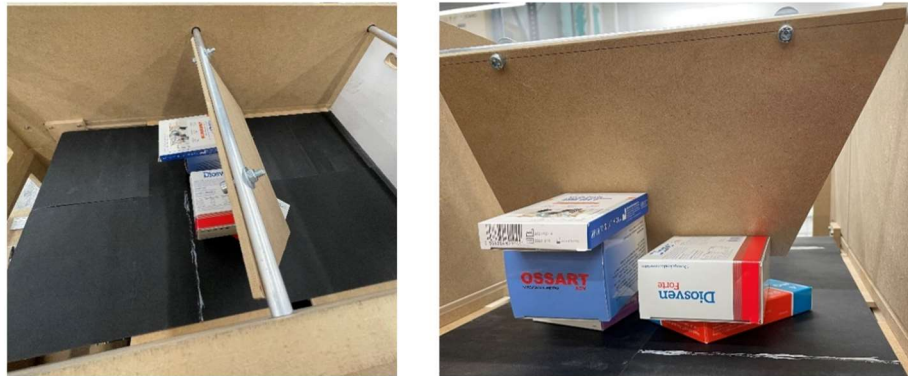


Figure 3.14 - Tests with 5mm thickness barrier

Furthermore, it is important to mention some aspect that may influence the final result. The conveyor belt that was used has low coefficient of friction on the top surface which was something that should not happen as the boxes should ideally stick to the belt so that when they hit the barrier they do not bounce back so easily as it happened in some experiments. Furthermore, the belt will have small steps that are made of resin and glued to the belt in the proper manner, in this experimental test they were made of hot glue which does not have precise dimensions, neither the geometrical accuracy, but for what it was intended to do, this alternative worked.

In general, the results obtained with the tests for this concept were quite satisfactory, which leave good prospects for the Z-axis division system, as it was expected, and the distance between the barriers also seems to be ideal. Due to the fact that the belt is too short, the boxes did not have much space to reorganise after the last barrier, being an aspect to be changed later in the modelling of the final project. But for these tests this was not a very important point since the goal was to understand what type of barrier thickness suits better on this system.

### - Curve's test

After concluding the first part of the test, it was time to test the idea presented in the third concept presented above. The conveyor used was the same and the curve was made from boards of PVC, that were very malleable, and with hot glue. In order to give more stiffness to the structure, a cardboard plate was also glued on the bottom part as shown in the Figure 3.15.



Figure 3.15 – Curve maquette



Figure 3.16 - Testing with the curve model

By making the tests, it was understood that the results were not what was intended. Starting by the fact that the construction material was not rigid enough to support the heavier boxes and the surface finish of the curve also turned out imperfect due to the high malleability of the material, which made it difficult for the boxes to follow the trajectory imposed by the curved wall.

Furthermore, as it can be seen in Figure 3.16, the boxes did not line up one behind the other and when they moved on to the side conveyor, this movement was often interrupted due to the lack of inertia required to move the boxes. This idea was put aside as it does not work as expected.

### - Chicane's test

After seeing that the last idea did not get the desired results, it was time to move on to the study of the concept with the “chicanes”. Firstly, it was necessary to develop a concept in which it was possible to place the two conveyors followed by each other. In order to make the passage of the boxes from one conveyor to the other as smooth as possible, it was applied a configuration known as the Knife Edge, where the shafts that make the transition from one conveyor to the other have the smallest possible diameter, so that they can be closer to each other. An illustrative image of the concept is presented in Figure 3.17. Apart from that, the whole mechanism was repeated.

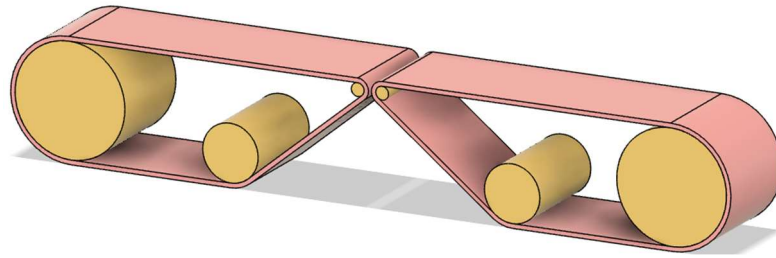


Figure 3.17 - Knife Edge 3D model concept

In the process of designing and creating the chicanes, it was necessary to take into consideration their dimensions, as it was necessary to avoid the creation of dead spaces along the path, in Figure 3.18, it is possible to see this aspect more clearly. Since the goal is to divide the boxes according to XX and YY it is necessary to avoid a path where the boxes do not pass through any of the chicanes, something that happens in the left part of the Figure. So, it is necessary that dimension "l" passes the middle of the belt or that  $\Delta X$  is smaller than the smallest width of the boxes, any of these solutions can be chosen.

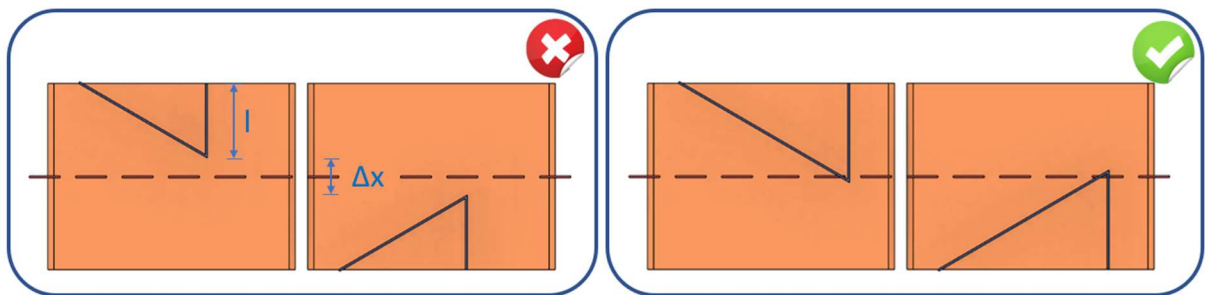


Figure 3.18 - Correct and Incorrect chicane alternatives

Beyond that, it was necessary to create free space in the beginning and the end of each conveyor, so that the boxes can rotate and adapt their orientation and do not get stuck inside the assembly, something that was taken into consideration, as it can be seen in Figure 3.19.



Figure 3.19 - Third concept testing model

After the boxes leave the first conveyor to the second, they will have a drop of 300 mm, which can cause some damage to them. In order to minimise this impact, there will be a ramp that will cushion the fall, thus reducing the risk of any defects created in the boxes. As can be seen in Figure 3.20, this ramp has some lateral slots in order to find the best inclination through this experimental phase.



Figure 3.20 – MDF ramp model

During the testing phase of this concept, some conclusions were drawn, as well as some adjustments needed to be made. Starting by the ramp inclination, it is important that the ramp is not too small inclined with the horizontal so that when the boxes leave the first conveyor, they do not advance the first chicane, without even touching it, or even get hooked on the inside of the first chicane, so it was chosen a 35° angle with the horizontal. Furthermore, the side slope of the chicane has to be as smooth as possible, so that it does not create a bottleneck in the system, and it was chosen a 30° angle with the side support board.

One detail that had to be changed during this test phase was the height at which the chicanes were in relation to the conveyor belt. Initially, the smaller boxes could pass under the chicane losing the expected effect. However, this problem was easily solved by closing that gap. The final distance that was chosen was 10 mm, Figure 3.21.



Figure 3.21 - Third concept testing experiments with the gap problem solved



Other than that, the concept seems to work perfectly, delivering what was previously expected. Besides, it is interesting to notice that the boxes always come out with the face touching the highest point of the second chicane, making it easier to know how to proceed with the positioning operation, as it can be seen in Figure 3.22.

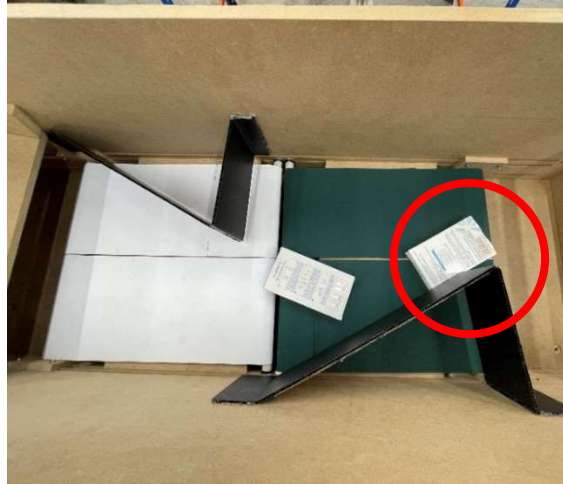


Figure 3.22 - Third concept testing experiments

Once again, the fact of reusing the belts caused some difficulties in the development of the process, but in terms of testing the concept, the results were obtained as it was expected, as all the boxes were properly spread in the XX and YY axes.

#### - Positioning concept

For building the component of the positioning concept, it was used the same technique as it was used to make the curve and the chicanes, ending up having the model as it is represented in Figure 3.23. The ramp was glued to the foots of the structure which turned out to be a fairly stable alternative, as it was able to deliver what it was intended for.



Figure 3.23 - Ramp for the positioning process

In Figure 3.24 it is possible to see the sequence of the boxes after leaving the last conveyor and how the positioning system works. With the testing of this concept, it was discovered some important aspects that previously were not paid much attention. Characteristics such as the length of the ramp (the distance available for the box to travel) and its inclination with the floor are extremely important aspects. In the first attempts, the ramp was extremely short and with a steeply sloping, which resulted in the boxes falling directly for the last conveyor and not having space to do their correct positioning, so it was needed to make some changes on the ramp. In Figure 3.24 it is possible to see the final model produced for the ramp, which worked as it was expected, the dimensions of the ramp as well as the inclination it has are presented in the chapter dedicated to the construction of the final model (Chapter 6.1). In addition, another important aspect to mention is the fact that the smaller dimension of the box is always parallel to the positioning wall. This is very important for the next phase, which is not the subject of this report, since it facilitates the continuity of the process.



Figure 3.24 - Positioning system in operation

In Figure 3.25 it is represented the final prototype that ended up working as it was expected. The construction of this prototype was important to understand the restrictions that some concepts have to work in a desired manner, and it was also a very useful tool to validate the ideas presented. Once the ideas have been proved, it becomes necessary to develop a final model where the concepts tested here are applied but developed with the necessary dimensional accuracy.



Figure 3.25 - Testing phase final prototype

*(Blank Page)*



## 4 Development of the final concept

After having finished the testing phase and having concluded that the chosen concept fully performed the functions required of it, it was time to develop a detailed solution. Therefore, in this chapter, it is going to be presented the justifications for the selection of each of the components, as well as the calculations that validate the structural integrity of the entire module are also presented.

### 4.1 Materials selection

Starting with the choice of materials, it was done research on which manufacturing processes were used to produce the components designed for this project and thus be able to choose the type of material that best fits that manufacturing project.

Although the price is more expensive when compared to other materials available in the industry, it was chosen aluminium alloys because it is possible to get a much lighter structure when compared to steel. In addition, aluminium has a very good surface finish so there is no need for post-processing operations or the application of products on the surface of the component, which also reduces operating costs. Therefore, in the PolyLanema [22] catalogue, a Portuguese distributor of this type of material, some alternatives that were selected are the following ones:

- **Al 5083** – this type of aluminium alloy was applied to all non-structural components that need to be machined by a 3-axis CNC. Being characterised as having good machinability properties the elements from which they are constructed with this material should not require such dimensional rigour. In addition, this aluminium alloy has a lower density which is also beneficial when it comes to reducing the weight of the structure. The properties of this material presented for a thickness of 18 mm blocks since are the ones that were required on the development of those components.
- **Al 7074** – This aluminium alloy has been selected for components that require high dimensional accuracy as well as better build quality, as it has excellent machinability properties. All structural components were made from this alloy due to its high surface hardness, thus ensuring better rigidity to the structure. Once again, the properties for which values have been presented are for 18 mm thick blocks.
- **Al 5754** – For the components that were obtained through a bending process it was advised by PolyLanema, to use this aluminium alloy. In addition, this alloy presents great mechanical properties and an easy conformation, something beneficial when it is intended to obtain components from this manufacturing process. Regarding the properties of this material, the values were taken for a 3 mm thick plate.

In Table 4.1, the technical data of each selected material are available which will be useful later on in the dimensioning part of certain elements, to understand if they support the efforts they are subject to.

Table 4.1 - Selected aluminium alloys specifications [22]

	Al 5083	Al 7075	Al 5754	Units
<b>Young's Modulus</b>	71	71	70	<i>GPa</i>
<b>Yield Stress (0.2)</b>	115	470	80	<i>MPa</i>
<b>Poisson's Ratio</b>	0.30	0.33	0.30	-
<b>Density</b>	2.66	2.80	2.67	<i>g/cm<sup>3</sup></i>
<b>Brinell Hardness</b>	75	161	52	-

## 4.2 Conveyor components

### 4.2.1. First conveyor

Starting with the presentation of the constructive model of the first stage of the whole process that splits the boxes in height. The constructive process began with the assignment of spatial measures for the whole set. Based on the measurements applied in the testing phase and trying to replicate the process, the overall dimensions of the conveyor can be seen in Figure 4.1.

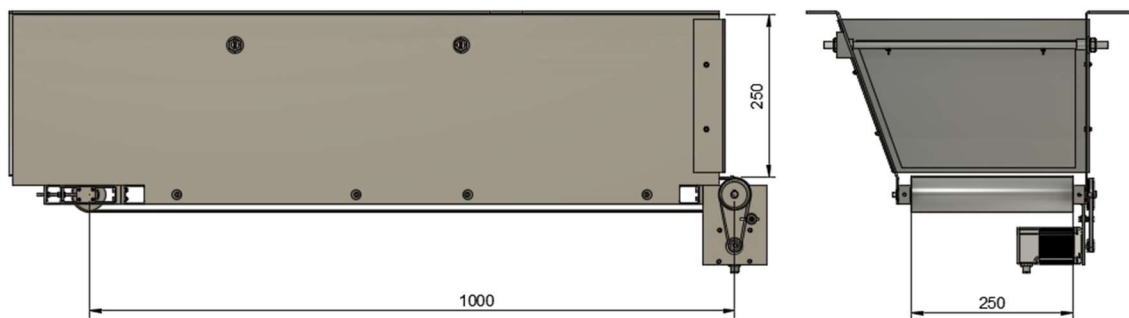


Figure 4.1 – First conveyor dimensions

As already mentioned in previous chapters, the main goal of this first stage was to split the boxes in height, so that at the end of the conveyor there were no boxes stacked on top of each other. The idea of putting up barriers emerged as the simplest and most viable alternative. However, there is another detail that needs to be taken into account. When the bottom boxes are making their linear movement and hit the barrier they tend to move backwards, and the aim was to try to make this reaction generated by the weight of the smaller barrier. The solution found to resolve this event was to try to create the maximum friction between the surface of the box and the conveyor belt, and this was the starting point for the selection of the first belt.

## - Belt selection

One of the suppliers of conveyor belts that *ENGINIS* works with is *MegaDyne* [23], after going to their catalogue and search for possible solutions where the friction of the top of the belt was the highest, as much to value the 1 as possible, it was founded a model where the surface finish had the geometry of an inverted pyramid configuration.

The model of the belt selected was the P9/Z, and these types of belts are generally used for the transport of small loads where it is necessary the minimum movement of the product during the movement of the load, something that fits in this system. In addition, on the upper part of the belt, there is an option that has small notches so that when the boxes get stuck on the barrier these small ribs force them to move and follow their course. This type of feature is manufactured by the supplier itself, and in the chosen belt two of them were applied separated by 1050 mm between each other.

Regarding the bottom part, this also has a special feature. In order to guarantee a better guidance of the belt there were guides that are placed exactly in the middle of the belt and that help to increase the life of the equipment, since it makes the belt not leave the central position of the roller.

In the supplier's catalogue there were many possible configurations for this feature, and one of the restrictions that was imposed was that the minimum diameter of the roller did not have to be much larger than the restriction imposed when choosing the belt, as the aim was to optimise the available space. Having said this, the choice ended up being the model NA.X04.62, since it was the one with the smallest dimensions and with a trapezoidal section, something very useful later in the selection of the roller, being in this case the value that limits the minimum diameter that the roller could have.

Table 4.2 contains important data about the belt, namely the total mass, an important variable in the sizing of the motors, there is also represented the tensile force for the elongation of 1% and other variables.

Table 4.2 - P9/Z specifications [23]

Belt Brand	MegaDyne	Model	P9/Z
Guidance	NA.X04.62	Minimum Pulley Diameter	30 mm
Length	2150 mm	Width	250 mm
Mass per square meter	1.42 kg/m <sup>2</sup>	Area	0.54 m <sup>2</sup>
Mass	0.76 kg	Thickness	1.52 mm
Coef. Friction top side	-	Coef. Friction downside	0.25
Tensile Force (k=1%)	6 N/m	-	

To calculate the mass of the belt, Equation 4.2, it was needed to first calculate the total area of the belt, Equation 4.1 and then multiply by the density per unit of thickness given in the datasheet, so it was possible obtain the mass. The length of the belt depends on the diameter of the pulleys and the separation between them, the Equation 4.3 was obtained from the Shigley's book [24] and it was possible to calculate the length the belt.

$$A_{belt} = (\pi \times d \times c) + 2 \times (c \times w) \quad 4.1$$

$$A_{belt} = (\pi \times 0.048 \times 1) + 2 \times (1 \times 0.25) = 0.54 \text{ m}^2$$

$$m_{belt} = A_{belt} \times \rho_{belt} \quad 4.2$$

$$m_{belt} = 0.54 \times 1.42 = 0.76 \text{ kg}$$

$$l = \sqrt{4C^2 - (D - d)^2} + 1/2 (D \times \Theta_D + d \times \Theta_d) = 2150.80 \text{ mm} \quad 4.3$$

Where,  $d$  – roller diameter – 48 mm;  $c$  – distance between rollers – 1000 mm;  $A_{belt}$  = internal belt area;  $l$  – total belt length;  $\Theta_D$  is the belt contact angle with the roller, as both rollers have the same diameter  $\Theta_D = \Theta_d = \pi \text{ rad}$ .

#### - Rollers and shaft selection

After selecting the conveyor belt main dimensions, it was necessary to select or design the remaining components. The aim was to try to and choose as many products as possible from the catalogues of the company's suppliers, since this way we already have a guarantee, beforehand how these components work under defined operating conditions. When it was not possible to obtain these products through the catalogues, they were designed to support the efforts to which they were subjected.

The first component chosen was the rollers for the driving pulley. In this component some specific characteristics were considered, such as the material of the last layer of the roller which is in urethane in order to promote a greater friction coefficient between the belt and the roller, thus decreasing the belt slippage and consecutively the energy losses. Furthermore, the external diameter was imposed by the belt restrictions since it requires a minimum operating diameter.

The chosen product has the following brand reference RWBMG48-N10-230-X10-Y8-Z6 from *MISUMI* [25] and its specifications are presented in Table 4.3. The middle of the roller it has a characteristic slot that was mandatory to have due to the fact that the belt has a central guide as presented before. The dimensions of the slot created in the roller are represented by the numbers after the letters X, Y and Z, respectively in the reference number.

The technical data sheet did not reveal the total weight of the roller, so it was needed calculate the volume occupied by the urethane layer (10 mm thick from the catalogue) and the volume occupied by the aluminium and obtain an estimate of the total weight of the assembly through the densities of each of the materials.

Table 4.3 - Driving and driven pulley specifications

	<b>RWBMG48-N10-230-X10-Y8-Z6</b>	
<b>Outer Diameter</b>	48	<i>mm</i>
<b>Internal Diameter</b>	10	<i>mm</i>
<b>Length</b>	230	<i>mm</i>
<b>Density of Urethane</b>	1.06	<i>g/cm<sup>3</sup></i>
<b>Density of Aluminium</b>	2.7	<i>g/cm<sup>3</sup></i>
<b>Volume of Urethane</b>	274.58	<i>cm<sup>3</sup></i>
<b>Volume of Aluminium</b>	123.56	<i>cm<sup>3</sup></i>
<b>Total Mass</b>	0.63	<i>kg</i>

Although this type of urethane surface finish was not required for the driven roller, it ended up choosing the same product for this axis, as in the *MISUMI* catalogues, there were no rollers with the same external and internal diameter, as the one chosen for the driving roller without this coat. Therefore, and in order not to have different sizes in the two rolls, it was chosen the same roll for the driven axis. Furthermore, these rollers already have a simple system that allows the shafts to be coupled and connected to the structure, which was another reason for choosing them.

These rollers need to rotate freely and at the same time be fixed to the structure that supports the entire conveyor. One of the elements that made this connection were the shafts to which they had been chosen from the *MISUMI* catalogue. In the driven roller the two shafts were the same and have the following reference: PSHFHR10-30. On the driving roller the shafts have to be different. One of the shafts was the same as the previous one but the other has to have a slot for a key since the pulley that was chosen for the transmission system requires it to ensure that there is no slippage between components and consequently increasing the efficiency of this energy transmission system (reference of the shaft number: PSFGKR10-52-KA1-A16).

#### - Conveyor structure and components assembly

In what concerns to the elements that support the whole conveyor structure, these were entirely designed according to the specifications of this project. Furthermore, during their design, it was taken into consideration that these components could be adapted to all the conveyor systems that need to be incorporated in the module, thus making the assembly process simpler and more standardised.

In order to guarantee the free rotation when connected to the structure, the shafts need a mechanism where the influence of friction is minimal. In this way it was created an assembly that has a bearing attached to it, Figure 4.2, the bearings (pink components) are coupled inside a box to make easier the attachment to the structure, which was done by means of a screw system. It should be noted that there were two different systems depending on the pulley to which they are applied, since the driven pulley has to move linearly, to put tension on the belt, it was necessary to make some changes on the components.

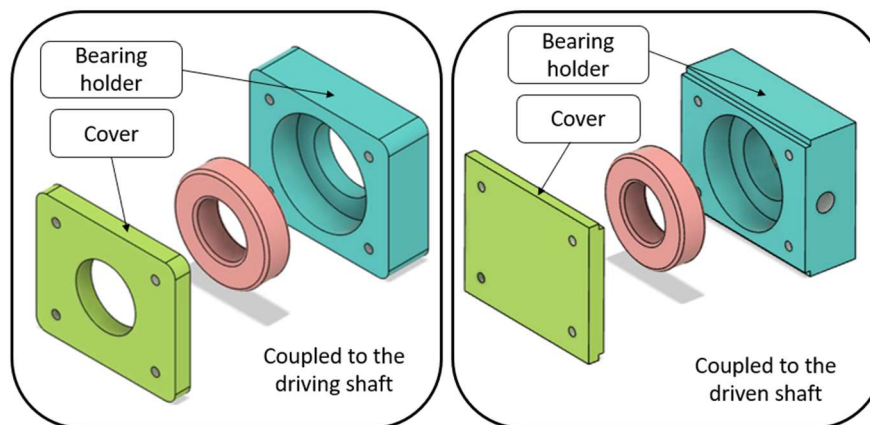


Figure 4.2 - Bearings couplings

The assembly that is connected to the driven shaft has a threaded lateral hole to which an endless bolt is attached. In addition, the upper and lower part of this assembly has small grooves to ensure linearity in the movement of the assembly and thus have a better adjustment of the conveyor.

The bearing reference is B6800ZZ, from the *MISUMI* catalogue. As for the other two components they were modelled according to the design needs, the constructive process of these elements is through the machining a solid aluminium block and a CNC that allows grinding in the 3 axes. As this was a structural element it was chosen the Al 7075 as the material of these products.

Table 4.4 - Bearing assembly components specifications

	Coupled to the driving shaft		Coupled to the driven shaft		Units
	Cover	Bearing Holder	Cover	Bearing Holder	
<b>Density</b>	2.80	2.80	2.80	2.80	$g/cm^3$
<b>Measurements</b>	28 x 24 x 3	28 x 24 x 8	28 x 24 x 3	28 x 24 x 8	mm
<b>Volume</b>	1641.58	3566.77	2075.17	5083.15	$mm^3$
<b>Mass</b>	4.60	9.99	5.81	14.23	g

The conveyors are going to be supported by horizontal guides. Along each guide there are different bars as shown in the Figure 4.3. The elements in orange are the ones that support the motor, and the driving shaft, in green the tensioners, which have been designed to be able to tension different belt sizes, while in pink are spacers that have the intended dimensions of the conveyor. Once again, all these components were connected together using a system of screws, washers and nuts.

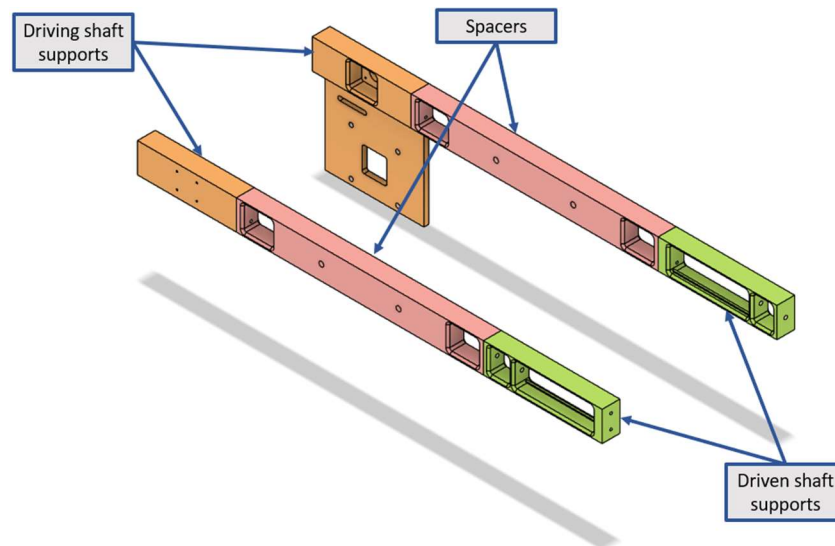


Figure 4.3 - Conveyor guide supporters

Focusing now on the orange elements, a distinction between them is going to be made, on where the block that holds just the shaft (left block on Figure 4.3), and the block that holds the shaft, the motor and the transmission system (right block on Figure 4.3). The block that only supports the shaft has a very simple configuration with a slot to couple the bearing system that makes the roller rotate freely. As this component was not a core structural element that compromises the proper functioning of the whole assembly it is going to be produced in the 5000 series aluminium alloy, Al 5083. Table 4.5 shows the driven shaft support specifications.

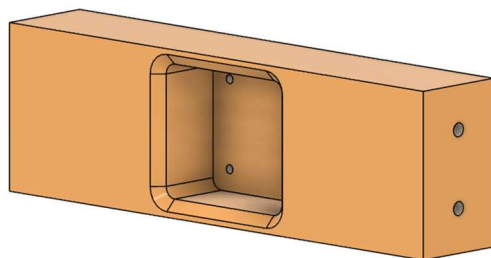


Figure 4.4 - Driving shaft support

Table 4.5 - Driven shaft support

	<b>Driven shaft Support</b>	
<b>Density (Al 5083)</b>	2.66	$g/cm^3$
<b>Measurements</b>	100 x 30 x 18	$mm$
<b>Volume</b>	44246.76	$mm^3$
<b>Mass</b>	117.70	$g$

The other component has a more complex structure due to the fact that is necessary to guarantee the correct positioning and parallelism between the pulleys that make up the transmission system of the energy from the motor to the shaft. For that reason, it was decided to design in one element all the details that meets the needs.

Initially it was intended to be separated into two parts, the upper part was supposed to be the same as the one presented before, while the lower part was a bent sheet that was going to support the motor and the transmission system. However, when producing a piece through a bending process, we cannot guarantee the dimensional quality required for the parallelism between the two components that was required for this type of system, and for this reason this alternative has been excluded.

Therefore, it was decided to create only a single piece where the lower part is where the motor is mounted. The ellipse-shaped slot is dedicated to give tension to the pulley that will make the transmission system, while the upper part is dedicated to the shaft support, which is the same as the one that is illustrated in Figure 4.4. Furthermore, the motor support holes are made according to the specifications of the chosen motor and has that circular central section slot for passing the motor shaft coupled with the pulley that makes part of the transmission system. As this is a structural part which requires maximum structural rigour and high mechanical strength, this product is going to be machined from a 7000 series aluminium alloy, being available from the supplier producing this type of machined component the Al 7075 aluminium series. Table 4.6 shows the motor support specifications.

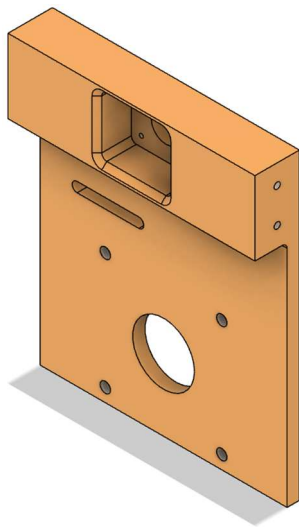


Figure 4.5 - Motor support

Table 4.6 - Motor support specifications

	<b>Motor Support</b>	
<b>Density (Al 7075)</b>	2.8	$g/cm^3$
<b>Measurements</b>	100 x 123 x 18	$mm$
<b>Volume</b>	87081.42	$mm^3$
<b>Mass</b>	243.83	$g$

Now looking at the spacers, as the name suggests these are only to make the connection between the motor support blocks and the tensioners. Its dimensions depend on the of the conveyor. This component is going to be produced in the Al 5083 aluminium series, since it is a piece that only makes the connection between two elements and does not need to be of a structurally rigid series neither does its dimensional quality need to have the rigour of other components, having opted for a 5000 series aluminium in order to minimise costs. Table 4.7 shows the spacer with 450 mm specifications.

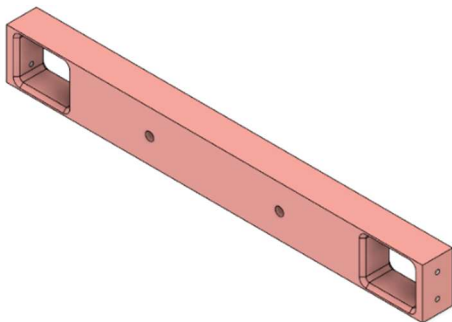


Figure 4.6 - Spacer

Table 4.7 – Spacer (450 mm) specifications

	<b>Spacers (450 mm)</b>	
<b>Density (Al 5083)</b>	2.66	$g/cm^3$
<b>Measurements</b>	450 x 30 x 18	$mm$
<b>Volume</b>	$2.155 \times 10^5$	$mm^3$
<b>Mass</b>	573.23	$g$



As this first conveyor has a linear distance between the roller's centre of 1000 mm and as the distance separating the motor support shaft and the tensioners is 900 mm these spacers have to fill this gap. As this is too big a difference to use only one piece, it was decided to make two equal components in order to make the structure more stable, thus reducing the effect of buckling to which this component would be subjected. This component has two central holes which is the solution founded to connect the conveyor to the structure as will be seen later.

Finally, for the tensioners, which are made to stretch the belt in order to create more friction between the belt and the roller, so the energy can be transmitted properly. By ensuring that we are putting the right tension on the conveyor it is guaranteed a better guidance of the belt, thus reducing problems that compromise the service life of the equipment. Additionally, these components serve to minimise defects derived from the manufacturing process of the belt, which generally have an associated error of about  $\pm 20$  mm of the desired length dimensions, according to the standard ISO 15147:2012 – “Light conveyor belts – Tolerances on widths and lengths of cut light conveyor belts” [26]. This standard defines the measurement tolerances of the widths and lengths to cut light conveyor belts, needing to be able to move the driven shaft in this spatial range with maximum accuracy [27].

Considering these restrictions, a component was then created to fulfil the requirements imposed on it, which can be seen in the Figure 4.7. In the larger open section is where the assembly with the coupled bearing goes, it is possible to see that in the lower part there is a notch that works as a guide in the process of tensioning the conveyor, which is very important since it is mandatory to guarantee that the bearing assembly only moves in a straight line along that axis. In addition, that small detail was also applied in the upper part of the support, and it was placed outside the symmetry axis of the part in order to avoid errors in the assembly process of the system.

Finally, as this is an extremely important component and considered a structural component of the assembly, it was produced from the 7000 series aluminium alloy, Al 7075. Furthermore, in the production of this part it is necessary to pay attention to the high dimensional accuracy in order to guarantee the linearity of the alignment guides, and this aluminium alloy presents an excellent machining quality making it a viable choice for production in this material. Table 4.8 shows the tensioner specifications.

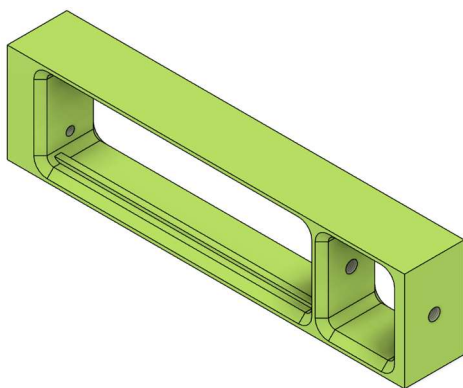


Figure 4.7 - Tensioner

Table 4.8 - Tensioner specifications

	<b>Tensioners</b>	
<b>Density (Al 7075)</b>	2.8	<i>g/cm<sup>3</sup></i>
<b>Measurements</b>	120 x 30 x 18	<i>mm</i>
<b>Volume</b>	20649.14	<i>mm<sup>3</sup></i>
<b>Mass</b>	57.82	<i>g</i>

The mechanism that stretches the belt is made by means of an endless bolt and three nuts, as shown in Figure 4.8. This mechanism has already been applied in many identical systems and has the advantages of high precision, easy usability and low production cost and these are reasons for the choice of this mechanism to tension the belt. As it is also possible to observe in the figure, it is noted that the mechanism that couples the bearings has the possibility to move linearly  $\pm 26$  mm, which ends up being more than necessary to comply with the standard requirements, being able to minimise potential errors due to the connections made between the blocks as it is not a joint with a high level of accuracy.

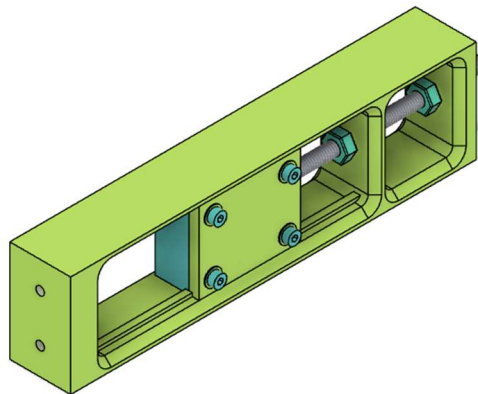


Figure 4.8 - Tensioner mechanism

Finally, all the systems that are part of the guides have an extra machining operation in order to remove the sharp edges of the components, thus promoting greater safety for the operator when handling these components. The milling diameter used for sharing the edges was of 2mm.

The way to assemble all these components is simple since the driving roller has a threaded holes already made, which allow to insert headless screws and thus make a more stable connection. In Figure 4.9, we can see the entire driving shaft assembly and ready to be placed on the frame. In addition, it is also possible to see how the power transmission system from the motor to the shaft is done.

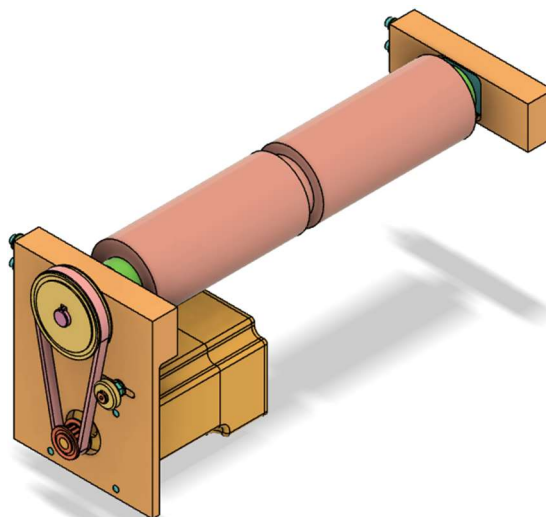


Figure 4.9 – Driving shaft assembly

Starting to introduce the transmission power system, it is also mandatory to stretch the transmission belt for the same reasons as of the conveyor belt. However, the approach was different where it is going to be used a specific screw available in the *MISUMI*'s catalogue. The screw has the following reference of the manufacturer BGPW4-7-L25-S5-F4 and has as main characteristics the fact of having a slot in its body that allows coupling a bearing. This set is going to be placed in the motor support bar that has an elliptical slot that allows it to move longitudinally until it has the desired tension.

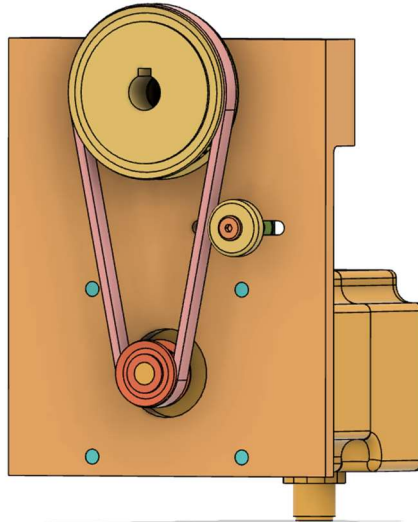


Figure 4.10 - Motor assembly

In Figure 4.11 you can see the whole mechanism of the driven shaft assembled. The roller is going to be coupled to the shafts by means of the system already incorporated by the supplier, with headless screws, as was the case with the driving roller. And then, these are going to be connected to the system that has the bearings coupled and subsequently to the structure, where in this case are the stretchers.

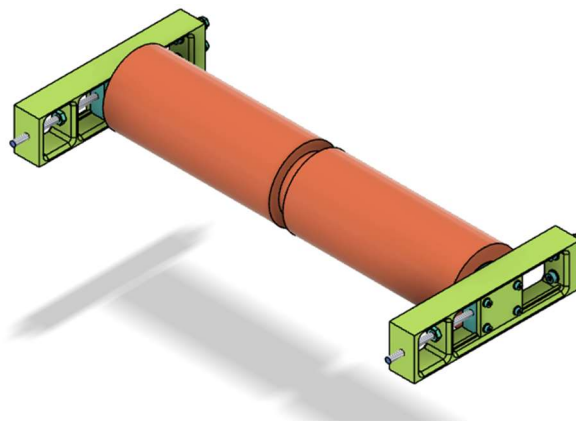


Figure 4.11 - Driven shaft assembly

Furthermore, as the distance between the two pulleys is 1000 mm, it was necessary to a supporting surface to support the belt and prevent it from bending with the weight of the load. For this, each of the spacers have a support plate screwed to it, in order to support the belt. This support plate is going to be bent in various directions and has a thickness of 2 mm as shown in Figure 4.12.

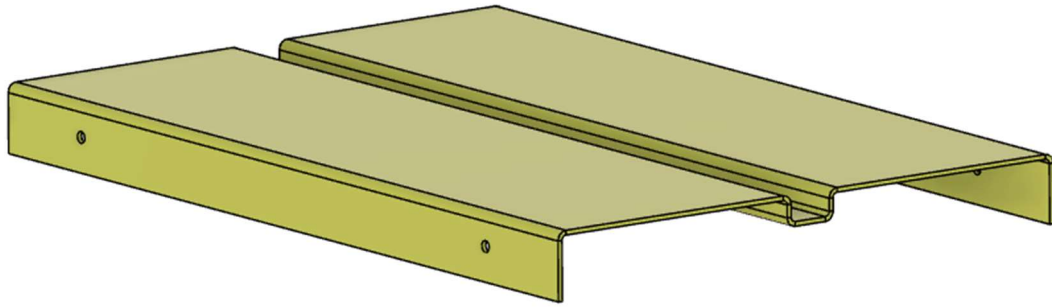


Figure 4.12 – Belt support

As can be seen by Figure 4.12 the support plate has specific folding in the middle due to the fact that the belt has the central guide. Furthermore, this component was made of aluminium alloy from the 5000 series, Al 5754, so as to have a low coefficient of friction and the belt can run more smoothly without the need to extra power from the motor.

#### - Motor and the transmission system

After having assembled the shafts that support the conveyor belt, it is time to focus on the power transmission mechanism. Due to space limitations, the motor rotation axis must be moved away from the shaft rotation axis, meaning that there must be a mechanism that transfers the power between the two shafts. The simplest way of transmitting the power from one axis to the other is through a mechanism of pulleys and belt. So, it was needed to look for transmission systems with toothed configurations that ensure a higher synchronism.

There are solutions for all types of systems, but for this case the choice was a toothed belt configuration that allows higher control of its movement, ensuring that there is no slipping when transmitting power. For the matter of maintaining the standard used by the company in other equipment developed internally, a \*GT, i.e., circular configuration of tooth was chosen (the \* means the pitch [in mm] value of the belt which for this case it was equals to 3 mm).

This type of configurations is mainly used in systems that require high torque transmission, something that fits in with the project in order to move the boxes easily. Furthermore, this belt has special characteristic as it has their teeth with a circular geometry which gives more control over the positioning pretended and allow a better control over the synchronism of the mechanism. Once again, the supplier which was recommended by the company was *MISUMI*.

It was analysed the possibility of having pulleys with the same diameter by having a 1:1 transmission ratio, or whether using pulley with different diameters, meaning introducing a ratio different than 1.

After carrying out some calculations, it was realised that with a 1:1 gear ratio the angular speed of the motor was lower, but the torque required was greater when compared with a ratio of 1:3 (the chosen ratio). Furthermore, the relation between the moments of inertia is also affected by this ratio, the sum of these moments is much lower when it is used a ratio of 1:3.

Therefore, the pulley that is connected to the motor must be smaller while the pulley connected to the shaft have to be larger. With this multiplication, it would demand a greater angular speed from the pulley connected to the motor, but the power would be greater at the opposite side (on the shaft). This conclusion is possible to obtain because as the linear speed and the tangential force are the same in both pulleys, by applying Equation 4.4, it is notable that the torque (T) is directly proportional to the radius (r), meaning that the larger the radius the larger the torque will be and consecutively the higher the power too.

$$T = F \times r \quad 4.4$$

The choice of the gear ratio was an iterative process until reaching the optimal solution, where it was known that the internal diameter of the pulley that is connected to the belt shaft has to be equals to 10 mm, while the internal diameter of the pulley that is connected to the motor shaft has to be equals to 6.35 mm (Note: this diameter comes from the choice of the motor to which a careful analysis was made to justify this choice) and the pitch has to be the same as the belt, in this case 3mm;

Having said that and following the advice of not exceeding a transmission ratio of 1 to 3 it was chosen the following pulleys which can be consulted at Table 4.9 as well as their specifications.

Table 4.9 - Big and small pulleys specifications

	<b>Big Pulley</b>	<b>Small Pulley</b>	
<b>MISUMI Serial Number</b>	GPA48GT3060-A-NK10	GPA16GT3060-A-H6.35	-
<b>Number of Teeth</b>	48	16	-
<b>Reference Diameter</b>	45	15	mm
<b>Internal Diameter</b>	10	6.35	mm
<b>Mass</b>	125	10.70	g

The choice of the pulley belt width was made considering the manufacturer's recommendation, being in this case of 6mm, for these types of applications. Regarding the size of the belt to be used, L [mm], a mathematical equation from Shigely's book [24] was applied to know which length to choose, Equation 4.3, where the values of  $\Theta_d$  and  $\Theta_D$  are calculated by Equations 4.5 and 4.6:

$$\Theta_d = \pi - 2 \operatorname{sen}^{-1} \left( \frac{D - d}{2C} \right) \quad 4.5$$

$$\Theta_D = \pi + 2 \operatorname{sen}^{-1} \left( \frac{D - d}{2C} \right) \quad 4.6$$

Where, L = belt length (mm); D = diameter of the biggest pulley (mm); d = diameter of the smaller pulley (mm); C = distance between the pulleys centres (mm);  $\Theta_x$  = contact angle on the pulley x

For this case, where the diameter of the larger pulley equals  $D = 45$  mm, the diameter of the smaller pulley equals to  $d = 15$  mm and the distance between pulleys equals  $C = 79$  mm, obtaining a total value for the belt length equal to  $L = 278.63$  mm, the measurement available on the store is with a circumference length of 282 mm, Table 4.10.

Table 4.10 - Transmission belt specifications

	<b>Timing Belt</b>
<b>MISUMI Serial Number</b>	GBN2823GT-60
<b>Belt Type</b>	3GT
<b>Belt Material</b>	Rubber
<b>Number of Teeth</b>	94

It was decided to choose a stepper motor, as this type of motor has several advantages, such as:

- Low cost;
- High reliability, requiring little or no maintenance due to being a mechanically simple mechanism;
- High torque at low speeds;
- Excellent speed and positioning control in open loop;
- Responds directly to digital control signals [28];

The choice of manufacturer for this type of components was simple, opting once again to choose one of the company suppliers, in this case *Nanotec* [29] which offers good construction quality for these types of motors, with IP65 protection (except in the shaft output), which is an International Protection against accidental contact with dust and water. In addition, they come equipped with pre-assembly cables that allow quick and error-free wiring and commissioning.

Within this category of motors, the supplier also offers several alternatives. The motor with the following reference [AS5918L4204] has been chosen due to the results obtained through the calculations presented in Section 5.2. The Table 4.11 is represented the specifications of the chosen motor.

Table 4.11 - First conveyor motor specifications [29]

	<b>AS5918L4204</b>	
<b>NEMA</b>	23	-
<b>Holding Torque</b>	187	<i>N.cm</i>
<b>Rotor Inertia</b>	480	<i>g.cm<sup>2</sup></i>
<b>Current per winding</b>	4.2	<i>A</i>
<b>Voltage</b>	24	<i>V</i>
<b>Weigh</b>	1.1	<i>kg</i>

In addition to the specifications presented in Table 4.11, it is important to note that this motor has a NEMA 23 frame size, and therefore the dimensions of this reference must be respected in the support of the motor. To verify the value of the moment of inertia ratios we must consider the value indicated for this type of motor, stepper, with the respective frame dimension, which in our case is equal to 10 [30].

In Figure 4.13 it is seen the set of all the components assembled, thus constituting the first conveyor belt.

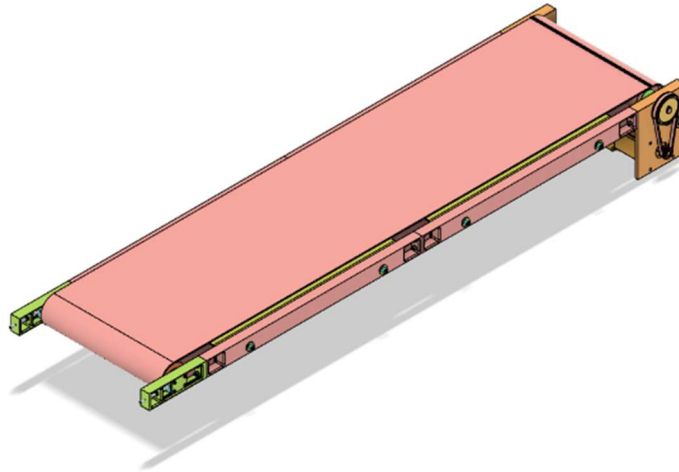


Figure 4.13 - First conveyor fully assembled

#### - Fixing the conveyor to the structure

Once the conveyor system is all assembled and with the parts correctly chosen and justified, it was necessary to fix this assembly to the structure. The simplest and most efficient way to solve this problem was using 3 mm thick, bent plates.

As these components are going to be obtained by bending aluminium alloy sheets and according to what was explained in the Section 4.1 these elements are going to be built with the AL 5754 aluminium alloy.

Therefore, a 3 mm thick aluminium sheet is fixed on each side of the conveyor. This first conveyor was not placed on the axis of symmetry of the structure, since for the second stage it is beneficial to ensure this condition. In this way, one of the sheets was bent with an inclination in order to increase the volume available for the introduction of the boxes, while the other sheet was bended in a 90° angle.

As it was presented, all the structure previously used by the company is made from technical profiles from the company *Item Portugal* [31], and there are already accessories produced by the supplier itself which are recommended for use to support external loads. Therefore, all the connections between the sheets and this structure were made using the accessories available from the supplier, so it was necessary to drill the sheets according to the specifications of these accessories.

In Figure 4.14 it is represented a drawing of the sheet planification that is going to be bent at different angles and is going to support the right side of the conveyor. On the upper part of the drawing, is represented the face that makes contact with the structure, while on the underside this is going to be connected to the conveyor spacers and is going to be done by means of a screwed connection.

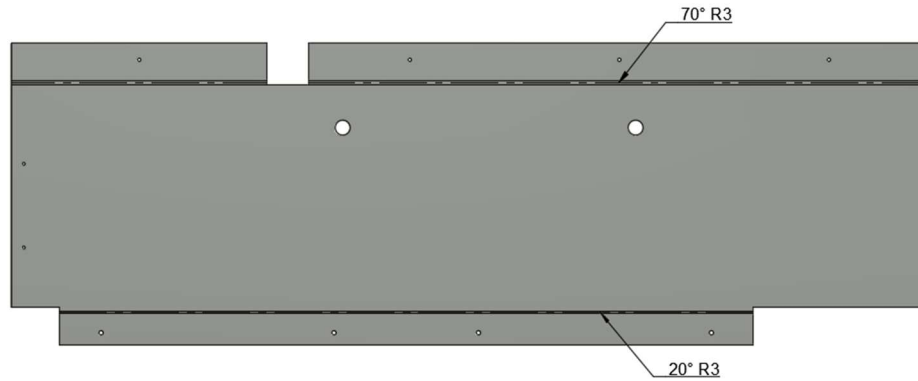


Figure 4.14 – Right side support sheet 2D planification

In Figure 4.15, it is illustrated the other support sheet that follows the same clamping principle to the structure. This support structure is going to be positioned on the left side of the conveyor.

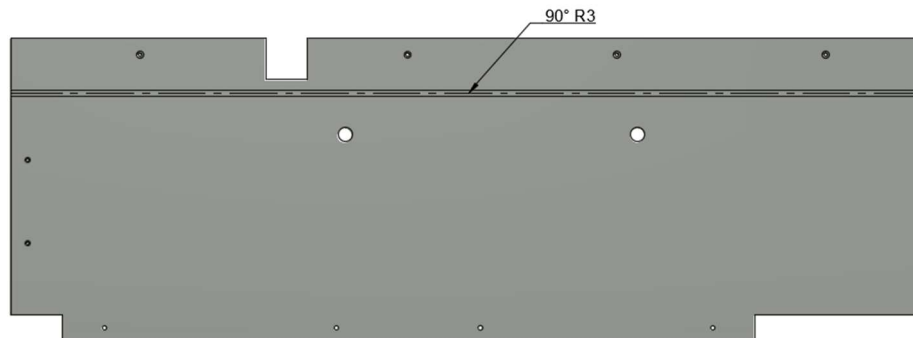


Figure 4.15 – Left side support sheet 2D planification

It was necessary at the beginning of the set to place a sheet par to ensure that the boxes do not move out of the system, our are dropped to the lower part of the mechanism. A 2mm thick aluminium plate, Figure 4.16, was also specified to be screwed to the support plates, thus ensuring that it was created a closed system where the boxes do not move into forward stages.



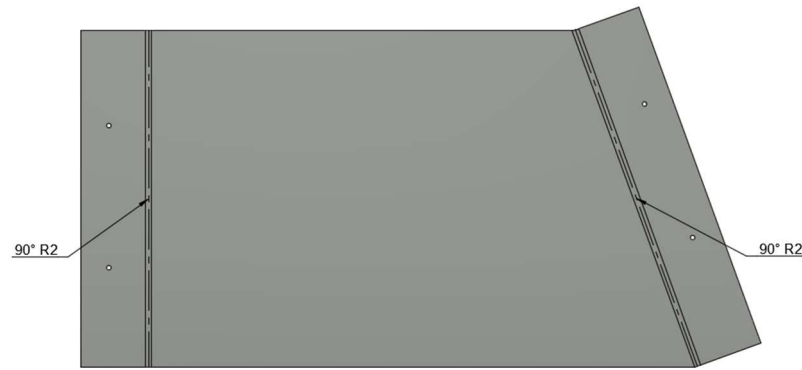


Figure 4.16 – Cover 2D planification

In Table 4.12 it is represented the masses of each component following the properties provided by the Al 5754 data sheet in the *PolyLanema* catalogue.

Table 4.12 – Al 5754 and first conveyor supports specifications

	<b>Left Support Side</b>	<b>Right Support Side</b>	<b>Cover</b>	<b>Units</b>
<b>Density</b>	2.67	2.67	2.67	$g/cm^3$
<b>Volume</b>	$1.157 \times 10^6$	$1.138 \times 10^6$	$2.093 \times 10^5$	$mm^3$
<b>Mass</b>	3.09	3.04	0.56	$kg$

#### - Barriers

Being the barriers one of the main components of this first stage it was necessary to make a more in-depth study in this section. After completing the testing phase, it was realised that two barriers of equal mass, separated by 350 mm were going to be used. As previously presented, each of these barriers have a mass of approximately 430 g.

As this mass worked perfectly for what was needed it is going to be used the same weight in the barriers for the final project. Since it was used the AL 5754 aluminium alloy, which had previously been chosen for other components that are produced by the same manufacturing process and knowing the available area inside the conveyor, it possible to define the required thickness, Equation 4.7. In Table 4.13, it is represented the surface area, which was taken through the FUSION 360 features, as well as the density and thickness required.

Table 4.13 – Barrier measurements

		Barrier	
Density	$\rho$	2.67	$g/cm^3$
Area	$A$	64571.44	$mm^2$
Mass	$m$	430	$g$
Thickness	$e$	2.50	$mm$

$$e = \frac{m}{A \times \rho} = \frac{430}{64571.44 \times 2.67 \times 10^{-3}} = 2.50 \text{ mm} \quad 4.7$$

Figure 4.17 shows a 2D plan of the configuration of the sheet, the holes that need to be made and where the bending will be done, for the 2.5 mm thickness aluminium sheet, which is going to be produced through a laser cutting process.

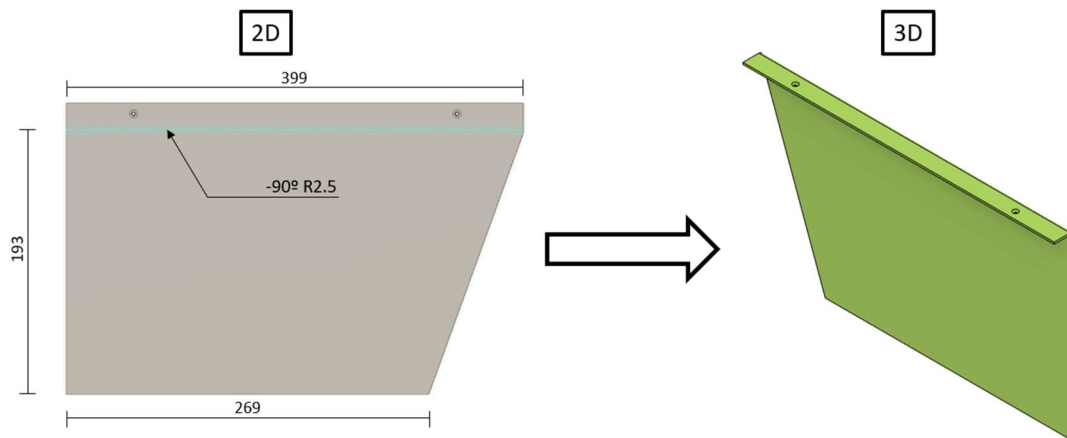


Figure 4.17 - Barrier folding principle

As the barrier has to rotate freely around an axis its assembly process was simple. The barrier is fixed with screws to a round section aluminium profile. This aluminium profile has 12 mm of diameter and is threaded at its ends so that a set of nuts and washers could be assembled, preventing it from moving longitudinally (YY axis in Figure 3.1).

This shaft passes over the plates that make up the attachment of the assembly to the main structure. In order to minimise the friction generated by this contact, as well as to increase the working life of the aluminium profile, a sleeve bearing was chosen to help minimise this damage. *IGUS* [32], a company specialised in the production of this type of components has a vast catalogue of solutions that can be used in various situations. After a detailed analysis, it was decided to choose a sleeve bearing with flange, with the following reference number: XFM-1416-17.

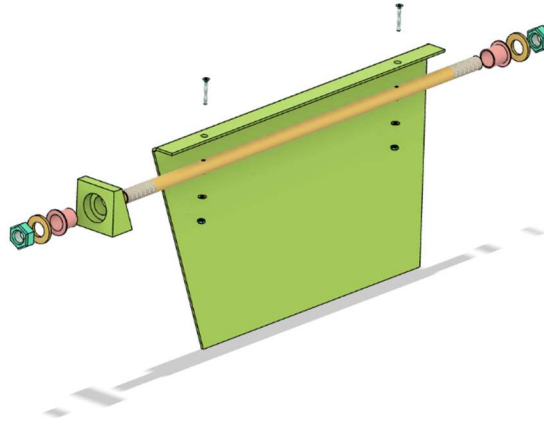


Figure 4.18 – Barrier exploded assembly view

One side of the carrier plate has an inclination that makes it not possible to mount the barrier directly on the conveyor due to that limitation. For this purpose, it was necessary to develop a small spacer in order to assist this assembly process, Figure 4.19. Being only a part with little importance in the final result it was printed in PLA, provided that when printing this component, the filament is reinforced in the most critical areas, particularly in the part in contact with the axis of rotation of the barrier. In Figure 4.20 shows all the assembly mounted on the structure of the first conveyor.

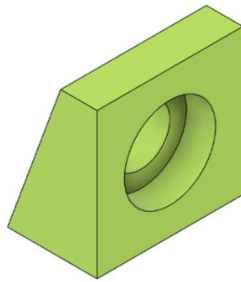


Figure 4.19 – Barrier spacer

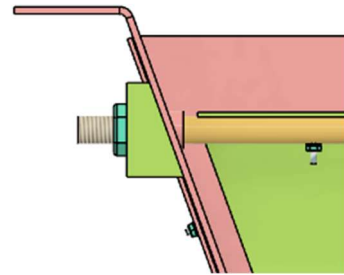


Figure 4.20 – Mounting the barrier spacing

In Figure 4.21, it is represented the whole assembly of the first conveyor belt assembled, ready to be introduced into the main structure.

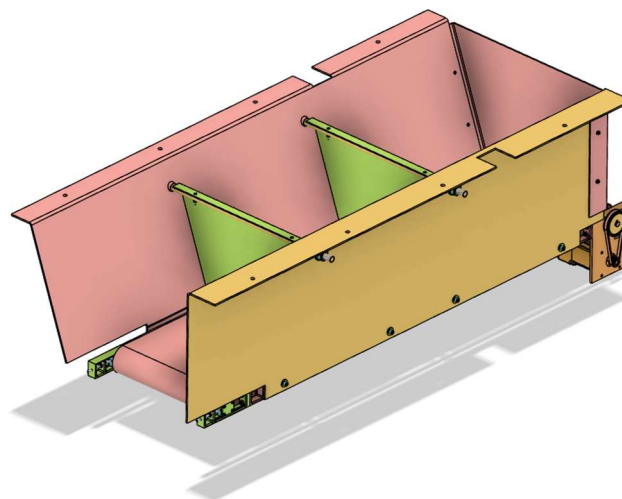


Figure 4.21 – First conveyor ready to be mounted on the principal structure

#### 4.2.2. *Second and third conveyors*

The second level of the box dividing system consists of two identical conveyor systems which are rotated through  $180^\circ$  in relation to each other. Therefore, the entire process of justifying the selection of materials and components for one conveyor applies to the other. In addition to what was mentioned in the first conveyor, the process of assembly and modelling of the whole system is the same as the previous one, in order to make all the logistics of the process simpler. Therefore, the dimensions of this second belt are shown in Figure 4.22.

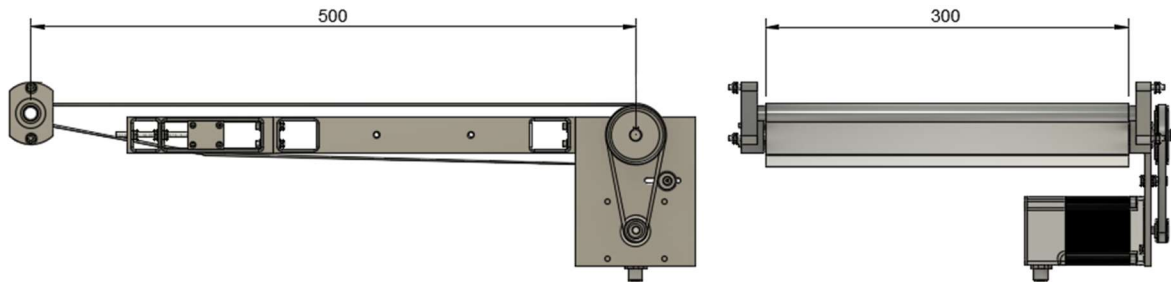


Figure 4.22 – Second and third conveyors dimensions

#### - **Belt selection**

Regarding the choice of the belt, the specific characteristics were the opposite to those that had been chosen for the first conveyor. In this context, it was required a belt with a slightly lower surface roughness in order to allow the boxes to be handled by the chicanes without having to make a great effort. Therefore, in the *MegaDyne* [23] catalogue, it was founded a solution that meets these requirements, which is a P9/A belt model, which was the same one that was used in the chicane test phase and to which we obtained great results, so choosing it was even simpler. Besides, on the technical sheet of this product is specific to be used in knife edge conveyor configurations which is another positive aspect for its selection. In Table 4.14 are represented the belt specifications.

As this belt works following the concept of a knife edge conveyor, it cannot have a central guide, otherwise the minimum diameter that is needed to have put on the rollers would not compensate the implementation of this concept.

Table 4.14 - P9/A specifications [23]

<b>Belt Brand</b>	<b>MegaDyne</b>	<b>Model</b>	<b>P9/A</b>
<b>Tensile Force (k=1%)</b>	8 N/m	<b>Minimum Pulley Diameter</b>	6 mm
<b>Length</b>	1097 mm	<b>Width</b>	300 mm
<b>Mass per square meter</b>	1.32 kg/m <sup>2</sup>	<b>Area</b>	0.33 m <sup>2</sup>
<b>Mass</b>	0.43 kg	<b>Thickness</b>	1.27 mm
<b>Coef. Friction top side</b>	-	<b>Coef. Friction downside</b>	0.25

Calculating the internal area and length of this belt was more complicated due to its knife edge configuration. Using the *FUSION 360* functionalities, the following results for these components were obtained.

$$\begin{aligned}
 A_{belt} &= 0.33 \text{ m}^2 & 4.8 \\
 m_{belt} &= A_{belt} \times \rho_{belt} = 0.33 \times 1.32 = 0.43 \text{ kg} & 4.9 \\
 l &= 1096.9 \text{ mm} & 4.10
 \end{aligned}$$

#### - Rollers and shaft selection

The construction model of this conveyor was slightly different, due to the implementation of the knife edge concept, which forces to create a new axis of rotation, with a smaller roller. In Figure 4.23 it is represented an overview of how this new conveyor system looks like. The driving pulley was the pulley through which the mechanical energy coming from the motor enters the conveyor, the knife edge was the pulley with the small diameter so when it assembles the two conveyors, the gap between them is minimal and the driven pulley works as the tensioner which serves only to stretch the belt so that the linear movement of the belt is optimal.

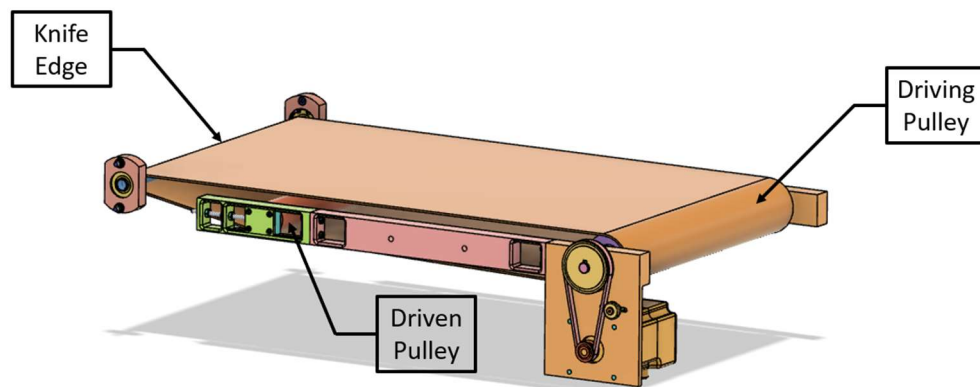


Figure 4.23 - Knife edge conveyor example

Once again, the choice of components was made from the catalogue of *MISUMI*. Maintaining the principle that the driving pulley roller had to have a top layer in urethane in order to have a greater friction between the inner surface of the belt and the roller, the choice of this component was the RWBMG48-N10-280-X10-Y8-Z6. It should be noted that for this conveyor it is not necessary to have that central slot in the roll, as the belt does not have an internal guide. However, the supplier only produces rolls in these dimensions with the urethane top cover with this feature incorporated.

The technical data sheet did not reveal the total mass of the roller, so it was needed to calculate the volume occupied by the urethane layer (10 mm thick) and the volume occupied by the aluminium and obtain an estimate of the total weight of the assembly through the densities of each of the materials, Table 4.15.

Table 4.15 - Driving roller specifications

	<b>RWBMG48-N10-280-X10-Y8-Z6</b>	
<b>Outer Diameter</b>	48	<i>mm</i>
<b>Internal Diameter</b>	10	<i>mm</i>
<b>Length</b>	280	<i>mm</i>
<b>Density of Urethane</b>	1.06	<i>g/cm<sup>3</sup></i>
<b>Density of Aluminium</b>	2.7	<i>g/cm<sup>3</sup></i>
<b>Volume of Urethane</b>	334.32	<i>cm<sup>3</sup></i>
<b>Volume of Aluminium</b>	150.42	<i>cm<sup>3</sup></i>
<b>Total Mass</b>	0.760	<i>kg</i>

As it was used a knife edge configuration, the rollers have to have different dimensions in order to be able to stretch the belt in the most appropriate way. For that reason, the driven roller has a smaller diameter otherwise it comes in contact with both sides of the inner side of the belt, something to be avoided as it interferes with the movement of the belt. Therefore, the chosen roller was made entirely from aluminium with the following reference according to the *MISUMI* catalogue: ROFAWC30-10-L300, since when the rolls have the topcoat in urethane, they are more expensive.

Table 4.16 - Driven roller specifications

	<b>ROFAWC30-10-L300</b>	
<b>Outer Diameter</b>	30	<i>mm</i>
<b>Internal Diameter</b>	10	<i>mm</i>
<b>Length</b>	300	<i>Mm</i>
<b>Density of Aluminium</b>	2.7	<i>g/cm<sup>3</sup></i>
<b>Volume of Aluminium</b>	188.49	<i>cm<sup>3</sup></i>
<b>Total Mass</b>	0.509	<i>kg</i>

The shafts that connect the rollers to the bearing and the pulley, in the case of the driven shaft, are exactly the same as the ones previously presented, since there was no need to choose other shafts.

Focusing now on the new element of this conveyor, the knife edge shaft, these were produced through an aluminium profile of circular section with a diameter of 12 mm. This configuration was chosen because it is a simple and viable solution to obtain the results required.

As it was needed to keep these elements rotating freely, it was necessary to come up with a mechanism that had bearings attached. Since this is a knife edge system, it was necessary to find a bearing mechanism that was as small as possible and had an internal diameter of 12 mm.

In the *MISUMI* catalogues was founded a solution to these problems, where a system comes with everything needed and ready to be assembled, being only necessary to screw this set to the structure. Besides, its characteristic geometry makes the space needed to assemble it very optimized. In Table 4.17, it is represented all the specifications of this assemble and it is possible to notice that the bearing which is used in this coupled is the same as the one previously chosen for the first conveyor, changing only the internal diameter, Figure 4.24.



Figure 4.24 - MISUMI coupled bearing [25]

Table 4.17 - *MISUMI* coupled bearing specifications

	<b>BACA6001DD</b>	
<b>Bearing Part Number</b>	6001	-
<b>Inter Diameter</b>	12	mm
<b>External Diameter</b>	52	mm
<b>Thickness</b>	13	mm

#### - Conveyor structure and components assembly

As it can be seen from Figure 4.25, the modelling of some components of this conveyor has many similarities with the modelling of the components of the previous conveyor. Items such as the tensioners and the two blocks that support the driving shaft are exactly the same as the components used to make the previous conveyor.

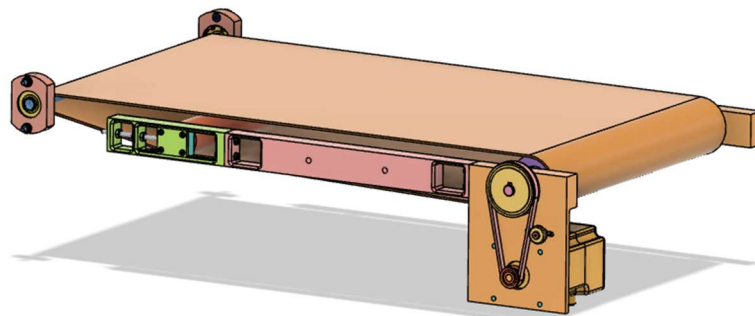


Figure 4.25 - Second conveyor assemble

Its initial modelling process was developed so these components would always be the same, regardless of the system intended to be used, changing only the size of the spacers depending on the distance required, which for this case was smaller, 250 mm. The specifications of this product are represented in Table 4.18.

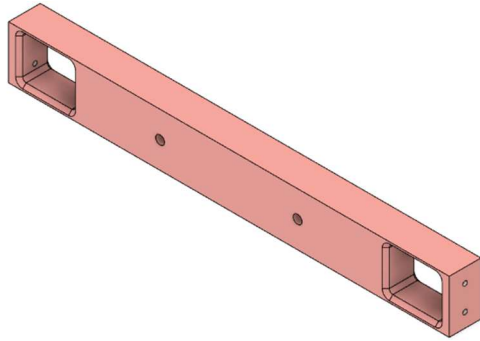


Figure 4.26 - Spacer (250 mm)

Table 4.18 - Spacer (250 mm) specifications

	<b>Spacers (250 mm)</b>	
<b>Density (Al 5083)</b>	2.66	$g/cm^3$
<b>Measurement</b>	250 x 18 x 30	$mm$
<b>Volume</b>	$1.075 \times 10^5$	$mm^3$
<b>Mass</b>	285.95	$g$

The chosen motor has the same dimensions (NEMA 23), but with different specifications, as we will see in the topic regarding this component. Anyway, the fact that the motor has the same dimensions in all the conveyors, means that even the modelling of the block that supports it was the same reducing costs in the production of these components.

#### - Motor and transmission system

After carrying out the mathematical calculations, which are presented in Topic 5.3, to size and select the motor that best suits the variables imposed by the system, it was selected the AS5918L2804 motor from *Nanotec*.

Table 4.19 - Second and third conveyor motor specifications [29]

	<b>AS5918L2804</b>	
<b>NEMA</b>	23	-
<b>Holding Torque</b>	99	$N.cm$
<b>Rotor Inertia</b>	230	$g.cm^2$
<b>Current per winding</b>	4.2	$A$
<b>Voltage</b>	24	$V$
<b>Weigh</b>	0.8	$kg$

Despite having the same frame size (NEMA 23) its specifications are slightly different when compared to the motor chosen for the first conveyor. In addition, the transmission system was kept the same since it was necessary to keep the same ratio in the diameter of the pulleys (1:3). In Table 4.20 are presented both pulleys specifications.



Table 4.20 - Transmission system pulleys

	Big Pulley	Small Pulley	
<b>MISUMI Serial Number</b>	GPA48GT3060-A-NK10	GPA16GT3060-A-H6.35	-
<b>Number of Teeth</b>	48	16	-
<b>Reference Diameter</b>	45	15	mm
<b>Internal Diameter</b>	10	6.35	mm
<b>Mass</b>	125	10.7	g

Once the size of the pulleys has been kept the same, it was decided to keep them with the same distance between axles so as to be able to choose the same transmission belt, Table 4.21.

Table 4.21 - Transmission belt

	Timing Belt
<b>MISUMI Serial Number</b>	GBN2823GT-60
<b>Belt Type</b>	3GT
<b>Belt Material</b>	Rubber
<b>Number of Teeth</b>	94

#### - Fixing the conveyor to the structure

The fixing method used to support the conveyor to the structure was once again identical to the method performed for the first one. In this phase, two identical conveyors were used following the Knife Edge concept, as previously presented. In order to guarantee the correct positioning of these two assemblies, rotated 180° in relation to each other, it was decided to fix them to a single aluminium sheet, thus minimising constructive errors of the project and ensuring a better alignment of both conveyors.

The sheets that support the conveyors have the same dimensions, with only changing the holes where the chicanes go. Figure 4.27 shows the 2D planification of the sheet that supports the conveyor on the left side as well as its dimensions and the axis for bending the sheet.

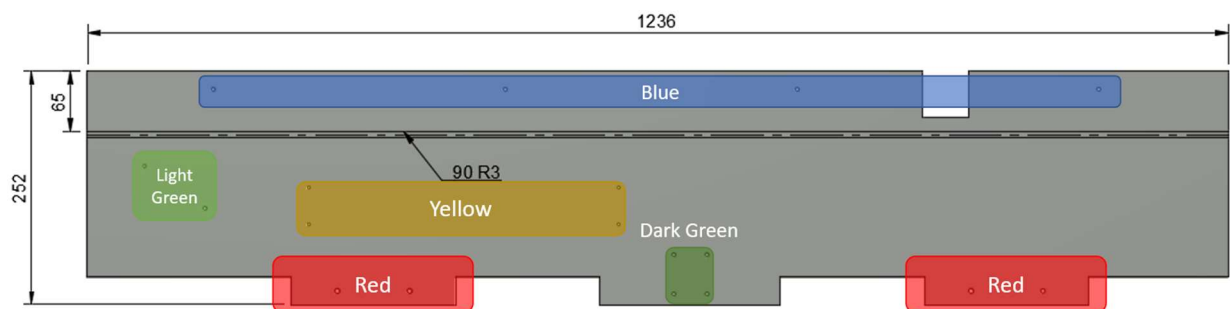


Figure 4.27 – 2D planification of the left support sheet for the second and third conveyor

Furthermore, in Figure 4.27, there is a distinction between some zones with different colours, meaning where each component was screwed.

- Blue – Drilling to fix the conveyor into the main structure;
- Light Green – Drilling to fix the ramp to the second conveyor system
- Yellow – Drilling to fix one chicane
- Red – Drilling to fix the spacers that support the conveyor assembly
- Dark Green – Drilling to fix the two knife edges rollers

In Table 4.22 are shown the characteristics of each of the support sheets, knowing that the material used is 5000 series aluminium, Al 5754, as already used in the supporting plates for the previous conveyor.

Table 4.22 - Second conveyor support specifications

	Left Side Support	Right Side Support	Units
<b>Density</b>	2.67	2.67	$g/cm^3$
<b>Volume</b>	$8.66 \times 10^5$	$9.398 \times 10^5$	$mm^3$
<b>Mass</b>	2.31	2.51	$kg$

#### - Chicanes

This second part of the system was characterised by the two chicanes. As this was the main component of this stage, it was necessary to pay attention to the way of manufacturing it, as well as some notes that were taken during the testing phase.

Therefore, it was decided to start out by finding a slope that was adequate for the straight line that would orientate the boxes. If the slope is too steep, this would create many constraints in the movement of the boxes. If the slope was not too steep it would create a dead zone and make the boxes not touch any of the chicanes, something to be avoided. Combining with the results obtained in the experimental phase it was concluded that the ideal slope would be a  $30^\circ$  angle with the horizontal. The other measurements started from this starting point. Figure 4.28 shows the final dimensions adopted for this component and proved to be the most suitable measures according to the experiences made in the test phase.

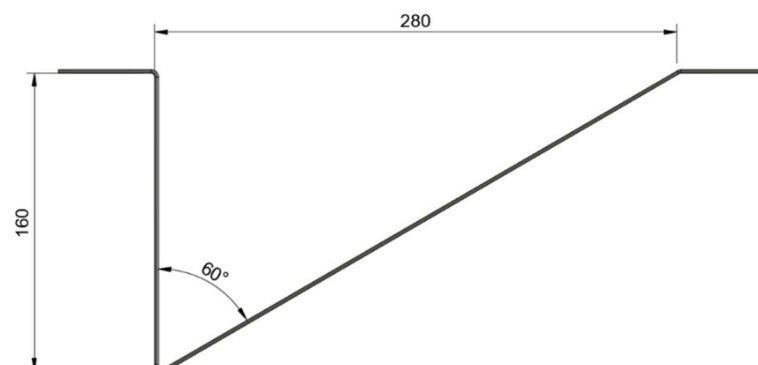


Figure 4.28 - Chicane dimensions

Furthermore, it is important to note that the dimension perpendicular to the drawing of Figure 4.28 has been taken into account on the study of the development of this product. This was important as it was necessary to ensure that the boxes lined up efficiently. In addition, the contact area between the surface of the box and the wall should be small so that the influence of friction is minimal but having always a minimum height, so that the larger boxes do not fall inside the chicane and get stuck there. Therefore, it was decided to choose this measure as being equal to 80 mm (dimension perpendicular to Figure 4.28).

With regard to the construction material, it was decided to select the same material as the one used for the barriers, as this would ensure greater standardisation in the manufacturing process, since only one supplier was needed to manufacture all these components. In addition, by using this aluminium series it was provided a reduction in the weight of this product due to their low density.

An aluminium plate with 2mm of thickness is used and is obtained through a bending process where the three folds were made according to the indications presented in Figure 4.29. Finally, the chicanes are screwed to the supporting structure, thus being a simple and effective connection.

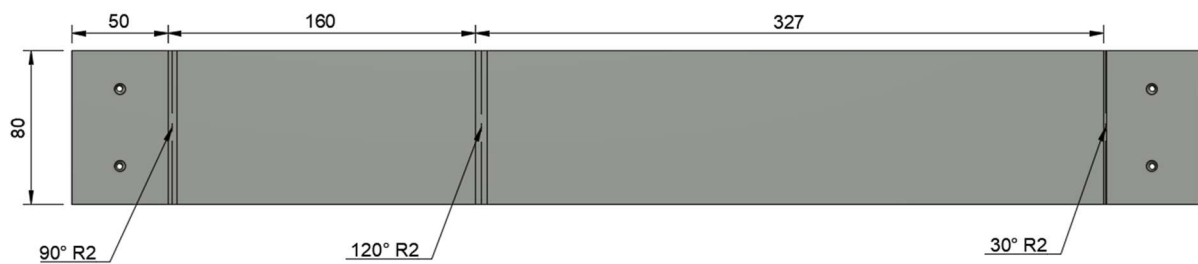


Figure 4.29 - 2D planification of the chicane

#### - Ramp

In order to make the fall of the boxes from the first to the second conveyor smoother, a ramp was designed and is obtained through bending a sheet of aluminium, AL 5754, with 2 mm of thickness and bent angle of 90° in points 1 and 2, shown in Figure 4.30 and Table 4.23.

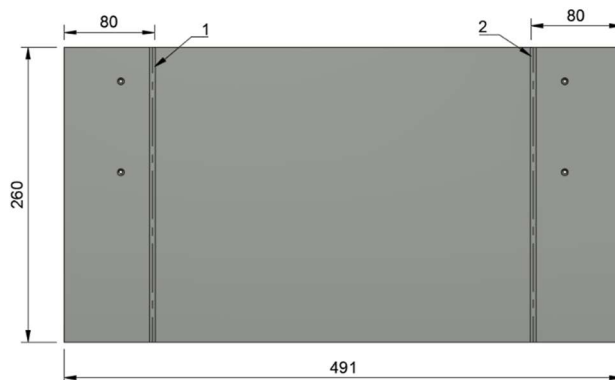


Figure 4.30 - Ramp 2D planification

Table 4.23 – Ramp specifications

	Ramp	Units
Young's Modulus	70	GPa
Poisson's Ratio	0.33	-
Density	2.67	g/cm <sup>3</sup>
Volume	2.307 x 10 <sup>5</sup>	mm <sup>3</sup>
Mass	0.62	kg

In Figure 4.31, it is represented the conveyor assembled and ready to be placed in the main structure.

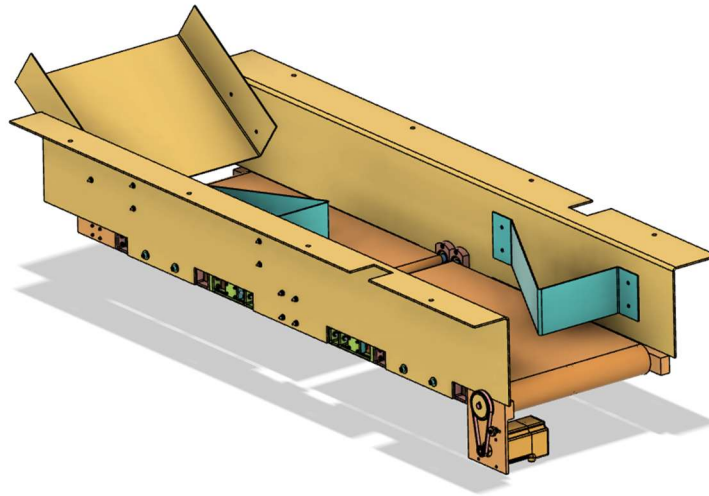


Figure 4.31 - Second and third conveyor full assembly

### 4.3 Verification of components resistance

After knowing how the configuration and assembly process of the whole structure, it was necessary to make some calculations that enable to check some components behaviour under certain forces. Therefore, it was used the tools available in the *ABAQUS* software to study the behaviour of the elements that were modelled for this work.

To do this analysis it was necessary to extract the STEP models of each of the elements to be analysed and then create a program that would allow to study their behaviour. For all the elements it was performed a static analysis, where it was used a step time of 1 second with increments of 0.1 seconds. The mesh was developed by the software using a free structure mesh due to the geometric complexities of the parts. In turn, the chosen mesh belongs to the 3D stress family being referenced as C3D10. As many parts are being used on both conveyors, the loading conditions to which they were subjected were considered as being the worst-case scenario, which in most cases refers to the boundary conditions applied to the first conveyor, as it is subjected to greater efforts.

After running the programs for each of the pieces, the software compiles the results and export the values of the Von Mises stress applied to each point of the mesh at the final instant of the simulation, as well as the deformation associated to each element.

The verification and validation process to prove that the element can withstand the efforts to which it is subjected was done by means of the ratio shown by the following equation. Where the yield stress of the material divided by the adopted safety factor, in this case 1.75, must be greater than the maximum value obtained for the Von Mises stress in the simulation.

$$\sigma^{V.M.} \leq \frac{\sigma^{Max}}{S.F.} \quad 4.11$$

Where,  $\sigma^{V.M.}$  - maximum stress according to Von Mises' criterion obtained by simulation;  $\sigma^{Max}$  – Yield Strength (0.2);  $S.F.$  – safety factor (1.75)

It should be noted that the units with which the results were extracted are in accordance with the international system measurements, being Pascal [Pa] for the case of Von Mises Stress and meter [m] for the deformation.

## - Tensioners

Starting the analysis with the tensioners, it is known that this component is bolted, through the two lateral holes, to the structure, and so this section was considered embedded. Subsequently, the weight of the piece itself and the tension coming from the driven roller were considered as the efforts to which this element was subjected. The results obtained are shown in Figure 4.32 and Figure 4.33.

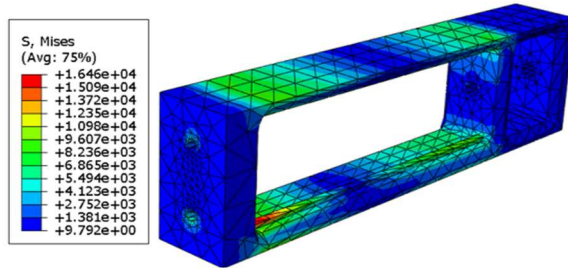


Figure 4.32 - Distribution of Von Mises stresses in the tensioner

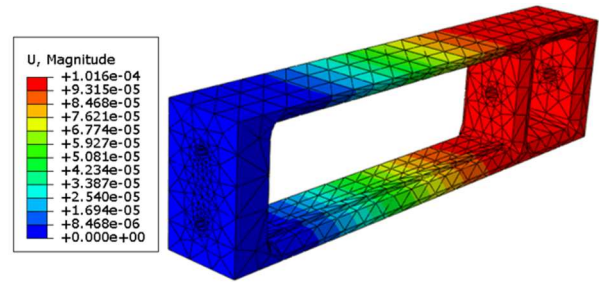


Figure 4.33 - Deformation of the tensioner

By making a visual analysis of the results obtained for the stress variation and the displacement along the piece for the final instant of the simulation, it is notice that the values where the stress concentration is maximum are in the places where there is less material thickness, something expected. Furthermore, it is possible to see that the displacement increases as we move away from the fixed section. To be able to correctly dimension the piece, it was extracted the results obtained for both stress and displacement for all the nodes of the mesh at the end of the simulation and the following maximum values were obtained, Table 4.24.

Table 4.24 - Maximum values obtained for the tensioner

	Tensioner	
Maximum Von Mises stress	16.26	MPa
Maximum displacement	0.10	mm

Applying the Equation 4.11 that allows to conclude if the piece can withstand the efforts, it can understand that the obtained value is within the acceptable parameters for the dimensioning of the piece, withstanding the efforts that it is subject to, Equation 4.12. With regard to the displacement and knowing that this is a part of great structural importance for the proper functioning of the conveyors, we see that the maximum displacement has a residual value, which is also very satisfactory.

$$16.26 \leq \frac{470}{1.75} ; 16.26 \leq 268.57 \quad 4.12$$

#### - Driving shaft support

Focusing on the driving shaft support it was applied the following boundary conditions: fixing the part in the two threaded side holes. As with the tensioners, the forces considered were the weight of the piece itself and the forces coming from the motion of the driving roller, which in this case were higher on the first conveyor, and for that reason were considered these forces. Figure 4.34 and Figure 4.35 shows the results obtained from the *ABAQUS* simulation.

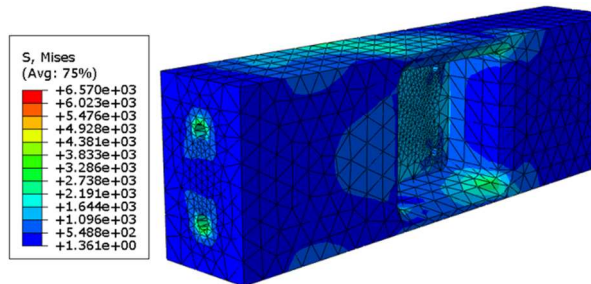


Figure 4.34 - Distribution of Von Mises stresses in the driving shaft support

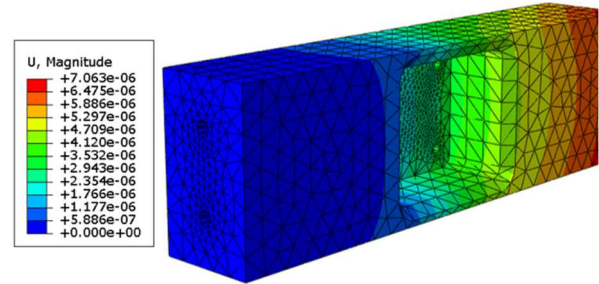


Figure 4.35 - Deformation in the driving shaft support

As with the tensioners the results followed the same trend, also verifying the mandatory conditions for the validation of the component, Table 4.25.

Table 4.25 - Maximum values obtained for the driving shaft support

	Driving shaft support	
Maximum Von Mises stress	7.15	MPa
Maximum displacement	0.0071	mm

$$7.15 \leq \frac{115}{1.75} ; 7.15 \leq 65.71 \quad 4.13$$

### - Motor and driving shaft support

Regarding the piece that supports the motor and the driving shaft the boundary conditions applied are exactly the same as the ones applied before adding the weight of the motor. The results obtained followed again the trend of the previous values, Figure 4.36, Figure 4.37 and Table 4.26.

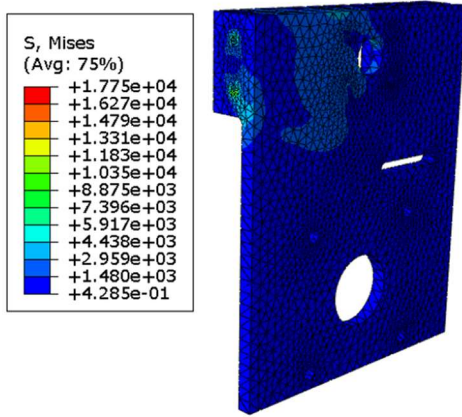


Figure 4.36 - Distribution of Von Mises stresses in the motor and driving shaft support

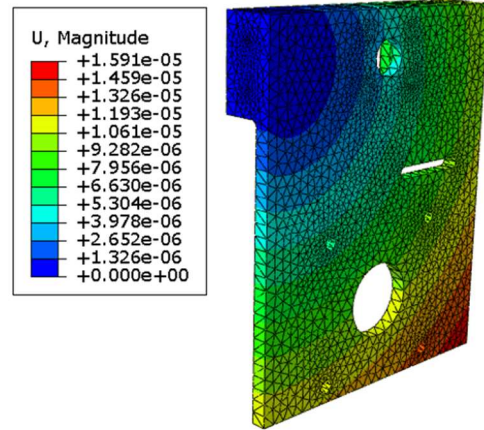


Figure 4.37 - Deformation in the motor and driving shaft support

Table 4.26 - Maximum values obtained for the motor and driving shaft support

	<b>Motor and driving shaft support</b>	
<b>Maximum Von Mises stress</b>	18.39	<i>MPa</i>
<b>Maximum displacement</b>	0.016	<i>mm</i>

It can be seen that the point furthest away from the attachment point of the component is the one which suffers the greatest deformation. The areas where the component has less thickness are the critical sections of the piece, since it is where a higher stress concentration value is, but this value does not present great risks to the integrity of the component, as it can be seen by the value obtained using the following equation.

$$18.39 \leq \frac{470}{1.75} ; 18.39 \leq 268.57 \quad 4.14$$



### - Right support of the first conveyor

With regards to the plate sheets that support the conveyor belts, it was applied the same principle analysis to all of them. The component was considered fixed to the structure in the respective area presented above and in this section the component was prevented from moving in any direction. Furthermore, the respective concentrated loads were applied to each one of the components depending on the assemblies attached to them.

In Figure 4.38 and Figure 4.39, it is possible to see the results obtained from the simulation of the sheet that supports the first conveyor on the right side. As it was bent at various angles, the stress concentration varies along the component section, with a maximum near the area where it was fixed to the conveyor (lower part). Regarding the deformation, its variation follows the same expected path, being higher as it moves away from the attachment section. Table 4.27 shows the maximum values for the Von Mises stress and displacement.

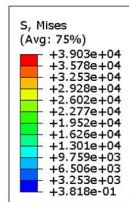


Figure 4.38 - Distribution of Von Mises stresses in the right support of the first conveyor

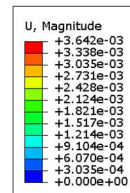


Figure 4.39 - Deformation in the right support of the first conveyor

Table 4.27 - Maximum values obtained for the right support of the first conveyor

	Right support of the first conveyor	
<b>Maximum Von Mises stress</b>	34.29	<i>MPa</i>
<b>Maximum displacement</b>	3.62	<i>mm</i>

Nevertheless, the condition that guarantees the structural rigidity of the piece is verified, Equation 4.15.

$$34.29 \leq \frac{80}{1.75} ; 34.29 \leq 45.71 \quad 4.15$$

Regarding the other plates that were bent according to a 90° angle, the results all follow the same trend in these components, with the value of stress concentration being maximum in the section where the bending operation was carried out, while the deformation is greater in the sections that are furthest away from the fixed section.

In all cases the condition that guarantees the structural functioning of the component was verified and the results obtained for each component are shown in from Figure 4.40 to Figure 4.45, from Table 4.28 to Table 4.30 and from Equation 4.16 to Equation 4.18.



- **Left support of the first conveyor**

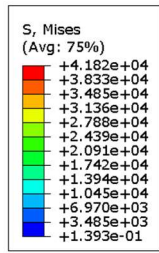


Figure 4.40 - Distribution of Von Mises stresses in the left support of the first conveyor

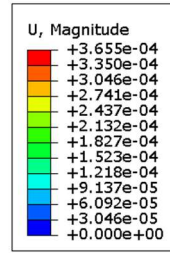


Figure 4.41 Deformation in the left support of the first conveyor

Table 4.28 - Maximum values obtained for the left support of the first conveyor

	Left support of the first conveyor	
Maximum Von Mises stress	31.64	MPa
Maximum displacement	0.37	mm

$$31.64 \leq \frac{80}{1.75} ; 31.64 \leq 45.71 \quad 4.16$$

- **Right support of the second conveyor**

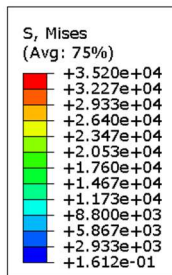


Figure 4.42 - Distribution of Von Mises stresses in the right support of the second conveyor

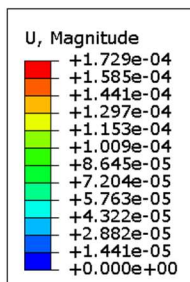


Figure 4.43 - Deformation in the right support of the second conveyor

Table 4.29 - Maximum values obtained for the right support of the second conveyor

	Right support of the second conveyor	
Maximum Von Mises stress	24.72	<i>MPa</i>
Maximum displacement	0.173	<i>mm</i>

$$24.72 \leq \frac{80}{1.75} ; 24.72 \leq 45.71 \quad 4.17$$

- Left support of the second conveyor

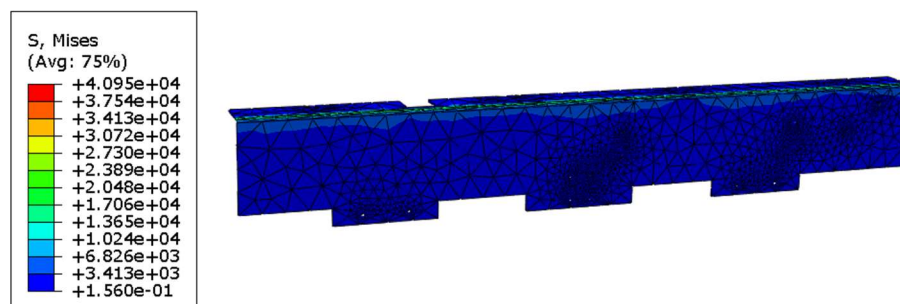


Figure 4.44 - Distribution of Von Mises stresses in the left support of the second conveyor

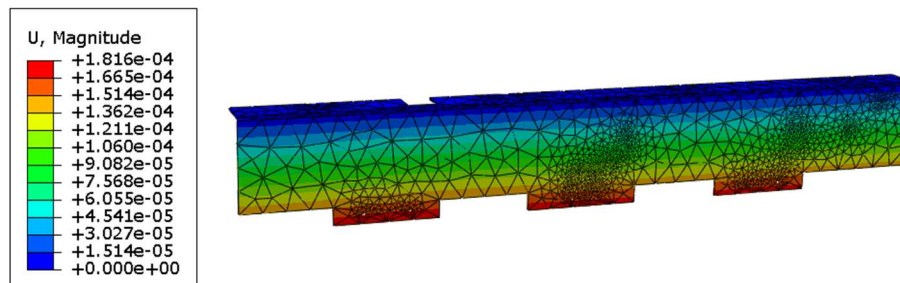


Figure 4.45 - Deformation in the left support of the second conveyor

Table 4.30 - Maximum values obtained for the left support of the second conveyor

	Left support of the second conveyor	
Maximum Von Mises stress	29.84	<i>MPa</i>
Maximum displacement	0.182	<i>mm</i>

$$29.84 \leq \frac{80}{1.75} ; 29.84 \leq 45.71 \quad 4.18$$

## 5 Power transmission system and automation system

This chapter describes the calculations made to size the driving motor and the power transmission system of the conveyors. The calculations are made based on a general analysis of the main forces involved in a belt conveyor system but focusing on the specifications of the conveyors for this work. So, it will take into account the design decisions previously made (i.e. Chapter 4) and the requirements established (i.e. load, velocity profile, intended operation mode) specified.

A stepper motor is chosen, as well as the respective controller. In addition, it is proposed an overall controller for the module developed and the basic sensors needed to implement the required operation cycles.

### 5.1 Force analysis on the belt conveyors

As the motor is one of the most important parts in ensuring the correct operation of the conveyor, its choice would have to be cautious and well-founded. Therefore, a mathematical model was developed that can be applied to the three conveyors used and be sure about the motor selection for each one. Firstly, a theoretical model is going to explain, subsequently, the results for each conveyor are presented, given the conditions intended to impose on it.

The Figure 5.1 represents a generic diagram for a conveyor where the axes that the system have been represented in order to facilitate the explanation of the mathematical method. In addition, the direction of movement of the loads is also shown. From this figure it is also possible to see the path adopted to make the mathematical method. Starting with the load applied to the belt, transferring it to the driving roller and then going into the transmission system "i" until it reaches the motor

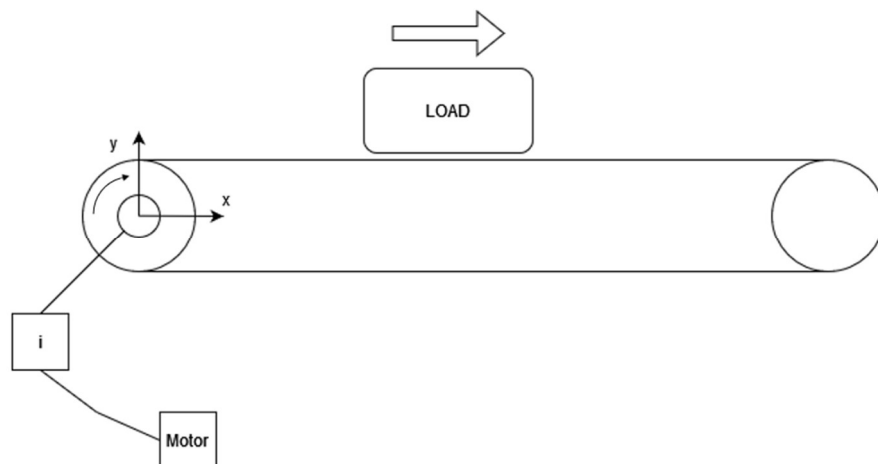


Figure 5.1 - Generic conveyor diagram

Starting with the analysis of the main forces opposing, the movement in the design of belt conveyors normally involve:

- Friction forces;
- Acceleration forces;
- Directing forces from tilting mechanisms, or guiding devices, or other special external forces.

In general, these forces vary along the movement path and some act locally. According to ISO 5048 [33], these forces are organised in five main groups as resistances to movement: main resistances, secondary resistances, special main resistances, special secondary resistances and slope resistances.

The friction forces along the moving direction (x) are calculated based on the forces acting vertically to the moving direction (y) and a coefficient of friction ( $\mu$ ), according to the Equation 5.1:

$$F_x = \mu \times F_y \quad 5.1$$

Friction resistances can originate from contact between the belt and supporting elements, such as idler rollers or surfaces, from contact of the load with the belt, contact with lateral guides and also support bearings. The friction involves sliding or rolling contact, in static or dynamic conditions, although static friction coefficient is normally considered as a worse case design scenario.

The acceleration forces must be included during start/stop operations. They include the masses (m) moving with a linear acceleration (a), Equation 5.2:

$$F_a = m \times a \quad 5.2$$

The torque associated with the acceleration of rotating bodies (rollers, or pulley) must also be included, considering the respective moment of inertia (J) and angular acceleration ( $\alpha$ ), using Equation 5.3:

$$T_a = J \times \alpha \quad 5.3$$

In the case of the driven rollers, this torque can be converted to a tensile force on the belt using the diameter (d) of the respective roller, according to Equation 5.4:

$$F_{Ta} = \frac{2 \times T_a}{d} \quad 5.4$$

The transmission of the actuating power, from the driven roller to the belt, depends on the friction coefficient of the belt/roller surfaces, the wrap angle and the initial tensile force imposed on the belt. In order to avoid slip, and therefore transmit power to the belt, this tensile force must overcome the tensile forces due to all resistances. According to the model presented in Shigley's book [24], the forces at both sides of the belt (Figure 5.2) can be related by the Equation 5.5:

$$\frac{F_1 - F_c}{F_2 - F_c} = \exp(f\theta) \quad 5.5$$

Where,  $F_1$  and  $F_2$  are the forces on the tight and loose ends, respectively, of the belt,  $F_c$  is the tension due to the centrifugal force,  $f$  is the friction coefficient belt/roller and  $\theta$  is the contact angle. This equation can be used to verify whether the selected belt can support the needed tensile force that overcomes the resistance forces on the belt.

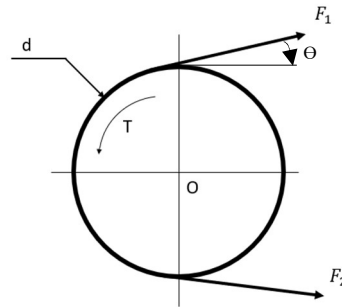


Figure 5.2 - Pulley diagram

Once the belt and rollers are selected, it can be established at the driving roller, the driving power, or maximum torque and speed, required to satisfy the conveyor specifications. With this information it can be defined the transmission system to the motor and the motor power, speed and torque requirements. Considering the worst-case scenario, starting phase considering a trapezoidal velocity profile, the power ( $P$ ) required to displace the opposing forces ( $F_{total}$ ) at the desired conveyor speed ( $v_l$ ) can be calculated by Equation 5.6:

$$P_{belt} = F_{total} \cdot v_l \quad 5.6$$

The power at the driving roller, Equation 5.7, will only differ from this power, so we have to include the driving roller's acceleration torque ( $T_a$ ), which can be calculated considering the angular velocity ( $\omega$ ), Equation 5.8, as well as the influence of some structural elements on which the roller is supported, such as the bearings, that we will analyse later on.

$$P_{roller} = \frac{F_{total}}{d/2} \cdot \omega + T_a \cdot \omega + P_{support\_elements} \quad 5.7$$

$$\omega_{roller} = \frac{v}{d/2} \quad 5.8$$

This power, associated torque and velocity, can be referred to the motor shaft considering a transmission relation ( $i$ ) and estimating an efficiency rate ( $\eta$ ), by Equation 5.9 to Equation 5.11:

$$P_{motor} = \frac{P_{roller}}{\eta} \quad 5.9$$

$$\omega_{motor} = \omega_{roller} \cdot i \quad 5.10$$

$$T_{motor} = \frac{P_{roller}}{\omega_{motor}} \quad 5.11$$

In addition to torque and speed requirements, it is especially important for sizing stepper motors to limit the inertia ratio, the total loads inertia compared to motor's inertia, Equation 5.12:

$$\frac{J_{total\ external}}{J_{motor}} < 10 \quad 5.12$$

## 5.2 First conveyor

Beginning with the static analysis, it has to be determined the total force that is generated by the exterior components applied on the belt. For this, these forces were divided into two stages. The forces that are moved at constant velocity,  $F_{Static}$ , and forces moved with constant acceleration,  $F_{Ac}$ , where it must be arbitrated a value for the acceleration time. In the Table 5.1 are described all the conditions that serve as a starting point for the analysis.

Table 5.1 - First conveyor specifications

<b>Barrier Mass</b>	$m_{Barrier}$	0.5	kg/barrier
<b>Total Boxes Mass</b>	$m_{Boxes}$	3	kg
<b>Belt Mass</b>	$m_{Belt}$	0.76	kg
<b>Coefficient of friction bottom part of the belt</b>	$\mu_{surf}$	0.25	-
<b>Linear Speed</b>	$v_l$	0.25	m/s
<b>Acceleration Time</b>	$t$	1	s
<b>Acceleration</b>	$a$	0.25	m/s <sup>2</sup>
<b>Roller diameter</b>	$d_3$	48	mm
<b>Big Pulley Diameter</b>	$d_2$	45	mm
<b>Small Pulley Diameter</b>	$d_1$	15	mm

- **Acceleration forces:** *Forces under constant acceleration*

Starting by calculating the accelerated forces of the load, it was only considering the effects produced by the mass of the boxes on the belt,  $F_{Boxes}$ , and the effect produced by the weight of the belt. The sum of these two variables results in the total force required to move the load with constant acceleration,  $F_{Ac}$ , Equation 5.13.

$$\begin{cases} F_{Ac} = F_{Boxes} + F_{Belt} \\ F_{Boxes} = m_{Boxes} \times a (=) \\ F_{Belt} = m_{Belt} \times a \end{cases} \begin{cases} F_{Ac} = 0.94 \text{ N} \\ F_{Boxes} = 0.75 \text{ N} \\ F_{Belt} = 0.19 \text{ N} \end{cases} \quad 5.13$$

- **Static forces:** *Forces at constant linear velocity*

In terms of the forces that are moving at a constant speed,  $F_{static}$ , it was considered for this case the forces produced by the weight of the barriers, the force generated by friction between the belt and the support plate, and the force produced by the weight of the boxes.

As the barriers are rotating around an axis, and the point of application of the forces is not constant throughout the system and throughout the time (depends on the height of the boxes we have at that moment) it was considered the worst-case scenario. For discovering the worst-case scenario, it was made a diagram (Figure 5.3) where only the box with greatest height (150 mm) pass through and by summing the moment on the axis of rotation (Point O) it was calculated the maximum force that would have to be made, Equation 5.14.

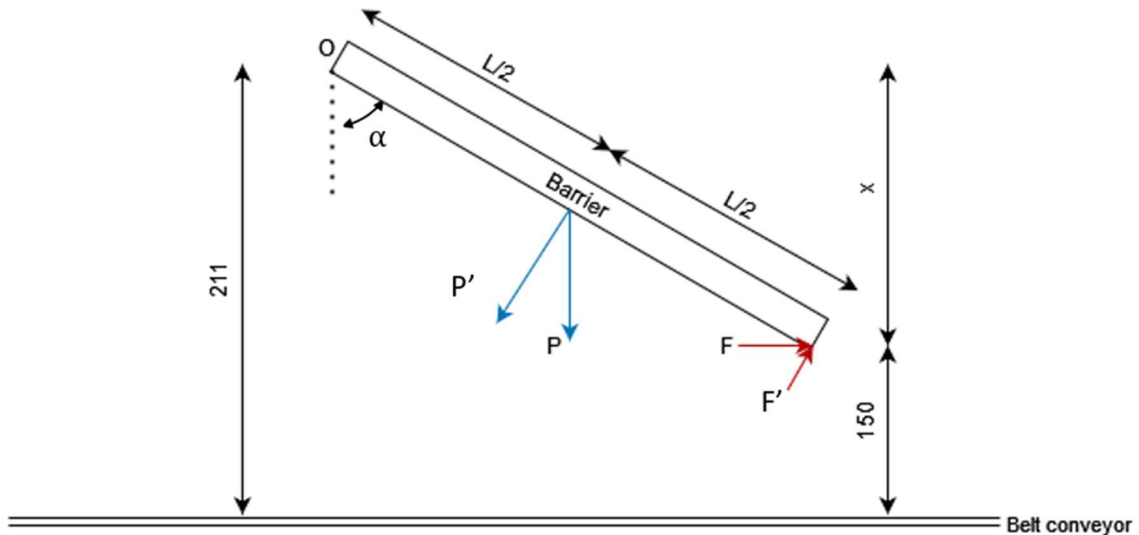


Figure 5.3 - Barrier diagram where ( $L$  is the length of the barrier [193 mm],

$P$  is the weight of one barrier and  $F$  the maximum force)

$$\begin{cases} P' \times \frac{L}{2} - F' \times L = 0 \\ \cos(\alpha) = \frac{X}{L} \\ P = m_{Barriers} \times g \end{cases} (=) \begin{cases} \left[ P \times \sin(\alpha) \times \frac{L}{2} \right] = [F \times \cos(\alpha) \times L] \\ \cos(\alpha) = \frac{X}{L} \\ P = m_{Barriers} \times g \end{cases} \quad 5.14$$

By replacing the variables with values and knowing that there are two barriers, this value of the force produced by rotating the barriers is:

$$\begin{cases} F = 1.5 \times P \\ \alpha = 71.58^\circ \\ F_{Barriers} = 2 \times F \end{cases} (=) \begin{cases} F = 7.36 \text{ N} \\ \alpha = 71.58^\circ \\ F_{Barriers} = 14.72 \text{ N} \end{cases} \quad 5.15$$

For the forces produced by the friction coefficient,  $F_{Belt-fric}$ , generated by the contact between the belt and the support plate,  $\mu_{surf} = 0.25$ , it is calculated by the following equation:

$$F_{Belt-fric} = m_{Belt} \times \mu_{surf} \times g = 1.87 \text{ N} \quad 5.16$$

Where,  $g$  is the gravitational acceleration ( $g = 9.81 \text{ m/s}^2$ )

Adding these two components, as well as the weight of the boxes, we get the total static force:

$$\begin{cases} F_{Box-fric} = m_{Boxes} \times g \times \mu_{surf} = 7.36 \text{ N} \\ F_{Static} = F_{Belt-fric} + F_{Barriers} + F_{Box-fric} = 23.95 \text{ N} \end{cases} \quad 5.17$$

By adding the last two variables, we have all the force that is needed to move on the upper side of the conveyor,  $F_{wght}$ .

$$\begin{aligned} F_{wght} &= F_{Ac} + F_{Static} \\ F_{wght} &= 0.798 + 23.95 = 24.89 \text{ N} \end{aligned} \quad 5.18$$

The power generated by the load,  $P_{load}$  [W], is obtained by multiplying the total load force previously calculated,  $F_{wght}$  [kg], with the linear velocity,  $v_l$  [m/s].

$$P_{load} = F_{wght} \times v_l = 24.89 \times 0.25 = 6.22 \text{ W} \quad 5.19$$

The linear velocity between the conveyor and the roller is the same as they are mechanically coupled.

$$v_l = v_3 = 0.25 \text{ m/s} \quad 5.20$$



With the value of the linear velocity applied we can obtain the value for the angular velocity of the roller through the Equation 5.21 and the number of rotations per minute through the Equation 5.22:

$$w_3 = \frac{v_3}{r_3} = \frac{0.25}{0.024} = 10.42 \text{ rad/s} \quad 5.21$$

$$n_3 = \frac{w_3 \times 60}{2 \times \pi} = \frac{10.42 \times 60}{2 \times \pi} = 99.47 \text{ r.p.m.} \quad 5.22$$

Where,  $w_3$  = Angular velocity in the shaft [rad/s];  $n_3$  = Rotations of the shaft [r.p.m.];  $r_3$  = roller radius [mm]

Furthermore, it is known that the tangential force produced by the load is equal to the tangential force on the roller. However, the tangential force produced on the roller will also be influenced by the centrifugal force generated by the belt, Equation 5.23, from the Shigley's book [24].

$$F_c = m_{Belt} \times r_3^2 \times w_3^2 \quad 5.23$$

$$F_c = 0.764 \times 0.024^2 \times 10.42^2 = 0.05 \text{ N}$$

Furthermore, the force created by the fact that the shaft is coupled to two bearings will also influence, Equation 5.24. To calculate this variable, it was only considered the influence of parameters, such as the weight of the roller itself and the tangential force obtained by the movement of the loads. The coefficient of friction of the bearings used was obtained by consulting the *SKF* catalogue, [34], and was used the biggest value for steel/steel connections, since it was always recommended to analyse the worst-case scenario. The most correct would be to use the reference value given by the technical data sheet of the bearing itself, however it was not available online for consultation, hence the use of this alternative.

$$F_{Bearings} = ((m_{roller} \times g) + F_{wght}) \times \mu_{Bearings} \quad 5.24$$

$$F_{Bearings} = ((0.625 \times 9.81) + 24.89) \times 0.2 = 6.20 \text{ N}$$

Finally, before calculating the tangential force generated in the roller, it was also calculated the value of the force caused by the fact that it is necessary to counteract the moment of inertia to move the roller, Equation 5.25 and Equation 5.26.

$$J_{rol} = m_{roller} \times \frac{r_{roller}^2}{2} = 0.625 \times \frac{0.024^2}{2} \quad 5.25$$

$$J_{roller} = 1.80 \times 10^{-4} \text{ kg.m}^2$$

$$F_{roller} = \frac{J_{roller} \times a}{r_{roller}^2} = \frac{1.80 \times 10^{-4} \times 0.25}{0.024^2} \quad 5.26$$

$$F_{roller} = 0.08 \text{ N}$$

Therefore, the tangential force generated on the motor shaft is obtained from the following equation:

$$F_3 = F_{wght} + F_c + F_{Bearings} + F_{roller}$$

$$F_3 = 24.89 + 0.05 + 6.20 + 0.08 = 31.22 \text{ N} \quad 5.27$$

After obtaining the tangential force, it is now possible to obtain the necessary torque and the power generated, by the equations 5.28 and 5.29:

$$T_3 = F_3 \times r_3 = 31.22 \times 0.024$$

$$T_3 = 0.75 \text{ N.m} \quad 5.28$$

$$P_3 = F_3 \times v_3 = 31.22 \times 0.25$$

$$P_3 = 7.80 \text{ W} \quad 5.29$$

With all the energy data on the roller calculated, it is necessary to transfer the variables to the second pulley. As these two elements are coupled to each other, the following equations are valid.

$$w_3 = w_2 = 10.42 \text{ rad/s} \quad 5.30$$

$$n_3 = n_2 = 99.47 \text{ r.p.m.} \quad 5.31$$

$$T_3 = T_2 = 0.76 \text{ N.m} \quad 5.32$$

Depending on the diameters of the roller and of the bigger pulley there is a transmission ratio and through this constant it was obtained a new tangential force, as shown in the following equation:

$$F_2 = F_3 \times \left[ \frac{D_3}{D_2} \right] = 31.22 \times \left[ \frac{0.048}{0.045} \right] = 33.30 \text{ N} \quad 5.33$$

Where,  $D_3$  = Roller Diameter [mm];  $D_2$  = Second Pulley Diameter [mm]

With the Equations 5.34 and 5.35 results the remaining variables, such as the linear velocity,  $v_2$  [m/s], and the power required,  $P_2$  [W], for the second pulley:

$$v_2 = w_2 \times r_2 = 10.42 \times 0.0225 = 0.23 \text{ m/s} \quad 5.34$$

$$P_2 = F_2 \times v_2 = 33.30 \times 0.23 = 7.80 \text{ W} \quad 5.35$$

After knowing all the components that characterise the movement of the second pulley, it was time to transfer that energy for the first pulley, which has a smaller diameter. These two pulleys are connected by a belt, which means that they have the same linear velocity, Equation 5.36.

$$v_1 = v_2 = 0.23 \text{ m/s} \quad 5.36$$

The tangential force transmitted is affected by the transmission efficiency, which can be assumed as to be 80% for this type of transmission system according to the literature.

$$F_1 = \frac{F_2}{\eta} = \frac{33.30}{0.8} = 41.62 \text{ N} \quad 5.37$$

By applying the same formulas used in the previous situations, it was possible to determine the parameters that characterise the first pulley movement:

$$w_1 = \frac{v_1}{r_1} = \frac{0.23}{0.0075} = 31.25 \text{ rad/s} \quad 5.38$$

$$n_1 = \frac{w_1 \times 60}{2 \times \pi} = \frac{31.25 \times 60}{2 \times \pi} = 298.42 \text{ r.p.m.} \quad 5.39$$

$$T_1 = F_1 \times r_1 = 41.62 \times 0.0075 = 0.31 \text{ N.m} \quad 5.40$$

$$P_1 = F_1 \times v_1 = 41.62 \times 0.23 = 9.75 \text{ W} \quad 5.41$$

Having calculated all the parameters that characterise the first pulley, those variables were passed directly to the motor and then proceed to its selection. For safety reasons and in order to minimise possible errors made by approximations, it was applied a safety factor for the required torque (S.F. = 1.75).

Table 5.2 - Motor needed specifications

	Nomenclature	Units
<b>Motor Power</b>	$P_m = P_1 = 9.75$	$[W]$
<b>Angular Velocity</b>	$w_m = w_1 = 31.25$	$[rad/s]$
<b>Rotational Speed</b>	$n_m = n_1 = 298.42$	$[r.p.m.]$
<b>Required Torque</b>	$T_m = T_1 \times S.F.$	$[N.m]$
	$T_m = 0.31 \times 1.75 = 0.55$	
	$T_m = 54.63$	$[N.cm]$

With these results, it was necessary to look for a motor that has an rotational speed of 298.42 r.p.m. and can deliver a torque equal to 0.55 N.m and a minimum power of 9.75 W.

The dynamic analysis was done by calculating the moments of inertia of all the components. First of all, it was necessary to calculate the moments of inertia of the objects with respect to their own axis of rotation. Subsequently, this moment of inertia has to be transferred to the motor shaft through the relationship of the rotation speeds. Finally, by adding all the calculated values, it results in the value that the motor has to deliver in order to move the load dynamically.

In order to simplify the identification process of each moment of inertia, the following nomenclature was used. This will only serve as an example that then must be adapted to the particular case.

$J_{1^{st}Pulley}^{Motor} [kg.m^2]$  = means the moment of inertia of the first pulley with reference to the motor shaft

It was started by calculating the moment of inertia of the load to be transported that was directly obtained in relation to the motor shaft, using the following equation:

$$J_{Load}^{Motor} = m_{Boxes} \times \left[ \frac{v_l}{w_{motor}} \right]^2 = 3 \times \left[ \frac{0.25}{30} \right]^2 = 1.92 \times 10^{-4} kg.m^2 \quad 5.42$$

For other components with cylindrical geometry, it was necessary to divide the process into two steps, first calculating the object's moment of inertia with respect to its own axis, Equation 5.43, and only then transferring this moment of inertia to the motor shaft, Equation 5.44.

$$J_{Pulley}^{Pulley} = \frac{m_{Pulley} \times \left[ \frac{D_{Pulley}}{2} \right]^2}{2} \quad 5.43$$

$$J_{Pulley}^{Motor} = J_{Pulley}^{Pulley} \times \left[ \frac{v_{Pulley}}{w_{motor}} \right]^2 \quad 5.44$$

In order to make the process more succinct, the results are represented in the following tables. In Table 5.3 are the moments of inertia applied to the product own axis, while in Table 5.4, are the moments of inertia applied to the motor rotational axis.

Table 5.3 – Moments of inertia applied to the object axis

$J_{Roller}^{Roller}$	$1.80 \times 10^{-4}$	$kg.m^2$
$J_{Pulley 2}^{Pulley 2}$	$3.11 \times 10^{-5}$	$kg.m^2$
$J_{Pulley 1}^{Pulley 1}$	$3.01 \times 10^{-7}$	$kg.m^2$

Table 5.4 - Moments of inertia applied to the motor axis

$J_{Roller}^{Motor}$	$1.15 \times 10^{-8}$	$kg.m^2$
$J_{Pulley 2}^{Motor}$	$1.75 \times 10^{-9}$	$kg.m^2$
$J_{Pulley 1}^{Motor}$	$1.69 \times 10^{-11}$	$kg.m^2$

After calculating the moments for each component individually, all of them were added together to obtain the total moment of inertia required for the motor.

$$J_{Total} = \left( \sum J_x^{Motor} \right) = 1.92 \times 10^{-4} kg.m^2 = 1920.13 g.cm^2 \quad 5.45$$

## - Verification

In addition, it was still necessary to check some parameters to be completely sure of the choice made. In Figure 5.4 it is represented the characteristic curve of the motor and in orange it is represented the operating point that the motor works. It is easy to see that given the requirements of the set, the motor can meet the needs, and could eventually increase the required torque as long as we maintain the rotation speed, being done the validation for the static analysis.

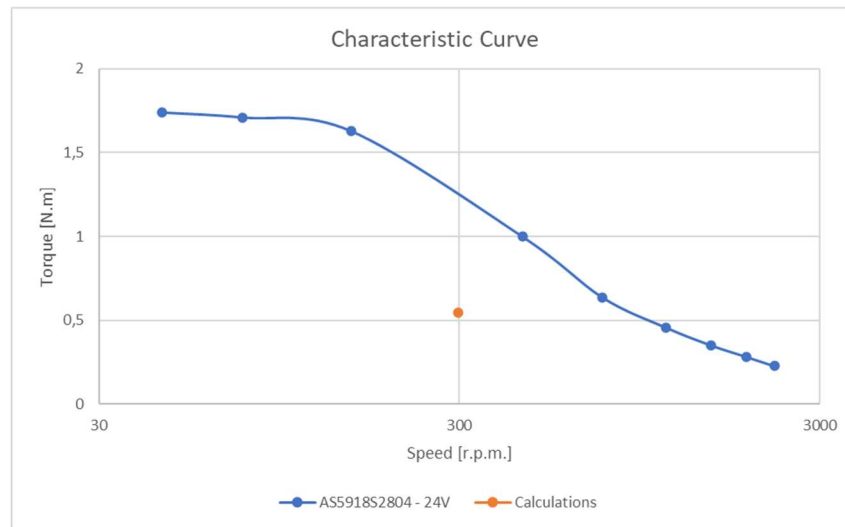


Figure 5.4 - First conveyor motor characteristic curve

Regarding the dynamic analysis, a validation is needed. When using stepper motors, it is necessary to comply with the following restriction [30], Equation 5.46:

$$Inertia\ Ratio \geq \frac{J_{Total}}{J_{Motor}} \quad 5.46$$

$$10 \geq \frac{1920.13}{480} ; 10 \geq 4.00$$

As we can see, the motor's operating point is in a zone where the torque drops quickly when we increase the speed. If it was used a 1:1 transmission ratio, this working point would move to the left of the diagram, being in a more stable zone of operation. However, the problem would be in the inertia ratio, which has a reference value of 10 for this type of motor. When we are using pulleys of the same diameter, we are working with the same rotation speeds, something proven by calculations. And as the inertia value depends directly on the square of the speed variation, the inertia value would increase very drastically invalidating the choice of this motor.

Furthermore, the value obtained for the inertia ratio is below the reference value for this type of motors. It was thought about selecting another motor with weaker specifications, but this one did not meet the requirements for the inertia ratio value. The choice of motor and pulleys made were based on these arguments.

### 5.3 Second and third conveyors

To select the motor for this conveyor system, it was used the same mathematical method as the previous system. As such, and in order to do not make the reading of the report too repetitive, the results obtained for each of the components of this conveyor will be presented in the form of a table. It should also be noted that the nomenclature used was exactly the same in order to unify the whole set.

The starting point for the analysis of this system was exactly the same as the previous one, having been arbitrated a mass for the boxes that would be in the belt, the linear velocity at which these boxes moved as well as their acceleration time, Table 5.5. As the behaviour of the chicanes is not the same as the barriers, the value of this variable was considered null, because the chicanes are fixed to the structure. Furthermore, as the conveyor does not have any support plate the static force was considered to be equal only to the force used to move the weight of the boxes.

Table 5.5 - Second and third conveyor specifications

<b>Chicane Mass</b>	$m_{Chicane}$	0.25	<i>kg/chicane</i>
<b>Total Boxes Mass</b>	$m_{Boxes}$	2	<i>kg</i>
<b>Linear Speed</b>	$v_l$	0.25	<i>m/s</i>
<b>Belt Mass</b>	$m_{Belt}$	0.47	<i>kg</i>
<b>Coefficient of friction bottom part of the belt</b>	$\mu_{surf}$	0.25	-
<b>Acceleration Time</b>	$t$	1	<i>s</i>
<b>Acceleration</b>	$a$	0.25	<i>m/s<sup>2</sup></i>
<b>Roller diameter</b>	$d_3$	48	<i>mm</i>
<b>Big Pulley Diameter</b>	$d_2$	45	<i>mm</i>
<b>Small Pulley Diameter</b>	$d_1$	15	<i>mm</i>

Although the conveyors run at different velocities, it was decided to make the calculations for the same speed and then figure out what would be the maximum speed that the conveyors could run at after having chosen the motor. Started by calculating the influence of the load to be moved at constant speed and the load to be moved at constant acceleration, we get the combined result of these two parameters for force and power, Table 5.6.

Table 5.6 – Moving the load needed specifications

<b>F<sub>Ac</sub></b>	0.37	<i>N</i>
<b>F<sub>Boxes</sub></b>	0.25	<i>N</i>
<b>F<sub>Belt</sub></b>	0.12	<i>N</i>
<b>F<sub>Static</sub></b>	4.91	<i>N</i>
<b>F<sub>wght</sub></b>	5.27	<i>N</i>
<b>P<sub>Load</sub></b>	1.32	<i>W</i>

Moving on to the analysis of the conveyor shaft.

Table 5.7 - Conveyor shaft obtained results

<b>w<sub>3</sub></b>	10.42	<i>rad/s</i>	<b>F<sub>c</sub></b>	0.03	<i>N</i>
<b>v<sub>3</sub></b>	0.25	<i>m/s</i>	<b>F<sub>Bearings</sub></b>	2.55	<i>N</i>
<b>n<sub>3</sub></b>	99.47	<i>r.p.m.</i>	<b>T<sub>3</sub></b>	0.19	<i>N.m</i>
<b>F<sub>3</sub></b>	7.94	<i>N</i>	<b>P<sub>3</sub></b>	1.99	<i>W</i>

The results obtained in both of the pulleys are shown in the following tables. In Table 5.8 is represented the results for the second pulley, the one with bigger diameter, while in Table 5.9 it is shown the results for the smaller one, when influenced by a transference efficiency of 80%, as used in the previous case.

Table 5.8 - Second pulley obtained results

<b>w<sub>2</sub></b>	10.42	<i>rad/s</i>
<b>v<sub>2</sub></b>	0.23	<i>m/s</i>
<b>n<sub>2</sub></b>	99.47	<i>r.p.m.</i>
<b>F<sub>2</sub></b>	8.47	<i>N</i>
<b>T<sub>2</sub></b>	0.19	<i>N.m</i>
<b>P<sub>2</sub></b>	1.99	<i>W</i>

Table 5.9 - First pulley obtained results

<b>w<sub>1</sub></b>	31.25	<i>rad/s</i>
<b>v<sub>1</sub></b>	0.23	<i>m/s</i>
<b>n<sub>1</sub></b>	298.42	<i>r.p.m.</i>
<b>F<sub>1</sub></b>	10.59	<i>N</i>
<b>T<sub>1</sub></b>	0.08	<i>N.m</i>
<b>P<sub>1</sub></b>	2.48	<i>W</i>

Finally, all that remains is to apply these values to the engine when influenced by the safety factor of 1.75. The results obtained can be seen in Table 5.10.

Table 5.10 - Second conveyor motor needed specifications

	<b>Nomenclature</b>	<b>Units</b>
<b>Motor Power</b>	$P_m = P_1 = 2.48$	<i>[W]</i>
<b>Angular Velocity</b>	$w_m = w_1 = 31.25$	<i>[rad/s]</i>
<b>Rotational Speed</b>	$n_m = n_1 = 298.42$	<i>[r.p.m.]</i>
<b>Required Torque</b>	$T_m = T_1 \times S.F.$ $T_m = 0.08 \times 1.75 = 0.14$	<i>[N.m]</i>
	$T_m = 13.90$	<i>[N.cm]</i>

With these results, it was needed to find a motor that at an rotational speed of 298.42 r.p.m. that can deliver a torque equal to 0.14 N.m and a minimum power of 2.48 W.

Having concluded the static analysis of the process, it was time to present the results of the dynamic analysis, where in Table 5.11 are presented the values of the inertia moments following the component's own axis and in Table 5.12 the inertia moments following the motor's rotation axis.

Table 5.11 – Moments of inertia applied to the object

	axis	
$J_{Roller}^{Roller}$	$1.8 \times 10^{-4}$	$kg.m^2$
$J_{Pulley 2}^{Pulley 2}$	$3.11 \times 10^{-5}$	$kg.m^2$
$J_{Pulley 1}^{Pulley 1}$	$3.01 \times 10^{-7}$	$kg.m^2$

Table 5.12 - Moments of inertia applied to the motor axis

$J_{Roller}^{Motor}$	$1.15 \times 10^{-8}$	$kg.m^2$
$J_{Load}^{Motor}$	$1.28 \times 10^{-4}$	$kg.m^2$
$J_{Pulley 2}^{Motor}$	$1.75 \times 10^{-11}$	$kg.m^2$
$J_{Pulley 1}^{Motor}$	$1.69 \times 10^{-11}$	$kg.m^2$

The total sum of the inertia required to be exerted by the motor is represented in the Equation 4.57:

$$J_{Total} = \left( \sum J_x^{Motor} \right) = 1.28 \times 10^{-4} kg.m^2 = 1280.13 g.cm^2 \quad 5.47$$

After finishing this part of the mathematical analysis, it was gone to the *Nanotec* catalogues to see what options were available on the market and compared them with results, so it was possible to choose the motor that most suits with the requirements, ending up picking the motor with the following reference: AS5918S2804. The motor specifications are presented in Table 5.13.

Table 5.13 - Second and third conveyor motor specifications

	<b>AS5918S2804</b>	
<b>NEMA</b>	23	-
<b>Holding Torque</b>	99	$N.cm$
<b>Rotor Inertia</b>	230	$g.cm^2$
<b>Weigh</b>	0.8	$kg$



## - Verification

Figure 5.5 shows the characteristic curve of the selected motor, with the orange point being the reference value required for the system. Making a visual analysis, it is notable that in terms of torque, the motor meets the necessary requirements.

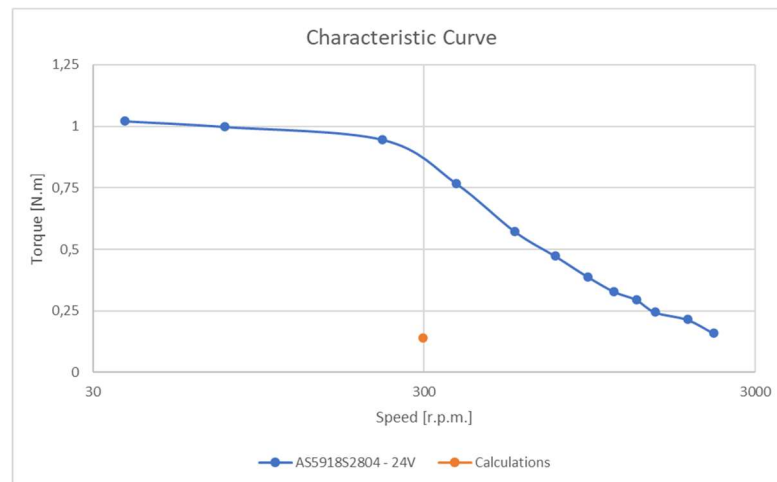


Figure 5.5 - Second conveyor motor characteristic curve

To validate the choice of this value, it was also needed to compare the inertia ratio with the reference values for this type of motor [30]. By doing the math equation for the obtained results, Equation 5.48, we realise that the value is about half of the reference value.

$$\begin{aligned}
 \text{Inertia Ratio} &\geq \frac{J_{Total}}{J_{Motor}} \\
 10 &\geq \frac{1280.13}{230} \quad (=) \quad 10 \geq 5.57
 \end{aligned}
 \tag{5.48}$$

However, if it was chosen a motor with the lowest specifications, this inertia ratio value was over exceeded. Furthermore, the size of this new motor and its shaft were smaller and there was a greater risk of bending the shaft and consequently a bad working principle in all set, thus excluding this option.

It is important also to note that the calculation was done using the same linear speed on both conveyors. However, a study was also made for a higher speed and this value can reach a maximum of 450 mm/s, something also quite satisfactory, given that it is intended to vary the speeds on these two conveyors.

To sum up, both motors chosen for the conveyors were with the same size, NEMA 23, changing only the working specifications of each other. Therefore, it was possible to use the same motor support block in all the conveyors, which is a positive aspect when it comes to standardisation of the whole assembly.

## 5.4 Module automatization

At this stage, the main objective of testing a working concept and specifying the structural and driving components of a solution is achieved. The next step is to describe the envisaged working principle, based on the control capabilities of the defined driving solution.

Additionally, the basic elements of the control system are selected and described, taking into account the need to integrate with the controller of the main system. This led to select a control architecture based on a Beckhoff / TwinCat platform [35].

### - Working principle

The envisaged solution takes advantage of the step motor control capabilities to implement either continuous with different velocities, or intermittent movements of the three conveyors, Figure 5.6, which is an advantageous for the control of the splitting and sequential separation of the loaded boxes. In order to decide on these working cycles, it is required to identify the various stages and boxes flow along the process. To provide this information sensors to detect the presence of the boxes at the start and the end of each conveyor, and also at the end position are considered. The programmable capabilities of the controllers allow for multiple combinations of working cycles to be defined, tested and implemented easily.

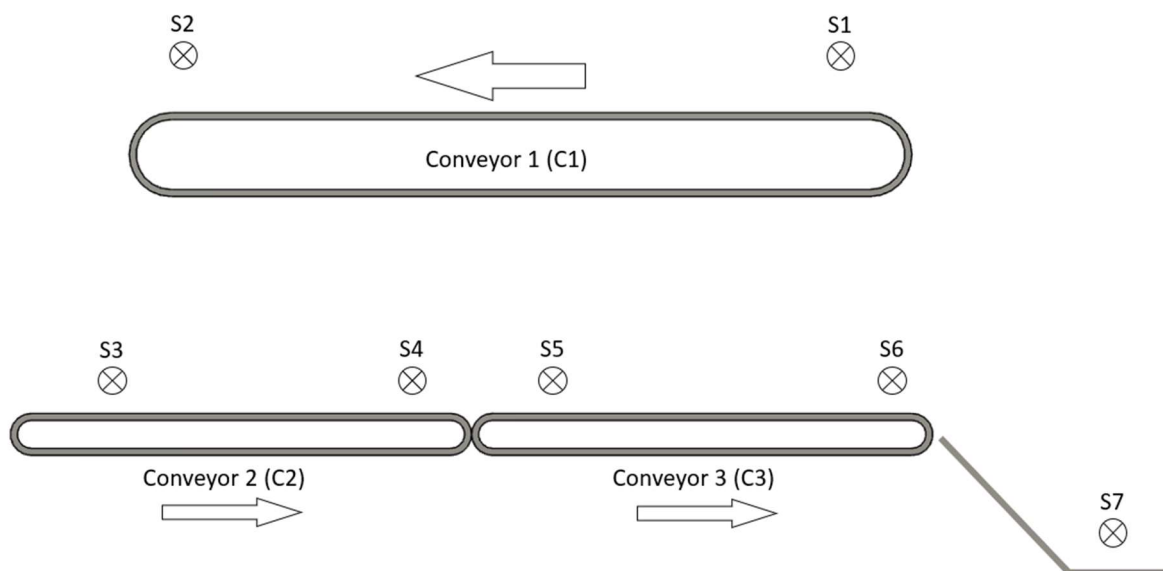


Figure 5.6 - Sensors position in a generic diagram

An example of the envisaged working cycles will include an initial cycle to guarantee that no boxes were left on the system previously. For example, each conveyor will run continuously, for a time that allows a box in any position along the conveyor path, to be directed to the end of the conveyor. This cycle ends when the conveyors run for the set time and no boxes are detected by the limit sensors.

After the initial cleaning cycle and having loaded the boxes on the input station, a processing starting cycle is initiated by the operator through the corresponding buttons available on an HMI (Human Machine Interface) select for this system. This cycle initiates with a continuous movement of the first conveyor (C1). When a box is detected by S2, the conveyor C1 pauses and starts an intermittent movement, to better control the fall of the boxes to the next conveyor (C2) is started at the same time. When S3 detects the presence of a box, conveyor 3 (C3) starts moving with a higher speed than C2. When a box is detected by S4 conveyor C2 pauses and starts its intermittent moves, as well as C1. The same movement behaviour is implemented with conveyor C3 when boxes arrive at sensor S6. The use of another sensor, S7, at the end positioning station, will be used to control C3. This basic cycle will be repeated until all boxes have left the system. At the end, a cycling cycle is going to be made, as it was done in the beginning of the process, to ensure that there are no boxes left inside the module.

The detailed and formal specifications of the working cycles, as well as safety measures, were not one of the main objectives of the current work and will be left out for the implementation phase. However, the specified elements, described next, guarantee the required programming capabilities for its implementation.

#### - Controller

The system is controlled by an industrial embedded computer (IPC - Embedded PC). This is a basic CPU model that is implemented in the Economy Plus range and can be supported on a DIN rail (EN 60715), which makes it easy to assemble. This compact model communicates with a PC for programming the module, storing the program that will control the cycles of this system depending on the information from the sensors installed in the module. In addition, there will also be a physical interface (HMI) that will allow the operator to communicate with the machine. Being chosen the CX 9020 controller for this application, Figure 5.7. Table 5.14 shows the controller specifications.



Figure 5.7 - Controller CX 9020 [35]

Table 5.14 - Controller CX 9020 specifications [35]

	CX 9020	
<b>Processor</b>	ARM Cortex™-A8, 1GHz	
<b>Power Supply</b>	24	<i>V</i>
<b>Max Power Consumption</b>	9	<i>W</i>
<b>Dimensions</b>	84 x 100 x 91	<i>mm</i>
<b>Main Memory</b>	1 GB DDR3 RAM (not expandable)	

## - Stepper motor terminal

When choosing the terminal to connect to the stepper motor, the current intensity passing through the motor and the voltage had to be taken into account. The terminal chosen to connect the stepper motor was EL 7041, Figure 5.8, with a maximum voltage of 48V and a current range up to 5A.

By choosing this terminal, the capacity of further developments of the system was increased. Imagine a case where the motor specifications need to be increased and use a consumption of 48V, this terminal can adapt to these changes. The question of choosing a terminal with lower specifications, like the EL 7031, could be raised, however this one does not check the current intensity condition imposed by the motors chosen.

The motor chosen has a step angle of  $1.8^\circ$ , which gives a total of 200 steps per rotation ( $[360^\circ \times 1 \text{ rotation}] / 1.8^\circ = 200 \text{ steps per rotation}$ ). Adding to this, the fact that the terminal can control up to micro steps, it is possible to increase the resolution of the motor step up to 64 times, which is the maximum resolution that the terminal allows. This gives a better control of the movement of the conveyor. This terminal also comes with an incremental encoder, which makes the response feedback even more precise, since it can control the loss of motor steps.

Finally, in terms of inputs / outputs, the EL 7041 provides two digital inputs, thus allowing to be associated two detectors to each motor, which guarantees a better control of the whole system, something very useful from the perspective of the application of the functionalities in the development of the project and the working principle of the module. It also provides an input of signals for an encoder, which however is not required at this stage, Table 5.15.

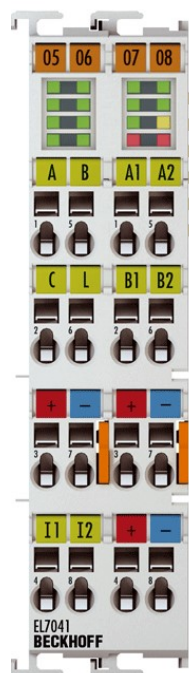


Table 5.15 - Terminal EL 7041 specifications [35]

	EL 7041	
<b>Number of outputs</b>	1 x stepper motor, 2 phases	
<b>Number of inputs</b>	2 x end position, 1 x encoder	
<b>Voltage</b>	48	<i>V</i>
<b>Output Current</b>	5	<i>A</i>
<b>Dimensions</b>	24 x 100 x 68	<i>mm</i>
<b>Step pattern</b>	64-fold micro stepping	

Figure 5.8 - Terminal EL 7041 [35]

## - Sensors Terminal

The availability of having various sensors terminals is important to not limiting the addition of sensors to the module. At this stage, the EL 1014 is selected to provide the capacity of using 7 sensors, Figure 5.9. Table 5.16 shows the sensor terminal specifications.



Figure 5.9 - EL 1014 [35]

Table 5.16 - EL 1014 specifications [35]

	<b>EL 1014</b>	
<b>Number Inputs</b>	4	
<b>Voltage</b>	24	V
<b>Input filter</b>	10	$\mu$ s
<b>Dimensions</b>	12 x 100 x 68	mm

## - Power Supply

Another component that must be included is a DC power supply to provide energy to the module. Considering the consumption of the three stepper motors and the controller, which are the components that consume more energy, the power supply characteristics are:

$$\begin{aligned}
 V &= 24 \text{ V} \\
 I &= 3 \times 4.2 = 12.6 \text{ A} \\
 P_{motor} &= V \times I = 24 \times 12.6 = 302.40 \text{ W} \\
 P_{Controller}^{Max} &= 9 \text{ W} \\
 P_{Total} &= P_{motor} + P_{Controller}^{Max} = 302.40 + 9 = 331.40 \text{ W}
 \end{aligned}
 \tag{5.49}$$

Based on these requirements, a power supply from Mean Week was selected, in this case the NDR-480-24. In addition, this module has the ability to be supported on the same rail as the controller [DIN (EN 60715)], which is also a positive aspect in terms of the uniformity of the whole set.



Figure 5.10 - Mean Well Power Supply [36]

Table 5.17 - Power Supply specifications [36]

	<b>NDR – 480 - 24</b>	
<b>Power</b>	480	<i>W</i>
<b>Voltage</b>	24	<i>V</i>
<b>Current Range</b>	0 – 20	<i>A</i>
<b>Dimensions</b>	85.5 x 125.2 x 128.5	<i>mm</i>
<b>Weight</b>	1.5	<i>kg</i>

Since this power supply can produce 480 W and the main components of the module need a much smaller amount of energy, it is easy to see that other components can be connected since there are about 190W of power still remaining.

#### - Module sensing

Regarding the type and number of sensors that best fit this module, its decision will depend on further approaches of the project. Due to the wide variety of sensors, as well as constraints that the system has, the current choice of sensors only considered photoelectric sensors placed at the start and at the end of the conveyors and one in the final positioning ramp. Later on, the type of sensors could be changed or even the need to add more sensors to the system, may be considered.

Therefore, it was chosen to use seven photoelectric sensors from *Banner*, the VS3, Figure 5.11. Their choice was mainly due to the fact that they are extremely compact and have the capability of detecting very thin objects. Furthermore, they can also operate in low-light environments and are available in a retroreflective detection mode.

Figure 5.11 - VS3 *Banner* photoelectric sensor [37]

In Figure 5.6 it is possible to see its positioning along the whole structure of the model. The final position will only be possible to know after running some tests of the concept and discovering the precise position that guarantees the correct functionality of the whole set. This figure is merely illustrative and serves only to have a generic idea on where the sensors should be placed. The last sensor is placed at the end of the ramp to detect if there are any boxes at the end of this stage.

*(Blank Page)*



## 6 Module assembly and Bill of Materials

### 6.1 Module assembly

After having the three conveyor belts completely assembled and with the choice of their components properly justified, it was time to mount them on the main structure. As previously stated, the main structure is constructed and supported by technical profiles of square-section with 40 mm of width. Furthermore, the main structure is divided into modules of 960 mm wide and 500 mm deep as it has already been presented in the Chapter 3.1, so there was no need to adapt the supports of the conveyors to fit within these restrictions. It was used the same profiles, as they can only be interconnected if they have the same measurements, according to the supplier of this product.

In addition, it was recommended that the height at which the boxes are dumped into the module should be easily accessible for a person of average height, opting for placing the first conveyor at 1200 mm from the floor. As the dimension according to the axis XX of both of the conveyors does not fit within a single module, the fixing structure has to occupy the second module as shown in Figure 6.1. In addition, the second and third conveyors were placed 400 mm below. As the profiles used were all the same, in terms of section measurements, and from the same supplier, they have a fixing mechanism between them also available on their catalogues, not being necessary to worry about the way of fixing the profiles between themselves.

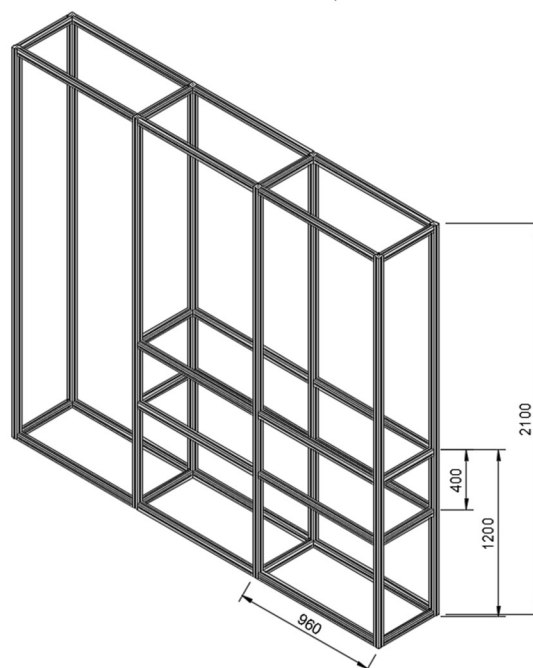


Figure 6.1 - Main support structure measurements

In addition, the supplier of these profiles also has another accessory available that enables components to be bolted onto the structure, Figure 6.1. This type of accessory is used to attach all of the previously presented conveyors assemblies to the main structure. This accessory was then placed inside the slots that the profile has and are specific for external components to be screwed on as they have a threaded hole. Furthermore, it was decided to choose an M6 thread diameter hole. Table 6.1 shows the accessory specifications.

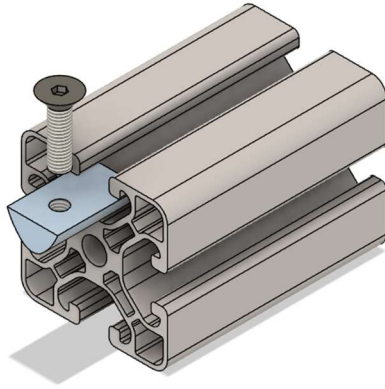


Figure 6.2 – External components support accessory

Table 6.1 – External components support accessory specifications [31]

<b>T-Slot Nut V 8 St M6</b>	
<b>Reference in Item Portugal</b>	0.0.480.50
<b>Line</b>	Line 8
<b>Weight</b>	10.3 g
<b>Thread</b>	M6
<b>Max. Force</b>	3500 N
<b>Torque</b>	14 N.m

The assembly method for the whole set was simple, starting by preparing the entire structure and the profiles to assemble the first conveyor. Next, it has to be mounted the bent sheets that support the conveyors with the accessories and the indicated screws. Finally, the conveyor has to be bolted to these structures as previously shown when it was presented the assembling of the first conveyor. Afterwards, the process has to be repeated for the second conveyor.

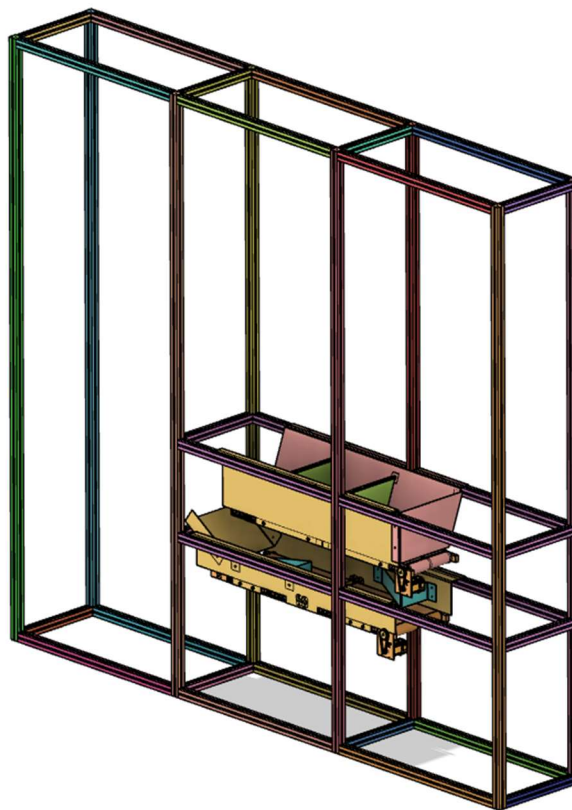


Figure 6.3 - Conveyors assembly in the main structure

For the module to be complete, the ramp that positions the boxes after they left the last conveyor still needs to be assembled. This ramp was obtained through a bending process and was made from 5000 series aluminium, AL 5754 with 2 mm of thickness.

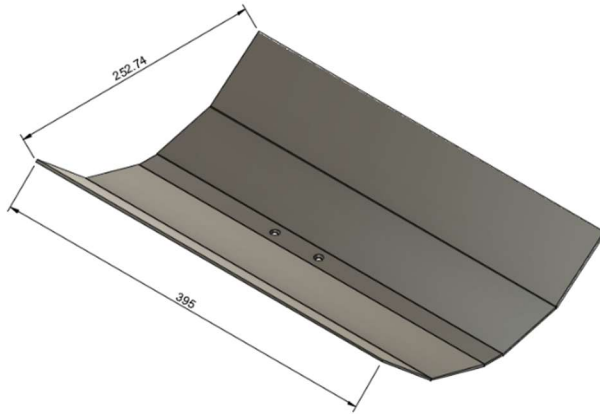


Figure 6.4 - Positioning ramp measurements

Table 6.2 - Positioning ramp specifications

		Ramp	
Density	$\rho$	2.66	$g/cm^3$
Volume	$V$	$2.307 \times 10^5$	$mm^2$
Mass	$m$	613.7	$g$
Thickness	$e$	2	$mm$

The assembly process of this component was simple, as the frame was made with the same technical profiles used in the structure. Subsequently, its assembled a bent sheet with the angle that the final curve needs to have for being connected to this structure, Figure 6.5. This sheet was made out of the aluminium series used in the previous components obtained through the same manufacturing process, Al 5754, and has 2 mm of thickness. It is also important to mention that the ramp that makes the positioning of the boxes has an inclination of  $25^\circ$  with the horizontal, being made from the construction of this component.

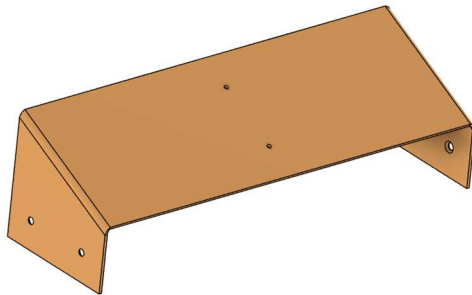


Figure 6.5 - Support for the positioning ramp

Table 6.3 - Support for the positioning ramp specifications

		Ramp support	
Density	$\rho$	2.66	$g/cm^3$
Volume	$V$	82544.16	$mm^2$
Mass	$m$	219.57	$g$
Thickness	$e$	2	$mm$

The wall that positions the boxes on the last required axis was made by a bending process and has the following geometry, Figure 6.6. Note that this sheet has 2 mm of thickness and has been made from the same material as the previous component, Al 5754.

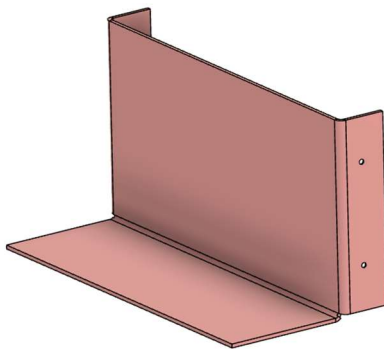


Figure 6.6 - Positioning wall

Table 6.4 - Positioning wall specifications

		Positioning wall	
Density	$\rho$	2.66	$g/cm^3$
Volume	$V$	$2.522 \times 10^5$	$mm^2$
Mass	$m$	670.85	$g$
Thickness	$e$	2	$mm$

The final assembly of this positioning module is represented in Figure 6.7.

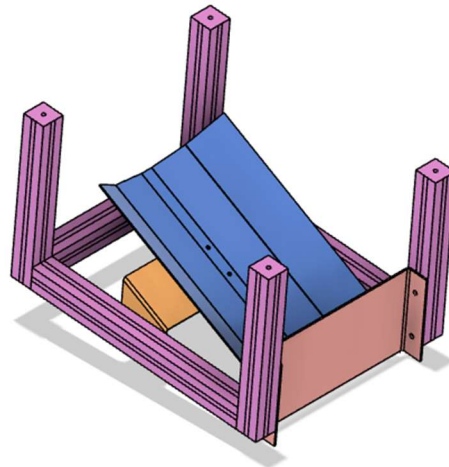


Figure 6.7 - Positioning module assembly

The whole model assembled is represented in Figure 6.8 and Figure 6.9. A human body with a height of 1800 mm was also introduced in order to have a point of comparison on the dimensions of the whole structure.

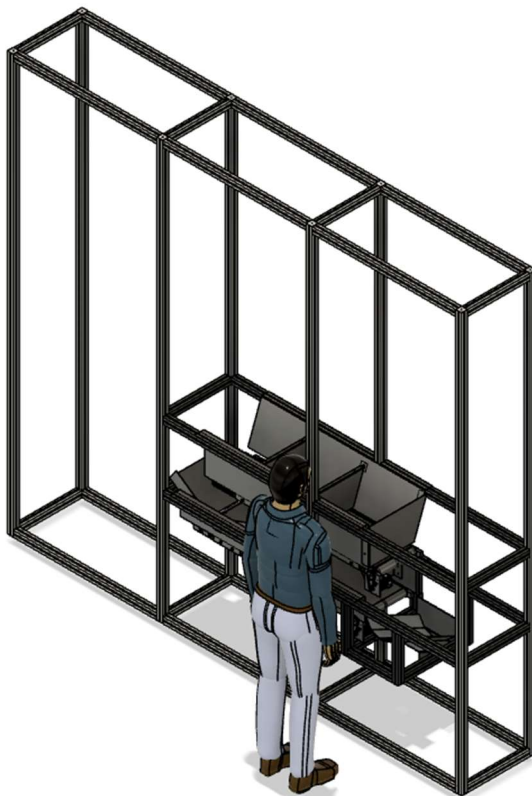


Figure 6.8 - Final assembly module 1



Figure 6.9 - Final assembly module 2

## 6.2 Bill of Materials (BoM) and cost estimation

A list of all the necessary materials was made where the main focus was the quotation of each component, even though there was not enough time to gather that information for all the components. Regarding machined components the quotation of such items was made through an on-line simulator in order to calculate an estimate price [38]. Many of the prices presented in the table are inflated due to the current state of the market and the lack of some materials in stock.

The list of all materials used is presented in Appendix C, while Table 6.5 presents the obtained cost that each section will have, as well as the total estimated price for all the components.

Table 6.5 – Total estimated costs

<b>Section</b>	<b>Price</b>
<b>First conveyor</b>	3132.736 €
<b>Second and third conveyor</b>	4303.75 €
<b>Positioning assembly</b>	539.31 €
<b>Control system</b>	-
<b>Total</b>	7975.79 €

*(Blank Page)*

## 7 Conclusions and future work

The main goal of this work was to develop a concept that would allow the separation, positioning and orientation of medicine boxes autonomously, which was entirely achieved and also a real prototype was built to verify its capabilities.

Besides, during the course of this work, the detailed design and specifications of the final concept was made, which includes the selection of standard products and the design of new components, whose behaviour under certain conditions was properly verified. Furthermore, with the development of this work, many of the competences acquired during this study cycle were put to the test, having also acquired new competences, due to the fact of carrying out the work in a business environment.

Despite having achieved all the objectives initially proposed for the completion of the project, there is still a long way to go to obtain a fully working model ready to be produced and marketed to the industry.

Although everything has been thought out and designed in detail, it is necessary to assemble the whole set and check that no possible flaws that were not detected during the development of this final model appear. Furthermore, it is necessary to develop a software capable of controlling the whole system autonomously.

On the other hand, and after having the whole system assembled, it is necessary to fine-tune small details, such as the correct positioning of the sensors to allow for maximum efficiency in the detection of the material and thus ensure the proper functioning of the system. It is also necessary to adjust some parameters that will only be possible to define after having the whole model assembled and with the performance of several tests until reaching a 100% operational synchronous movement.

Finally, and for this module to be fully complete, it is necessary to develop a mechanism that allows the removal of the box in its current position, so as to correctly identify each one of the boxes, leaving it up to the main system to store them on their warehouse.

Although the model is still far from being commercialised, the results achieved were quite satisfactory, considering the time interval in which all this work was carried out. Besides that, since this is the development of a model in which there are many associated variables, it is difficult to find a perfectly functional solution without going through an intensive testing phase.

*(Blank Page)*

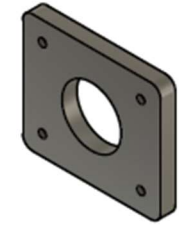
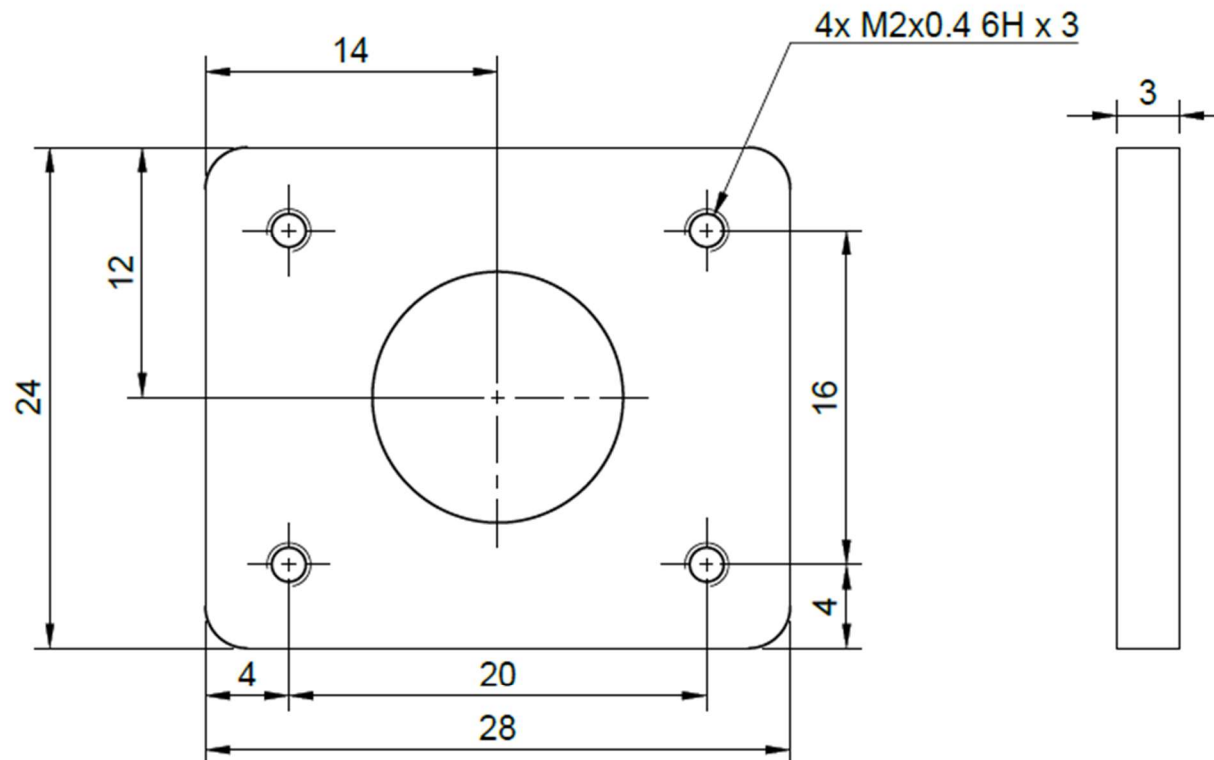


## References

- [1] SIER, “Sier Webpage,” 2022. <https://www.sier.pt/>.
- [2] L. Pečený, P. Meško, R. Kampf, and J. Gašparík, “Optimisation in Transport and Logistic Processes,” in *Transportation Research Procedia*, 2020, vol. 44, doi: 10.1016/j.trpro.2020.02.003.
- [3] C. Scott, H. Lundgren, and P. Thompson, “Introduction to Supply Chain Management BT - Guide to Supply Chain Management,” C. Scott, H. Lundgren, and P. Thompson, Eds. Berlin, Heidelberg: Springer Berlin Heidelberg, 2011, pp. 1–8.
- [4] A. S. U. Rembold; B.O. Nnaji, *Computer Integrated Manufacturing and Engineering*. Addison-Wesley, 1993.
- [5] T. Contributor, “Warehouse control system (WCS),” *TechTarget*, 2010.
- [6] J. Karásek, “An overview of warehouse optimization,” *Int. J. Adv. Telecommun. Electrotech. signals Syst.*, vol. 2, no. 3, pp. 111–117, 2013.
- [7] A. Solutions, “ASRS,” 2022. <https://adaptecsolutions.com/automation/asrs-cranes/> (accessed Jun. 06, 2022).
- [8] REMOCO, “Vertical Carousels,” 2022. <https://remcoequipment.com/product-solutions/lifts-carousels/vertical-carousels/> (accessed Jun. 06, 2022).
- [9] SwissLog, “Mini load ASRS for your light goods logistics,” 2022. <https://www.swisslog.com/en-us/products-systems-solutions/asrs-automated-storage-retrieval-systems/boxes-cartons-small-parts-items>.
- [10] SwissLog, “F. Hoffmann-La Roche, Switzerland: Industry 4.0 cold store logistics,” 2022. <https://www.swisslog.com/en-us/case-studies-and-resources/case-studies/2016/07/roche-kaiseraugst> (accessed Jun. 25, 2022).
- [11] Swisslog, “Automated guided vehicles AGV: The mobile solution of the future,” 2022. <https://www.swisslog.com/en-us/products-systems-solutions/transport/agv-automated-guided-vehicles> (accessed Jun. 06, 2022).
- [12] R. Automation, “Automated Guided Vehicles,” 2022. <https://www.roboticautomation.com.au/>.
- [13] N. AGV, “AGV in Hospitals. Autonomous Mobile Robots Disrupting Healthcare Automation,” 2022. <https://www.agvnetwork.com/Automation-Hospitals-AGV-Autonomous-Mobile-Robots>.
- [14] DEMATIC, “Healthcare solutions.” <https://www.dematic.com/pt-pt/industrias/visao-geral-de-industrias/saude/> (accessed Jun. 25, 2022).
- [15] KNAPP, “Healthcare Solutions,” 2022. <https://www.knapp.com/en/solutions/sectors/healthcare-logistics-from-pallet-to-pill/>.
- [16] M. O. Qureshi and R. Sajjad, “A study of integration of robotics in the hospitality sector and its emulation in the pharmaceutical sector,” *Heal. Sci. J.*, vol. 11, no. 1, p. 1, 2017.
- [17] R. E. Sarthois, “Quand un robot arrive à la pharmacie de l’hôpital,” 2019. [https://actu.fr/pays-de-la-loire/le-mans\\_72181/video-mans-quand-robot-arrive-la-pharmacie-lhopital\\_29983362.html](https://actu.fr/pays-de-la-loire/le-mans_72181/video-mans-quand-robot-arrive-la-pharmacie-lhopital_29983362.html) (accessed May 16, 2022).
- [18] ROWA, “Easy Load,” 2022. <https://rowa.de/en/products/store-pick/bd-rowa-vmax/> (accessed May 10, 2022).

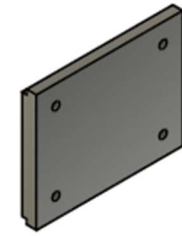
- [19] Gollman, “GoCompact,” 2022. <https://www.gollmann.com/de/> (accessed May 10, 2022).
- [20] Mekapharm, “MekaPharm,” 2022. <http://mekapharm.com/en/>.
- [21] Omnicell, “Fill in box,” 2022. <https://www.omnicell.com/products/fill-in-box-automated-filling-system> (accessed May 10, 2022).
- [22] PolyLanema, “Aluminium Materials Selection,” 2022. .
- [23] MegaDyne, “Flat Belt,” 2022. <https://megadynegroup.com/pt> (accessed Jun. 11, 2022).
- [24] J. E. Shigley, *Shigley’s mechanical engineering design*. Tata McGraw-Hill Education, 2011.
- [25] MISUMI, “Automation Components,” 2022. <https://uk.misumi-ec.com/>.
- [26] International Organization for Standardization, *ISO 15147:2012 – “Light conveyor belts – Tolerances on widths and lengths of cut light conveyor belts.”* 2012.
- [27] HABASIT, “CONVEY-SeleCalc,” 2022. [Online]. Available: <https://www.habasit.com/en/Support-and-Services/Selection-and-calculation>.
- [28] V. V Athani, *Stepper motors: fundamentals, applications and design*. New Age International, 1997.
- [29] Nanotec, “Nanotec,” 2022. <https://en.nanotec.com/products/154-stepper-motors-ip65>.
- [30] J. Tang, “Motor Sizing Basics Part 2: How to Calculate Load Inertia,” *OrientalMotors*, 2020. <https://blog.orientalmotor.com/motor-sizing-basics-part-2-load-inertia> (accessed Jun. 16, 2022).
- [31] I. Portugal, “Support Structure,” 2022. <https://pt-product.item24.com/pt/catalogo/products/mb-building-kit-system-1001009411/> (accessed Jun. 27, 2022).
- [32] IGUS, “Sleeve bearings,” 2022. <https://www.igus.co.uk/> (accessed Jun. 13, 2022).
- [33] S. Zhang and X. Xia, “Modeling and energy efficiency optimization of belt conveyors,” *Appl. Energy*, vol. 88, no. 9, pp. 3061–3071, 2011.
- [34] SKF, “Bearing coefficient of friction,” 2022. <https://www.skf.com/group/products/plain-bearings/spherical-plain-bearings-rod-ends/principles/friction> (accessed Jun. 08, 2022).
- [35] Beckhoff, “Controller Solutions.” <https://www.beckhoff.com/en-gb/> (accessed Jun. 25, 2022).
- [36] M. Weel, “Power Unit supplier.” <https://www.meanwell.com/productSeries.aspx?i=17&c=6#tag-6-17> (accessed Jun. 29, 2022).
- [37] Banner, “Photoelectric sensors.” <https://www.bannerengineering.com/us/en/products/sensors/photoelectric-sensors.html#all> (accessed Jun. 29, 2022).
- [38] WEERG, “Free Instant Quote,” 2022. <https://www.weerg.com/en/global/cnc-3d-print-online-services-quote?hsCtaTracking=b0d7f160-2ebc-43d9-902e-baed23531b4a%7C346bd6e5-8152-4d31-b64e-6f2fab4dba2b> (accessed Jun. 01, 2022).

# Appendix A - Technical Drawings

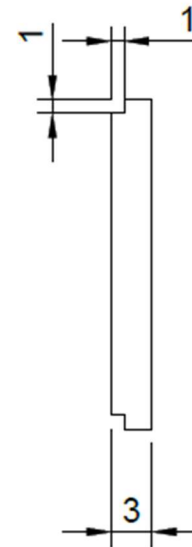
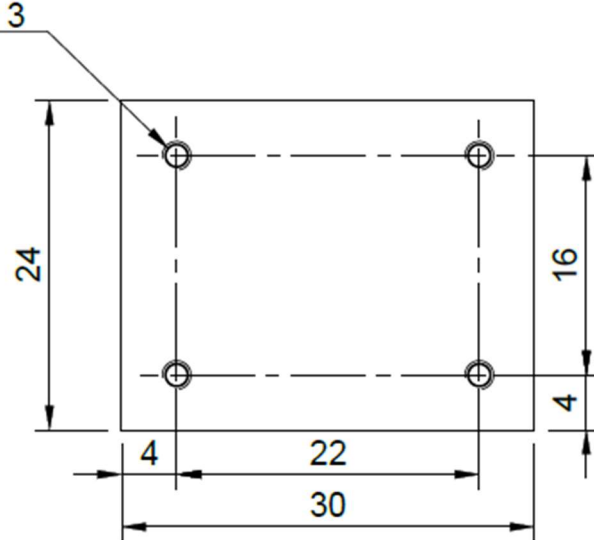


ISO 8015  
ISO 2768-mK

Dept.	Technical reference	Created by Tiago Barreira 03/07/2022	Approved by		
Material: Al 7075		Document type	Document status		
		Title Bearing Cover	DWG No.		
			Rev.	Date of issue	Sheet 1/1

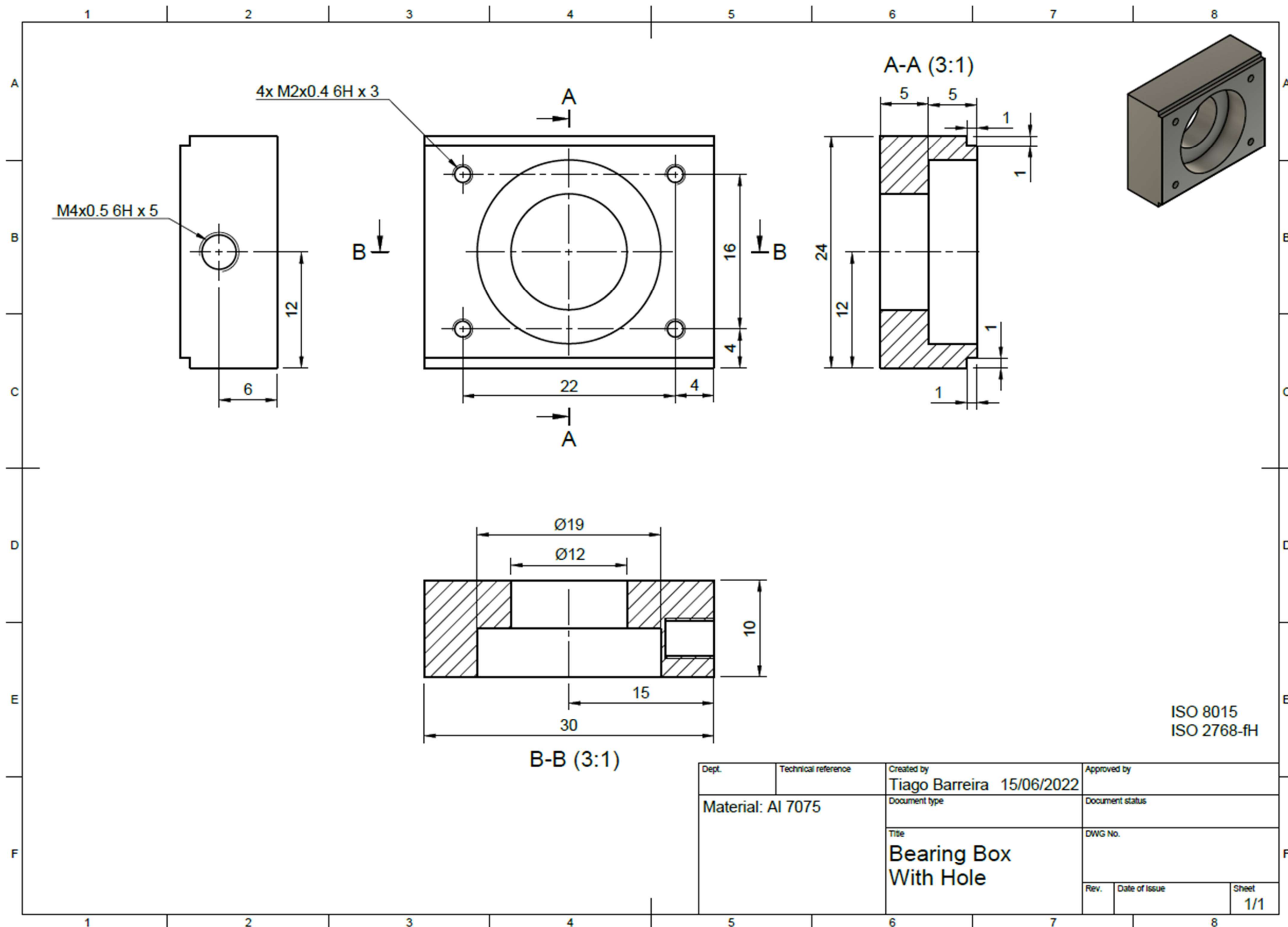


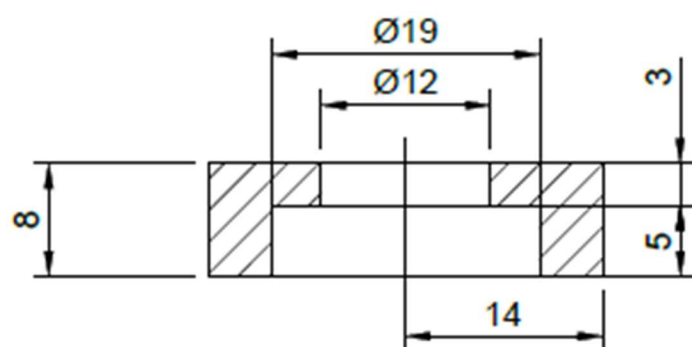
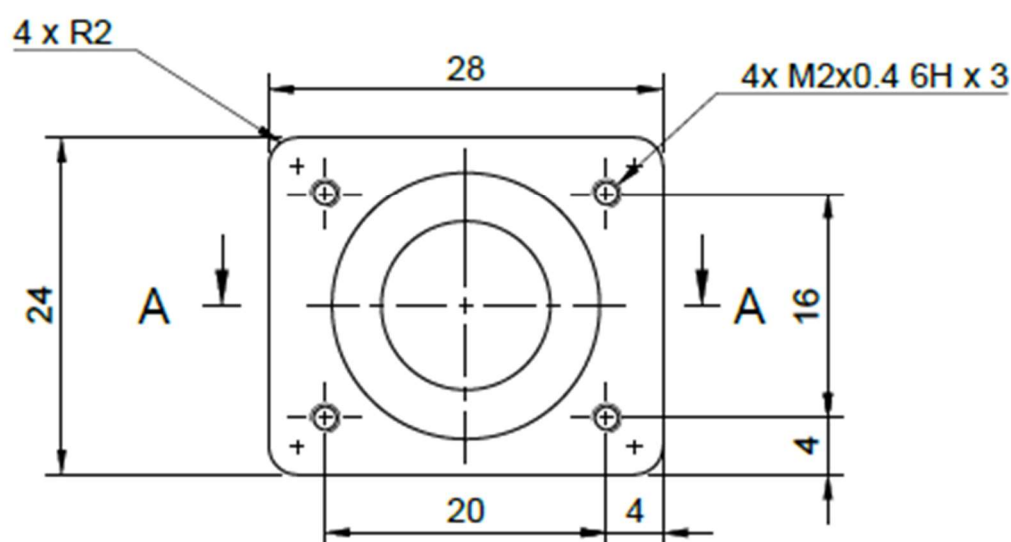
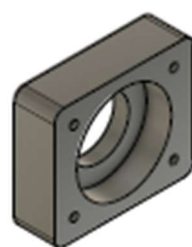
4x M2x0.4 6H x 3



ISO 8015  
ISO 2768-fH

Dept.	Technical reference	Created by <b>Tiago Barreira 15/06/2022</b>	Approved by	
<b>Material: Al 7075</b>		Document type	Document status	
		Title <b>Bearing Cover 2</b>	DWG No.	
		Rev.	Date of issue	Sheet <b>1/1</b>

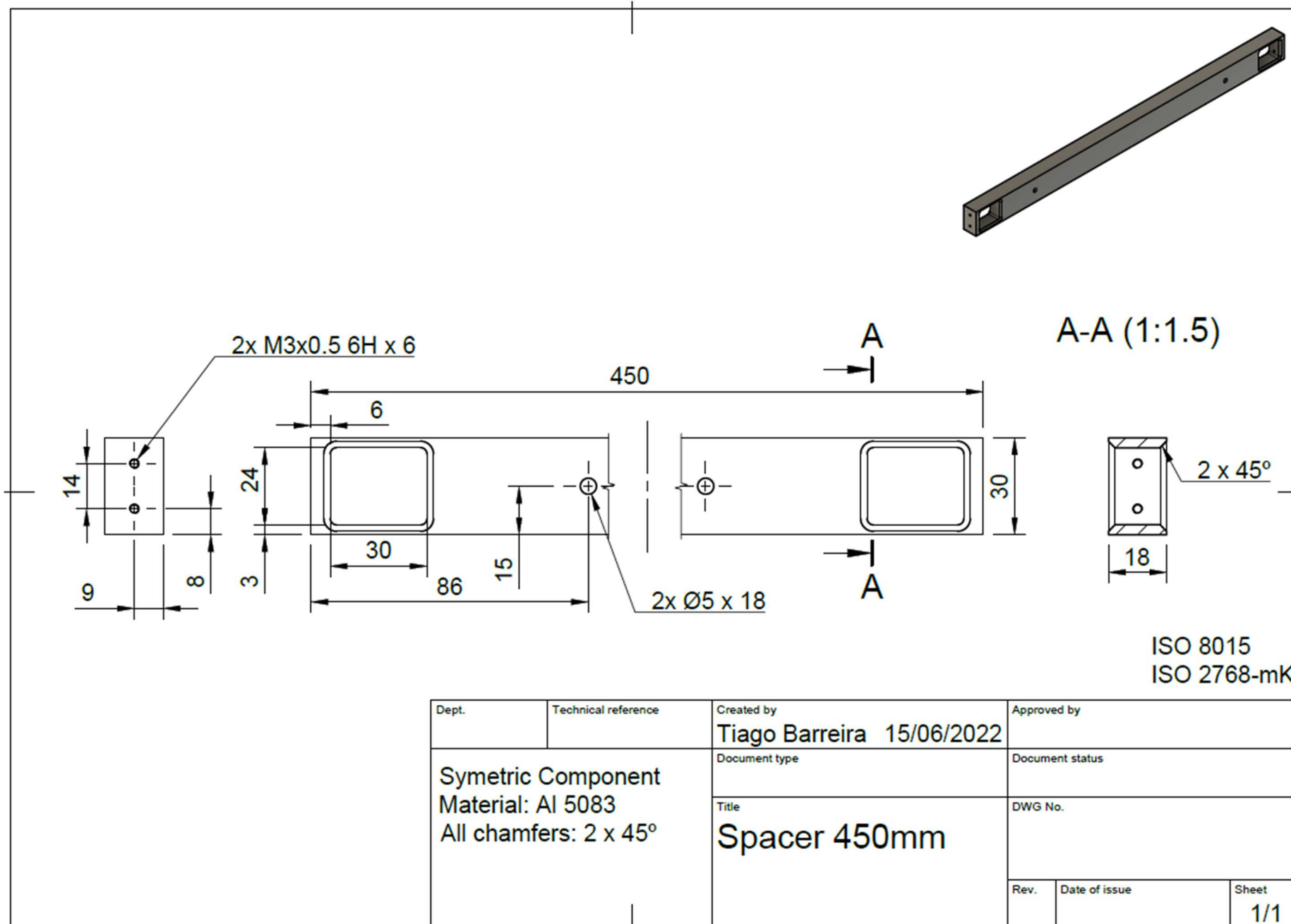




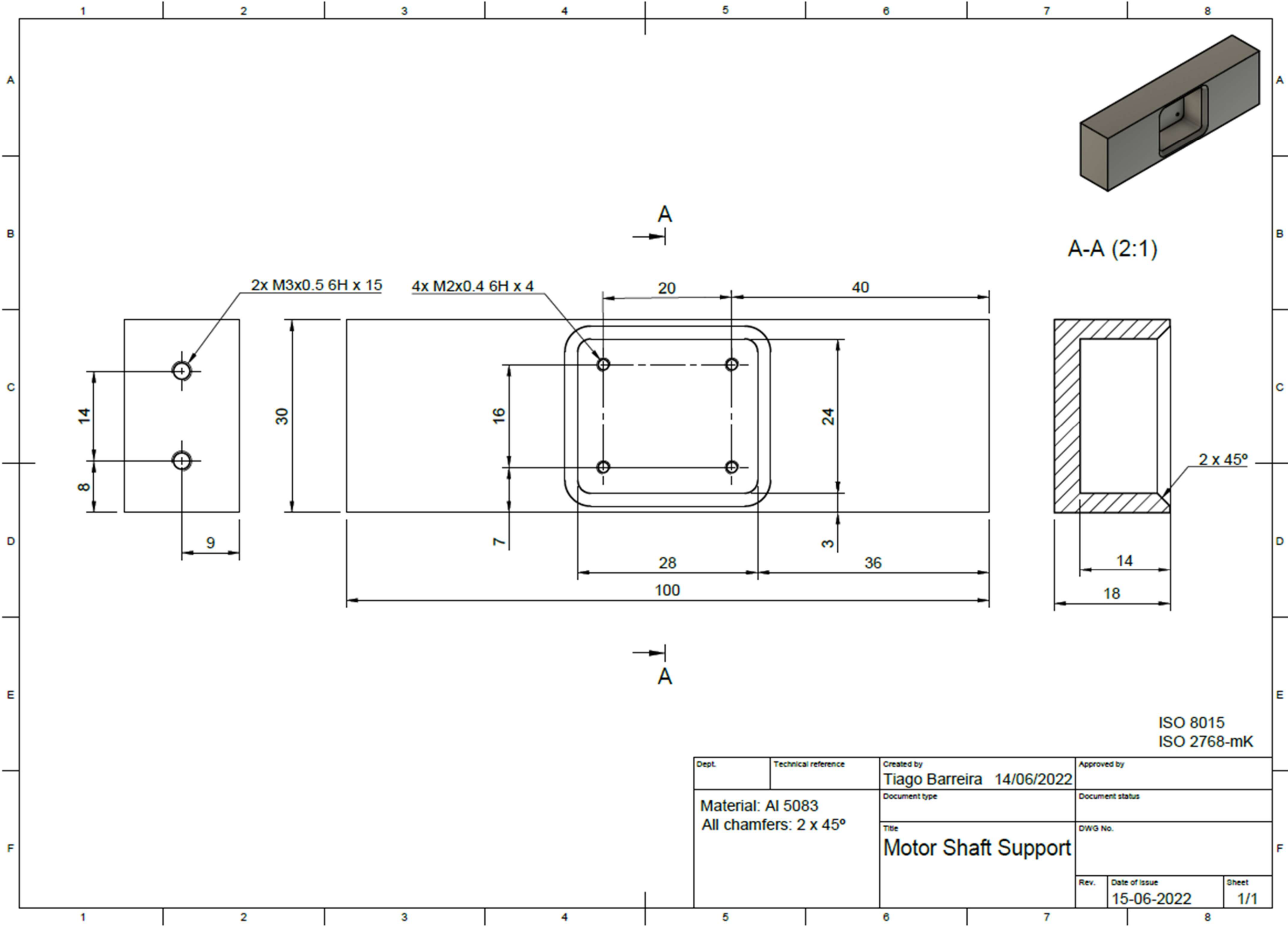
A-A (2:1)

ISO 8015  
ISO 2768-mK

Dept.	Technical reference	Created by Tiago Barreira 15/06/2022	Approved by
Material: Al 7075		Document type	Document status
		Title Bearing box Without hole	DWG No.
		Rev.	Date of issue
		Sheet	1/1

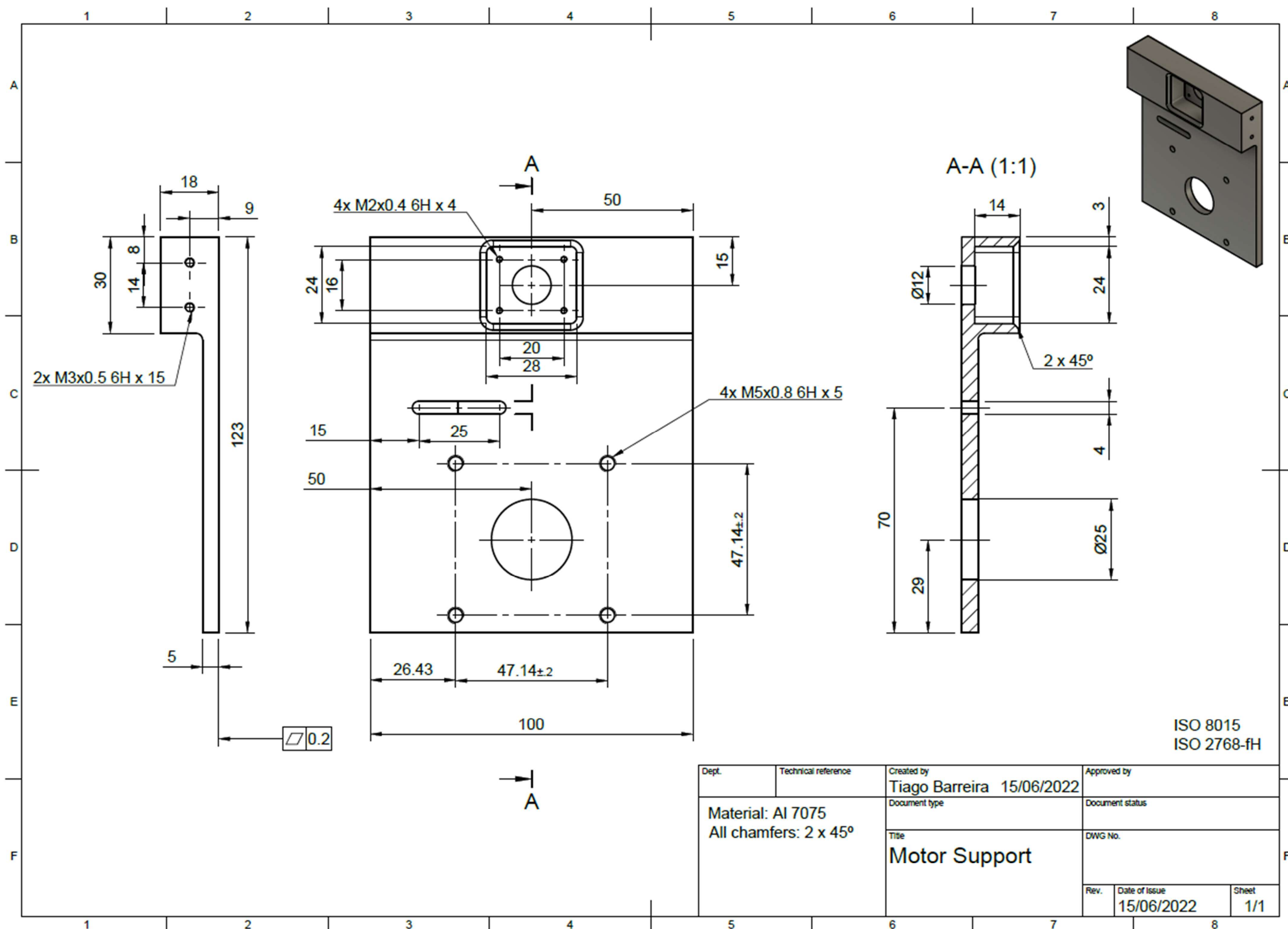


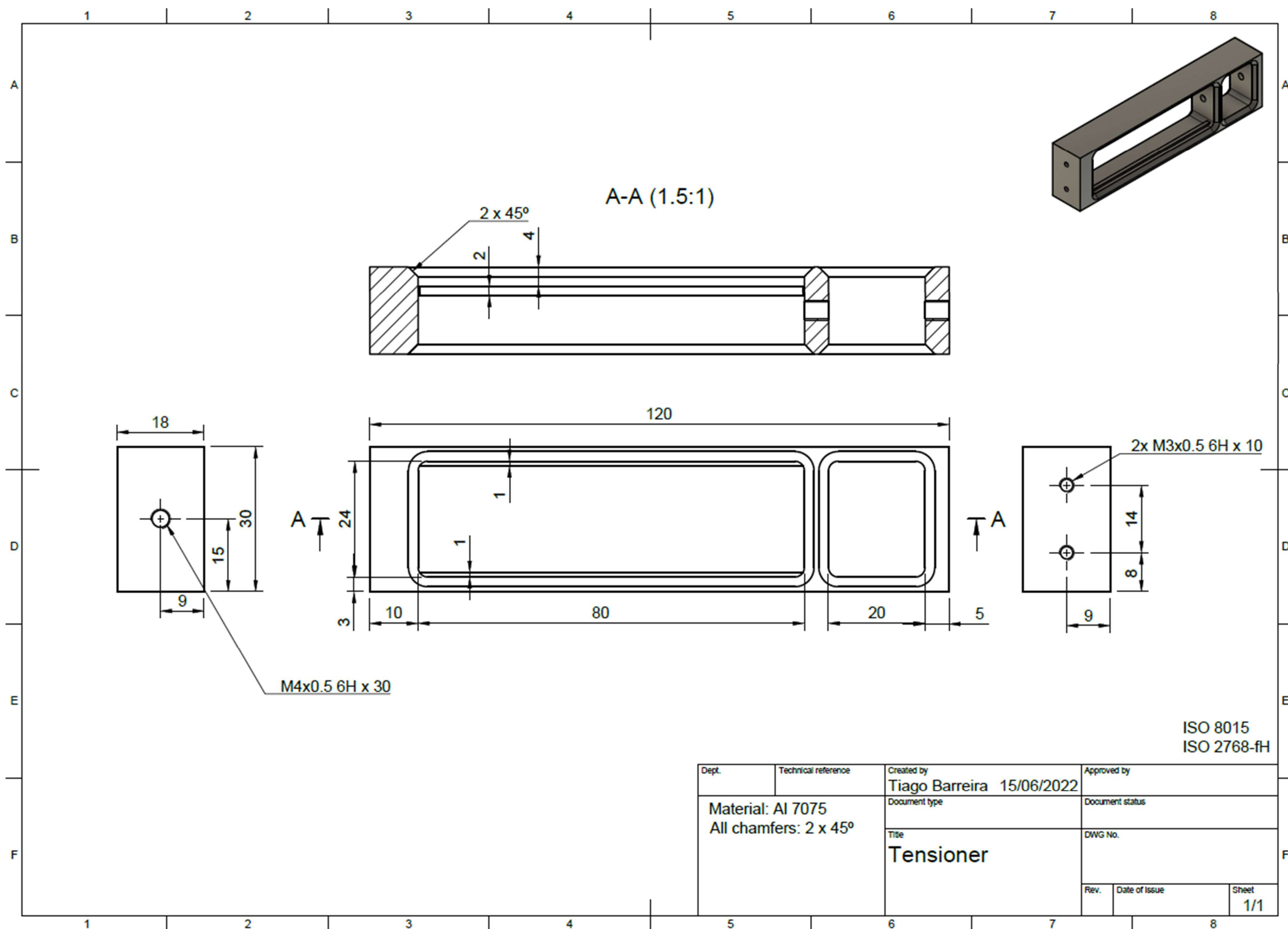


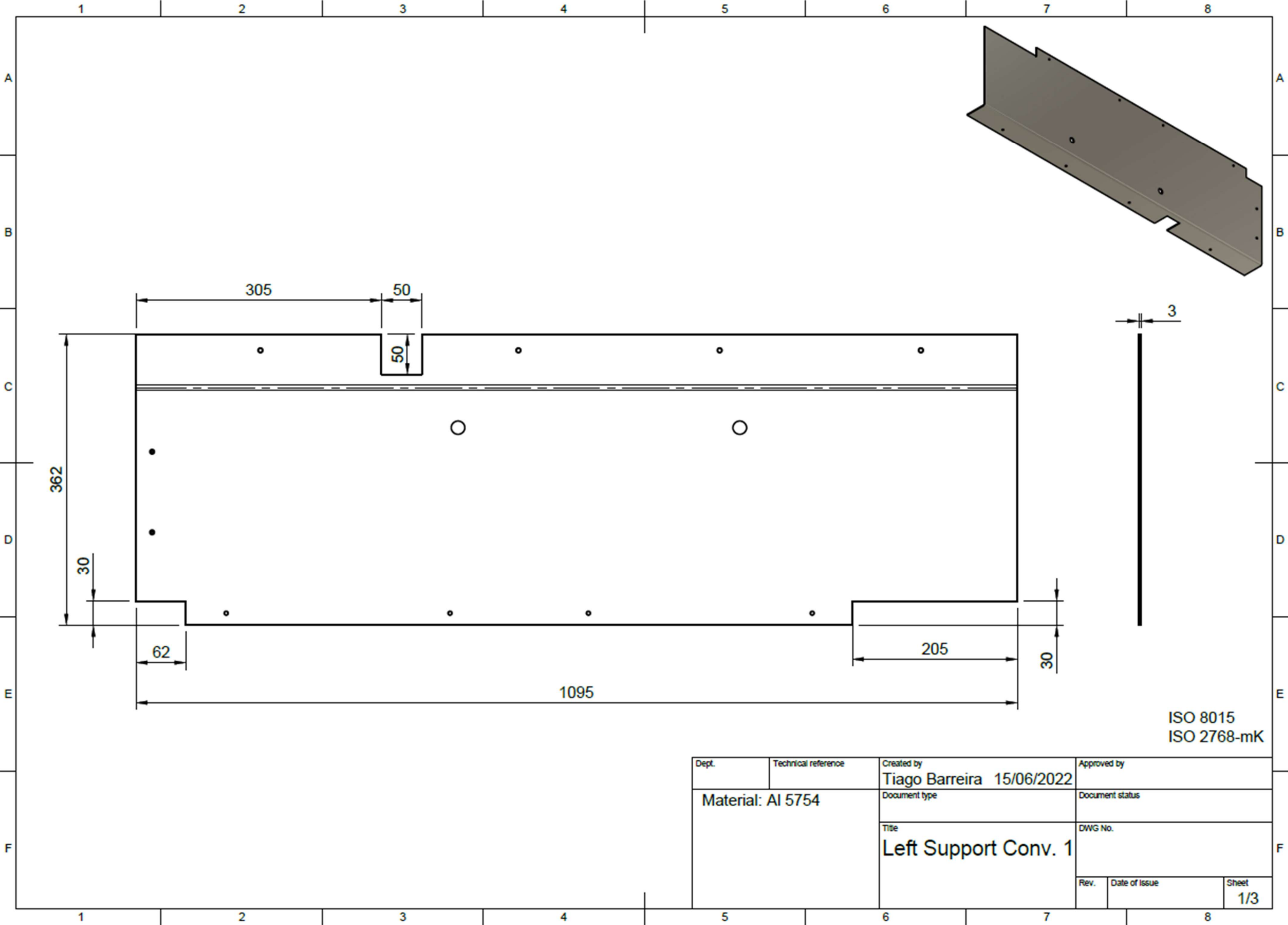


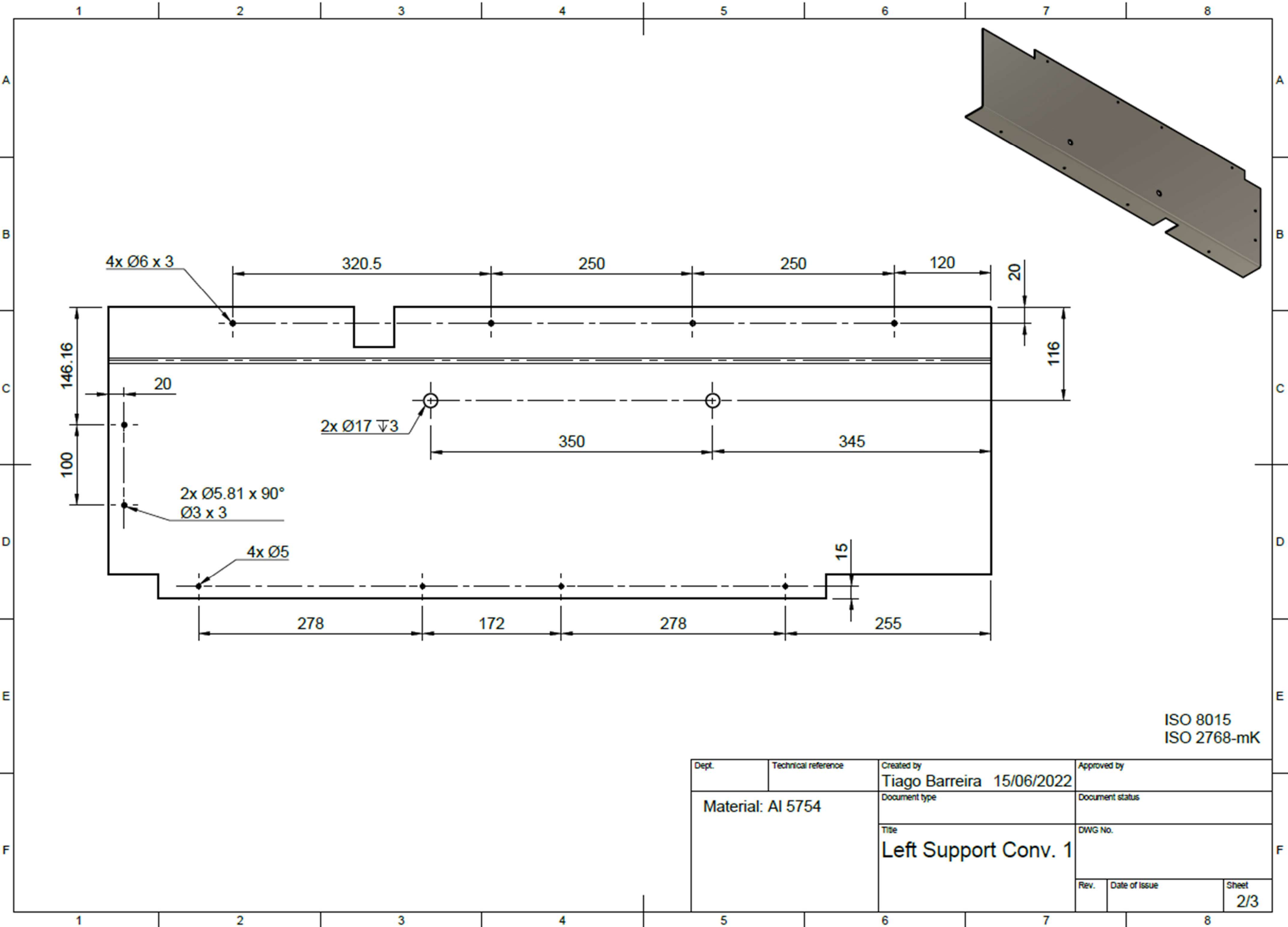
ISO 8015  
ISO 2768-mK

Dept.	Technical reference	Created by Tiago Barreira 14/06/2022	Approved by
Material: Al 5083 All chamfers: 2 x 45°		Document type	Document status
		Title Motor Shaft Support	DWG No.
Rev.	Date of issue 15-06-2022	Sheet 1/1	



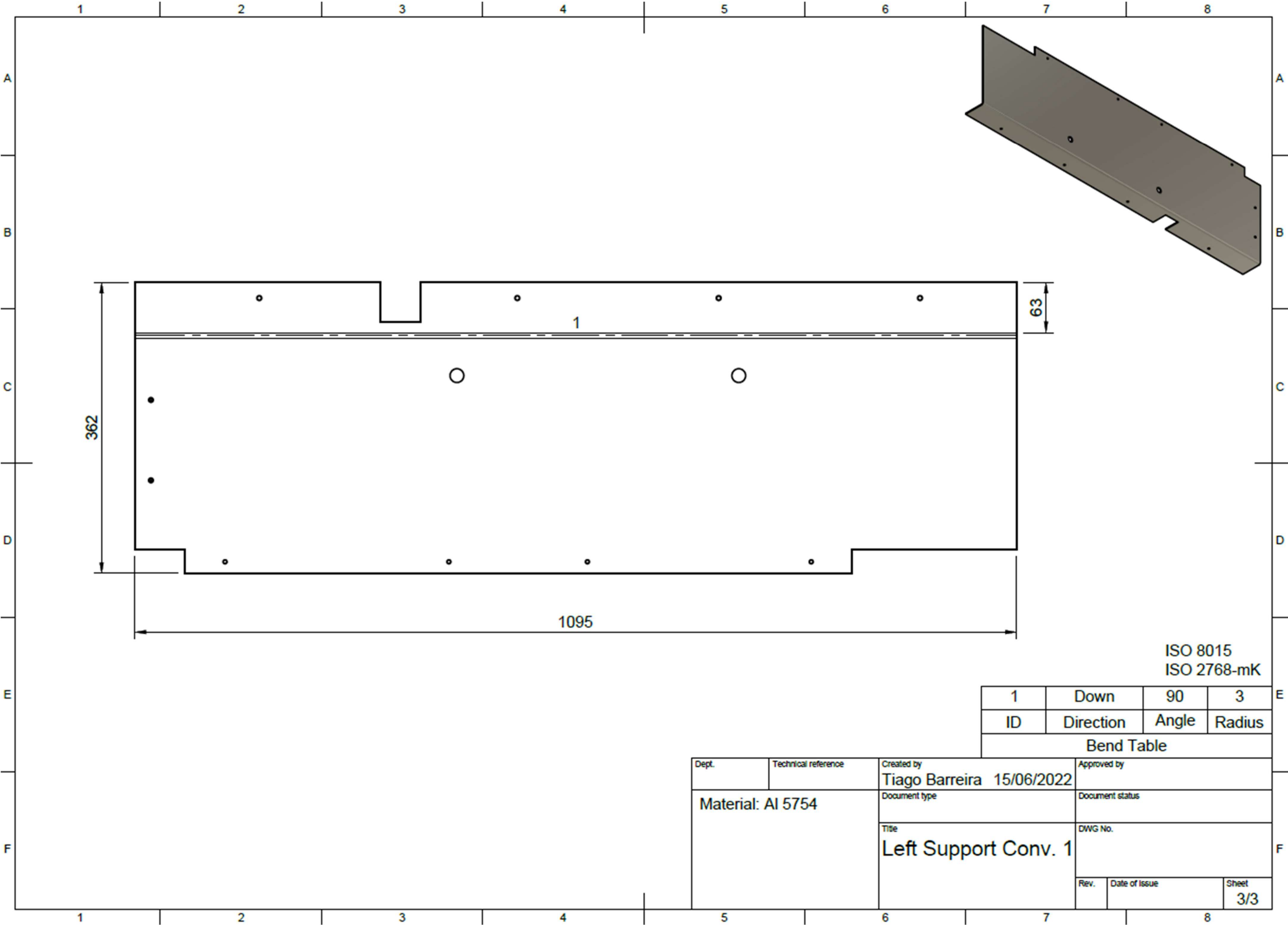


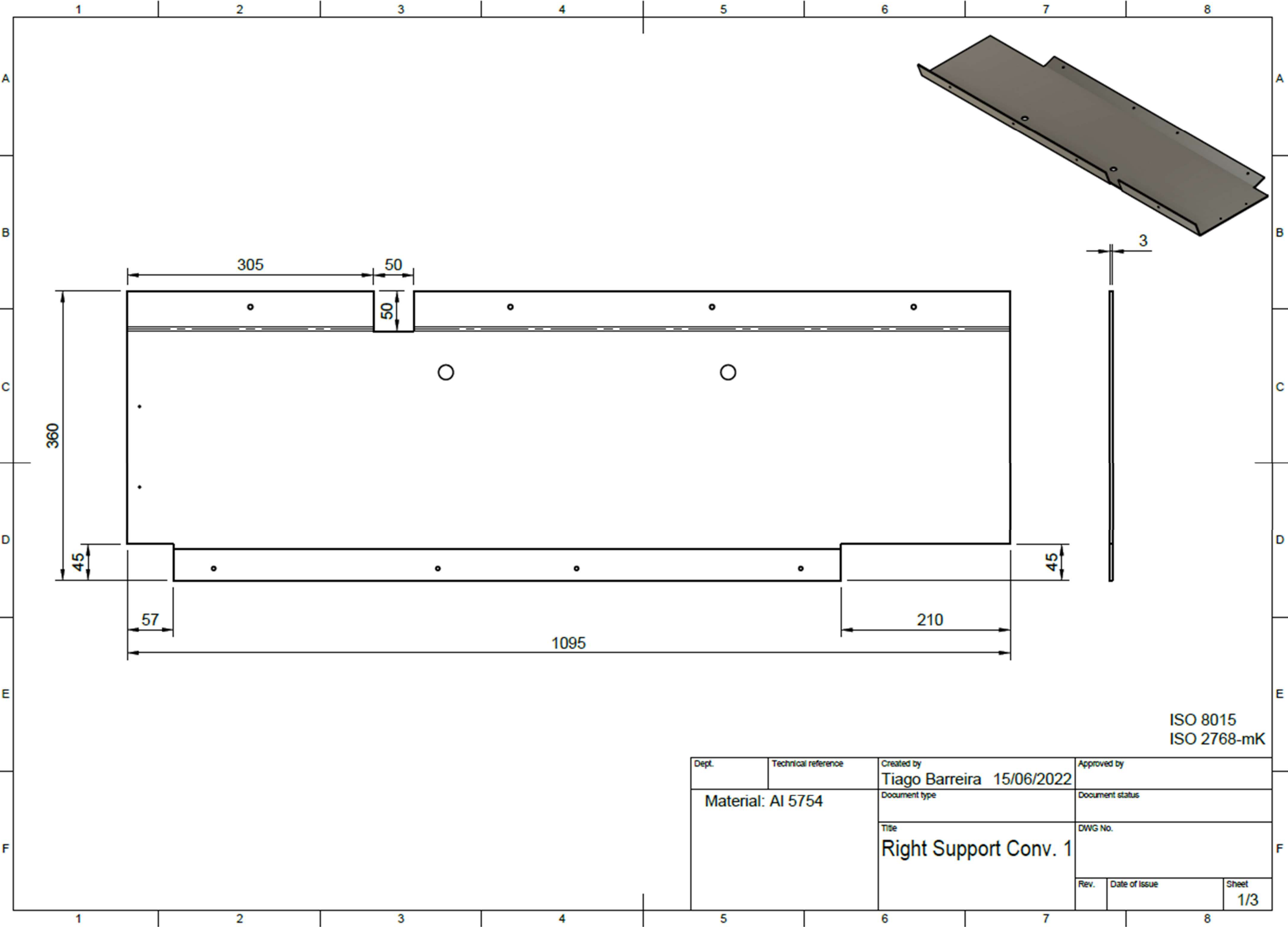




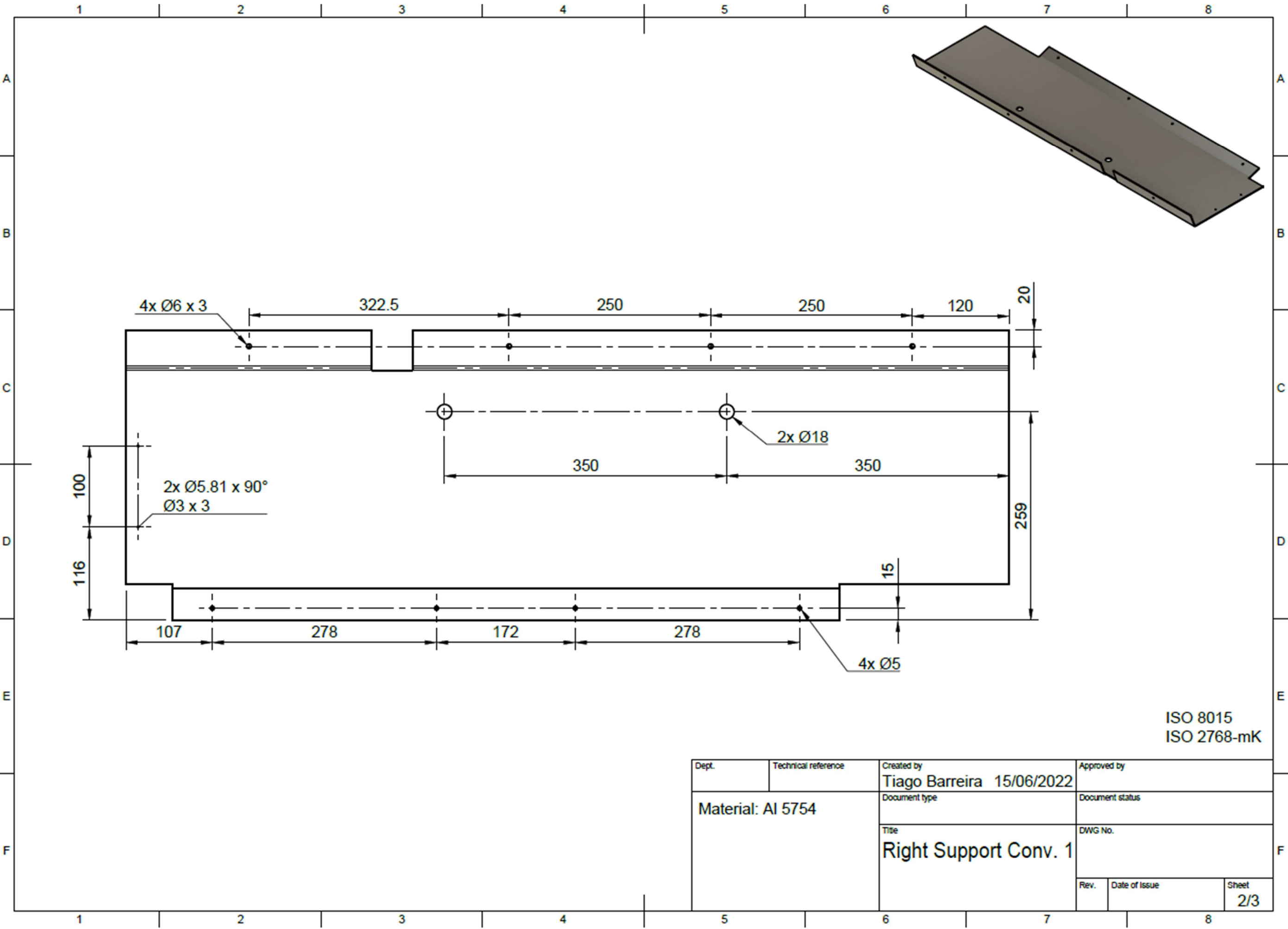
ISO 8015  
ISO 2768-mK

Dept.	Technical reference	Created by Tiago Barreira 15/06/2022	Approved by
Material: Al 5754		Document type	Document status
		Title Left Support Conv. 1	DWG No.
		Rev.	Date of Issue
			Sheet 2/3



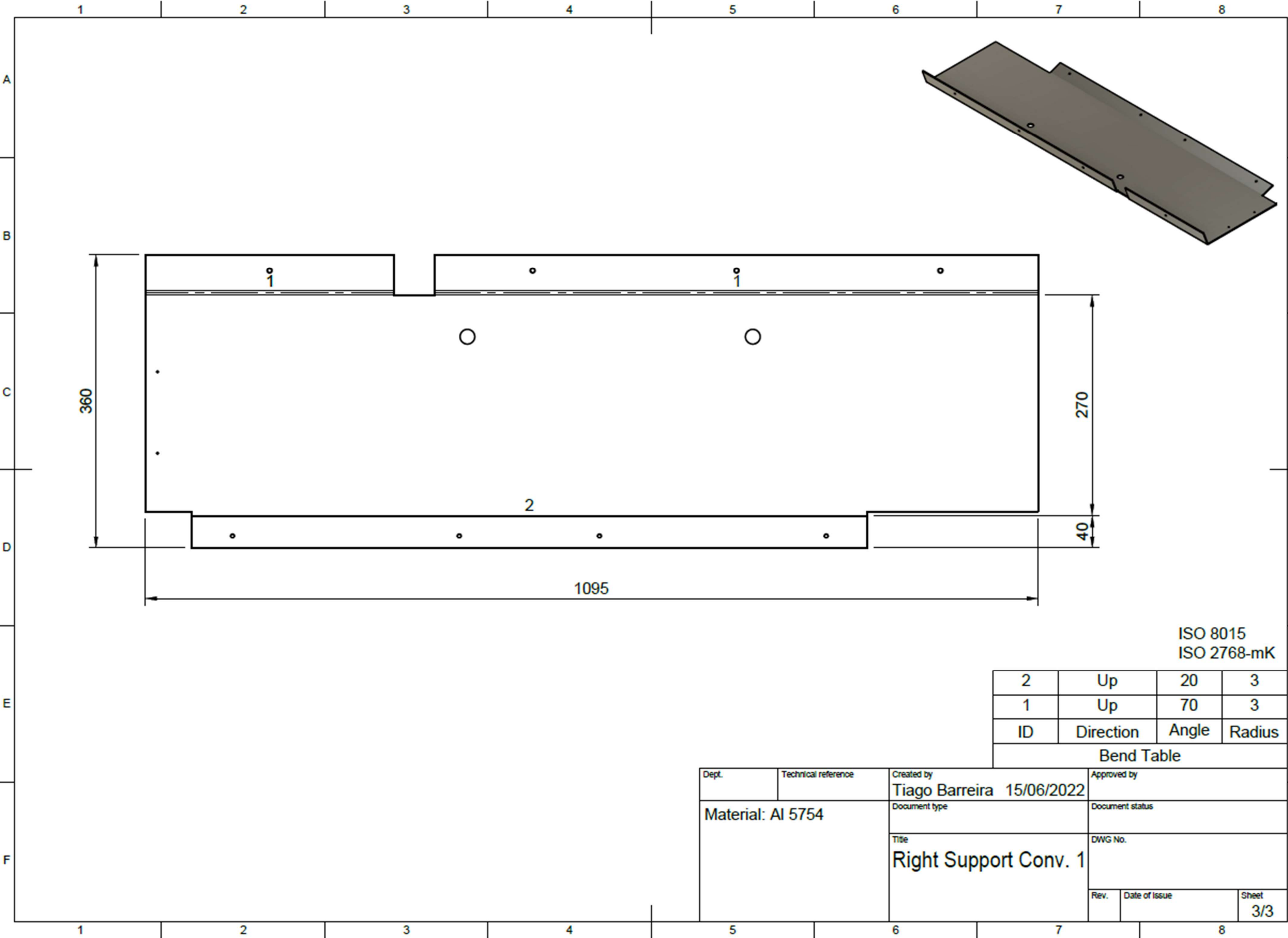






Dept.	Technical reference	Created by Tiago Barreira 15/06/2022	Approved by
Material: Al 5754		Document type	Document status
		Title Right Support Conv. 1	DWG No.
Rev.	Date of Issue	Sheet 2/3	



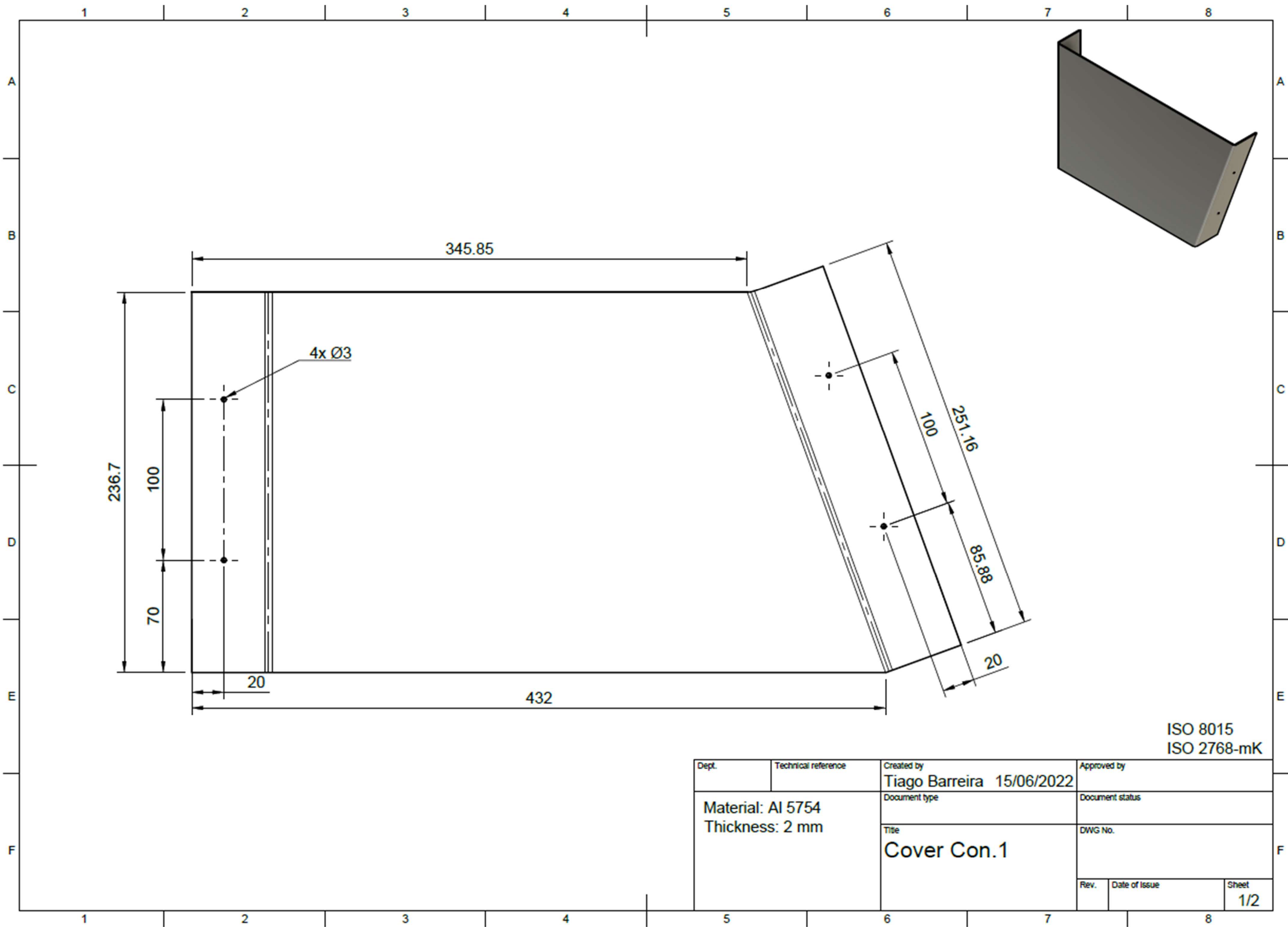


ISO 8015  
ISO 2768-mK

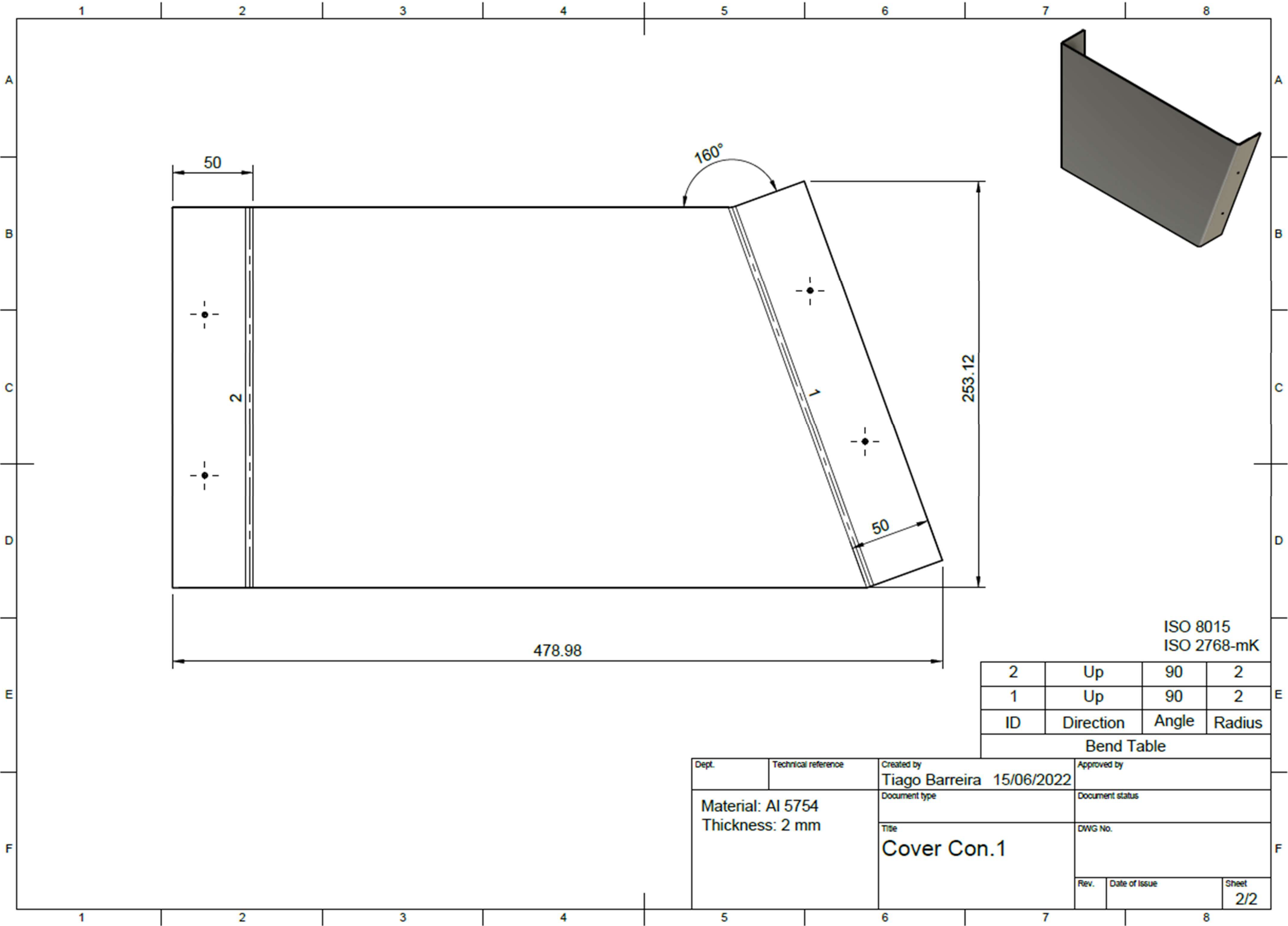
2	Up	20	3
1	Up	70	3
ID	Direction	Angle	Radius

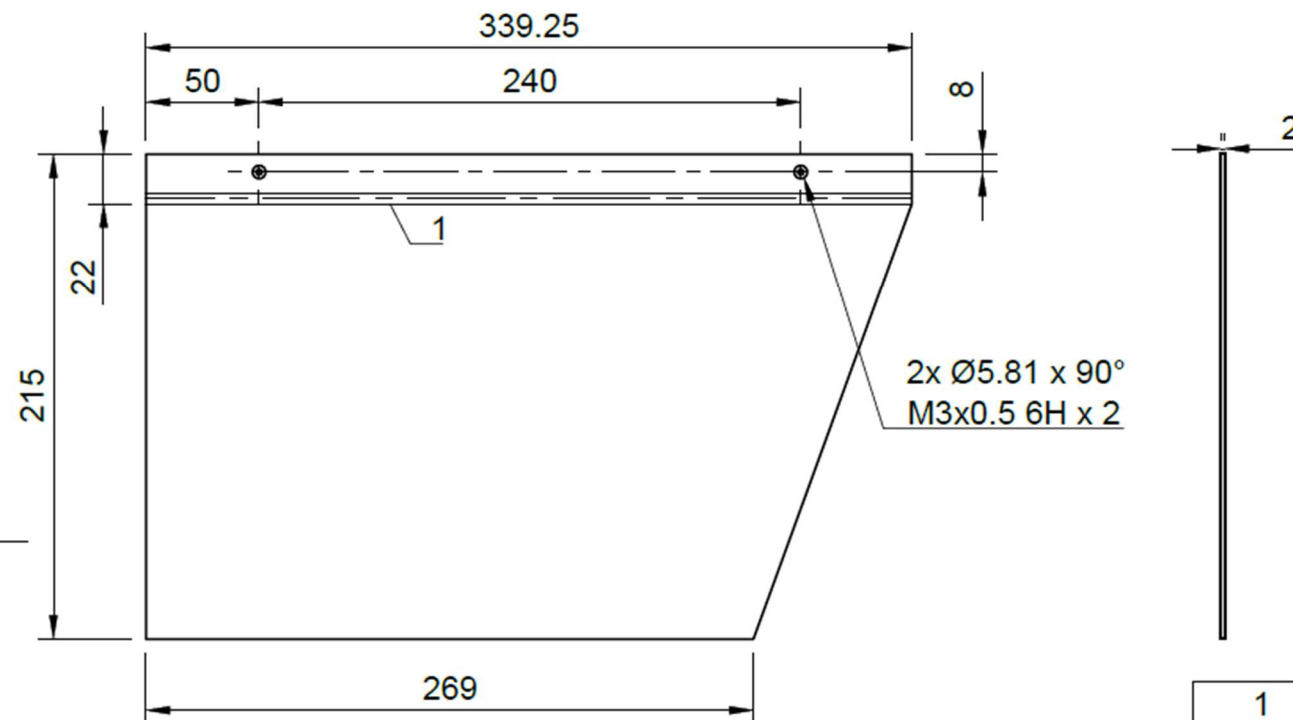
Bend Table

Dept.	Technical reference	Created by Tiago Barreira 15/06/2022	Approved by		
Material: AI 5754		Document type	Document status		
		Title Right Support Conv. 1	DWG No.		
			Rev.	Date of Issue	Sheet 3/3



0



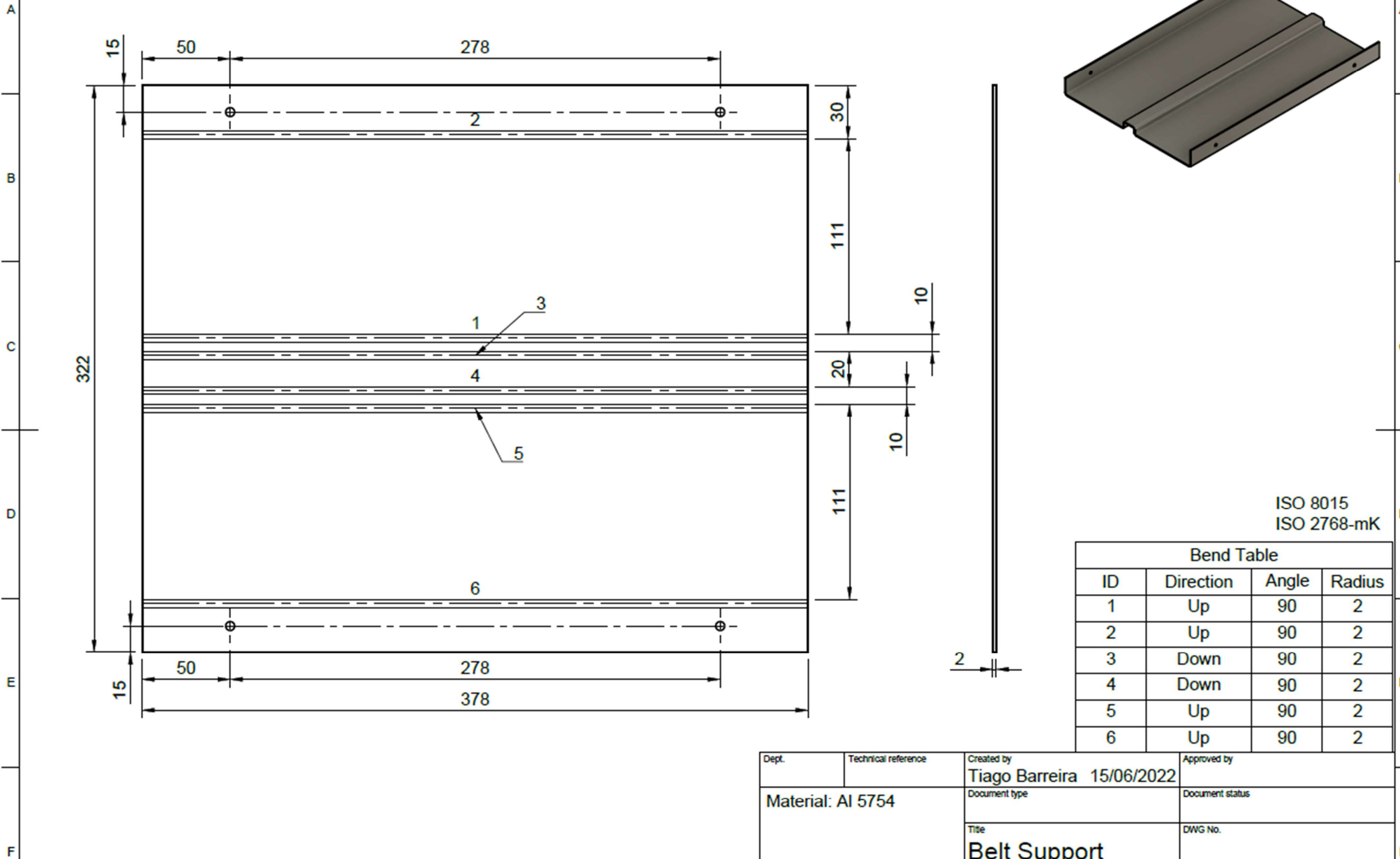


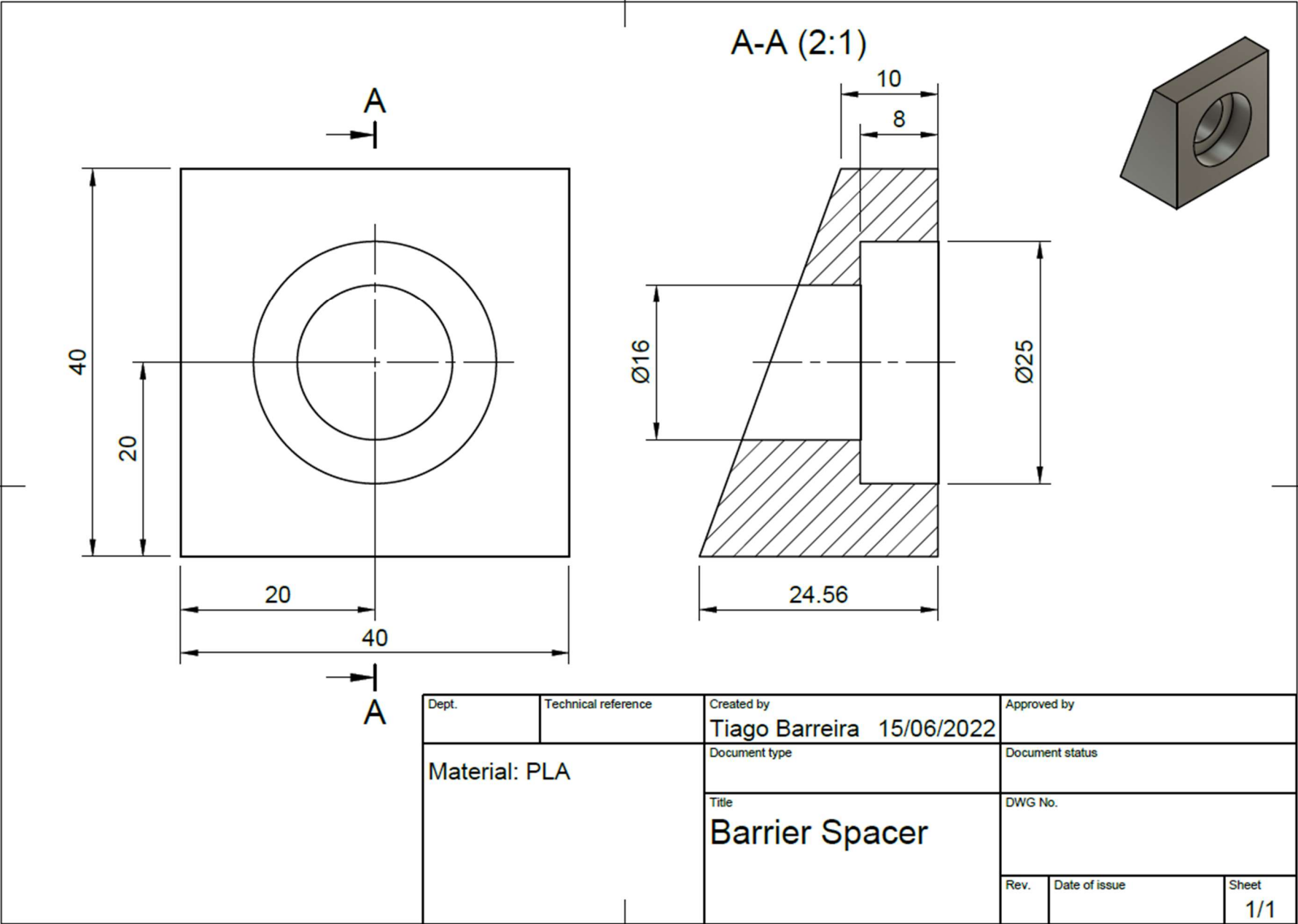
ISO 8015  
ISO 2768-mK

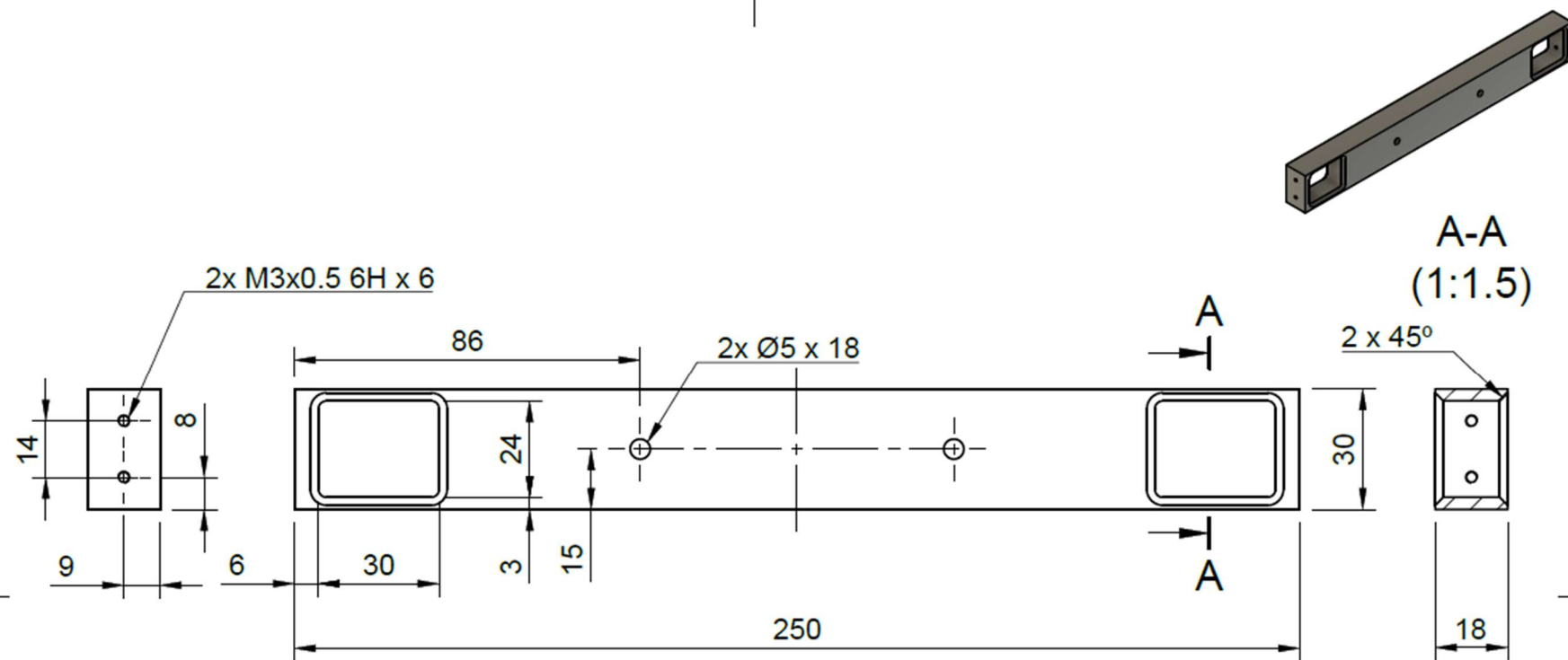
1	Down	90	2
ID	Direction	Angle	Radius

Bend Table

Dept.	Technical reference	Created by Tiago Barreira 15/06/2022	Approved by	
Material: Al 5754		Document type	Document status	
		Title Barrier	DWG No.	
			Rev.	Date of issue



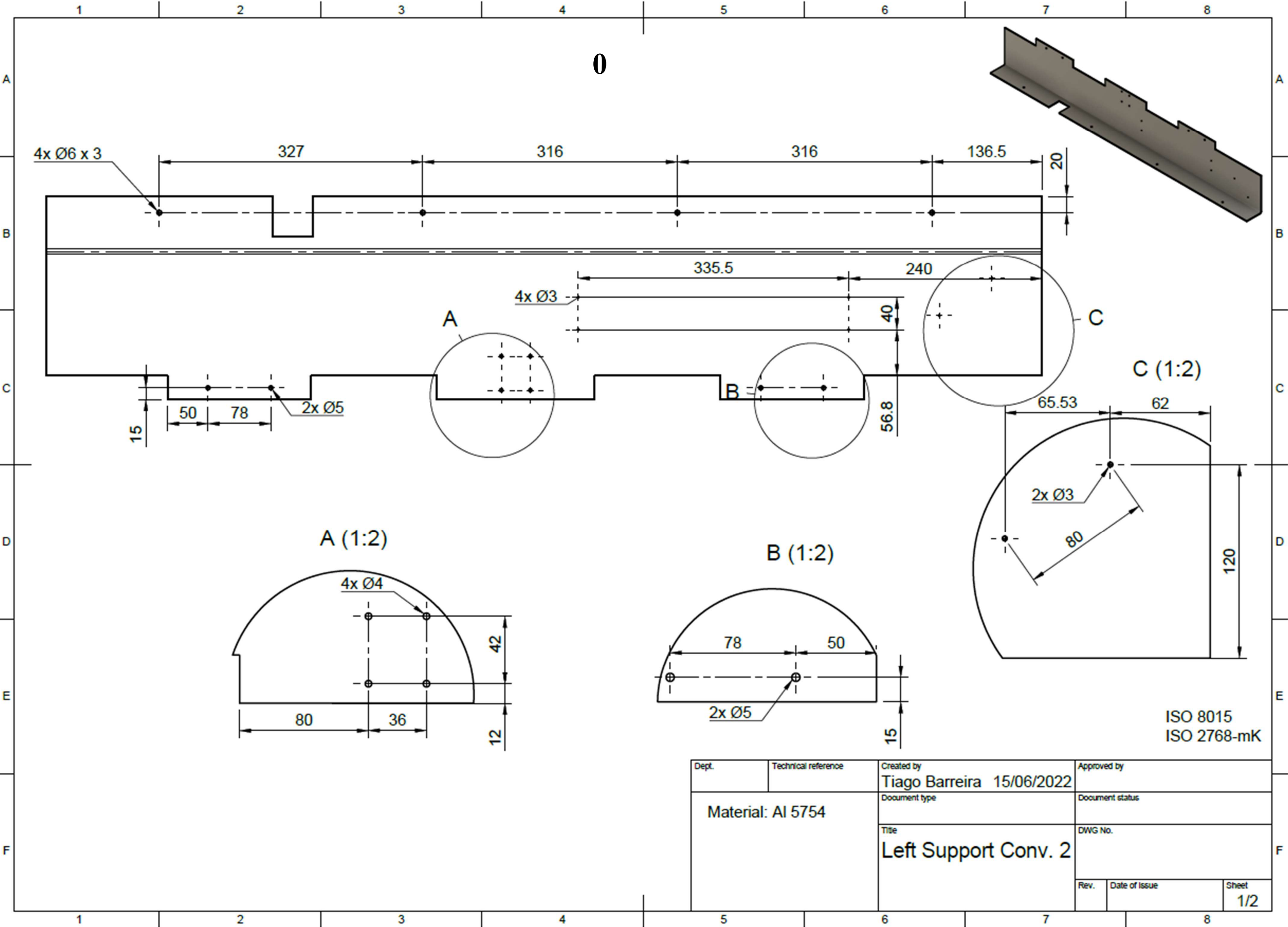




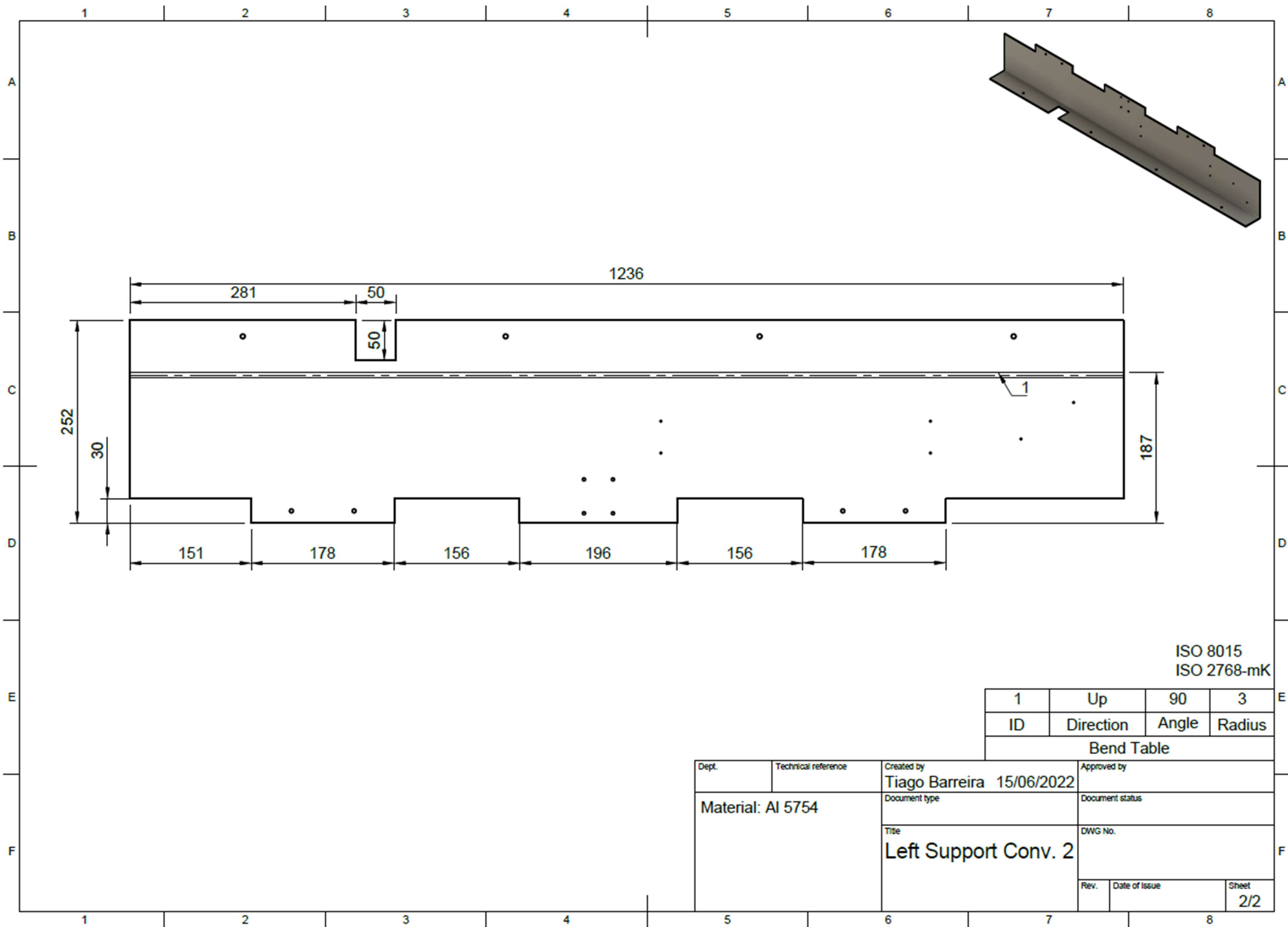
ISO 8015  
ISO 2768-mK

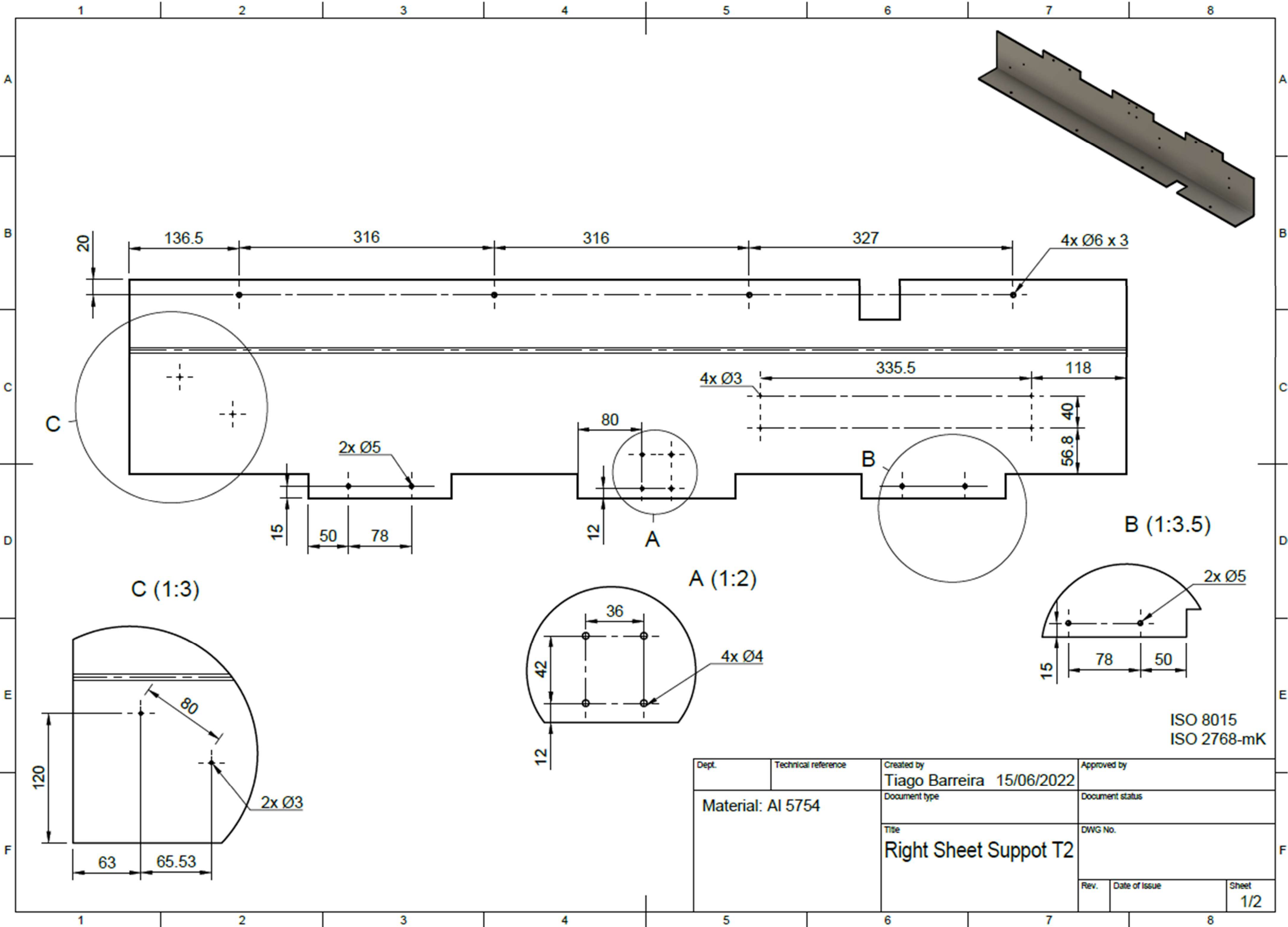
Dept.	Technical reference	Created by <b>Tiago Barreira 15/06/2022</b>	Approved by
Symetric Component Material: Al 5083 All chamfers: 2 x 45°		Document type	Document status
		Title <b>Spacer 250mm</b>	DWG No.
		Rev.	Date of issue
			Sheet <b>1/1</b>

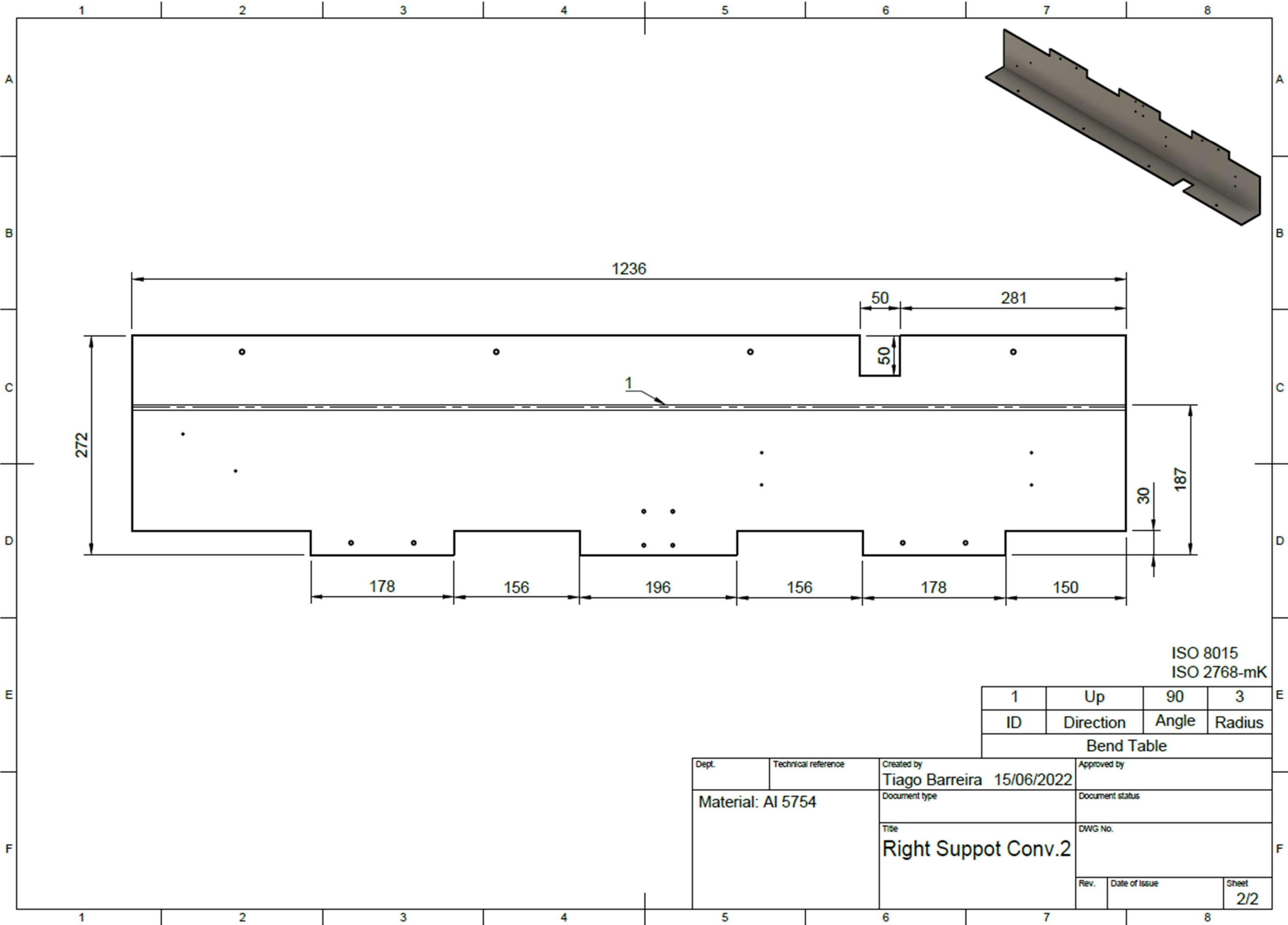


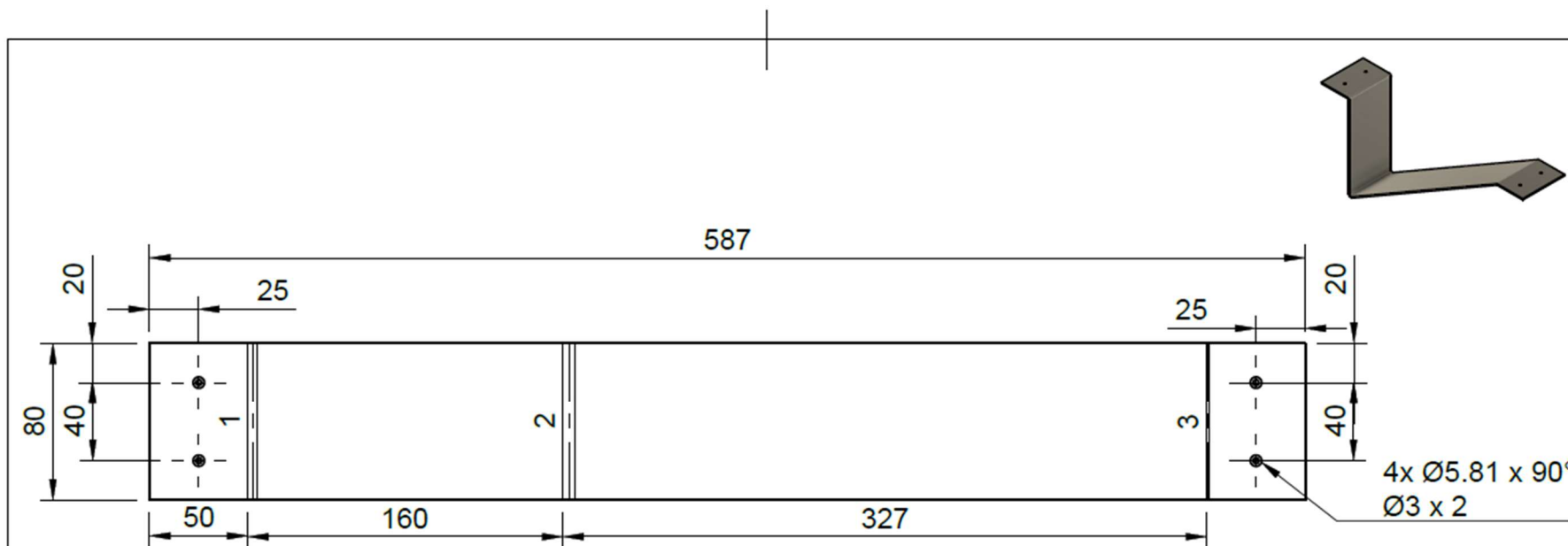










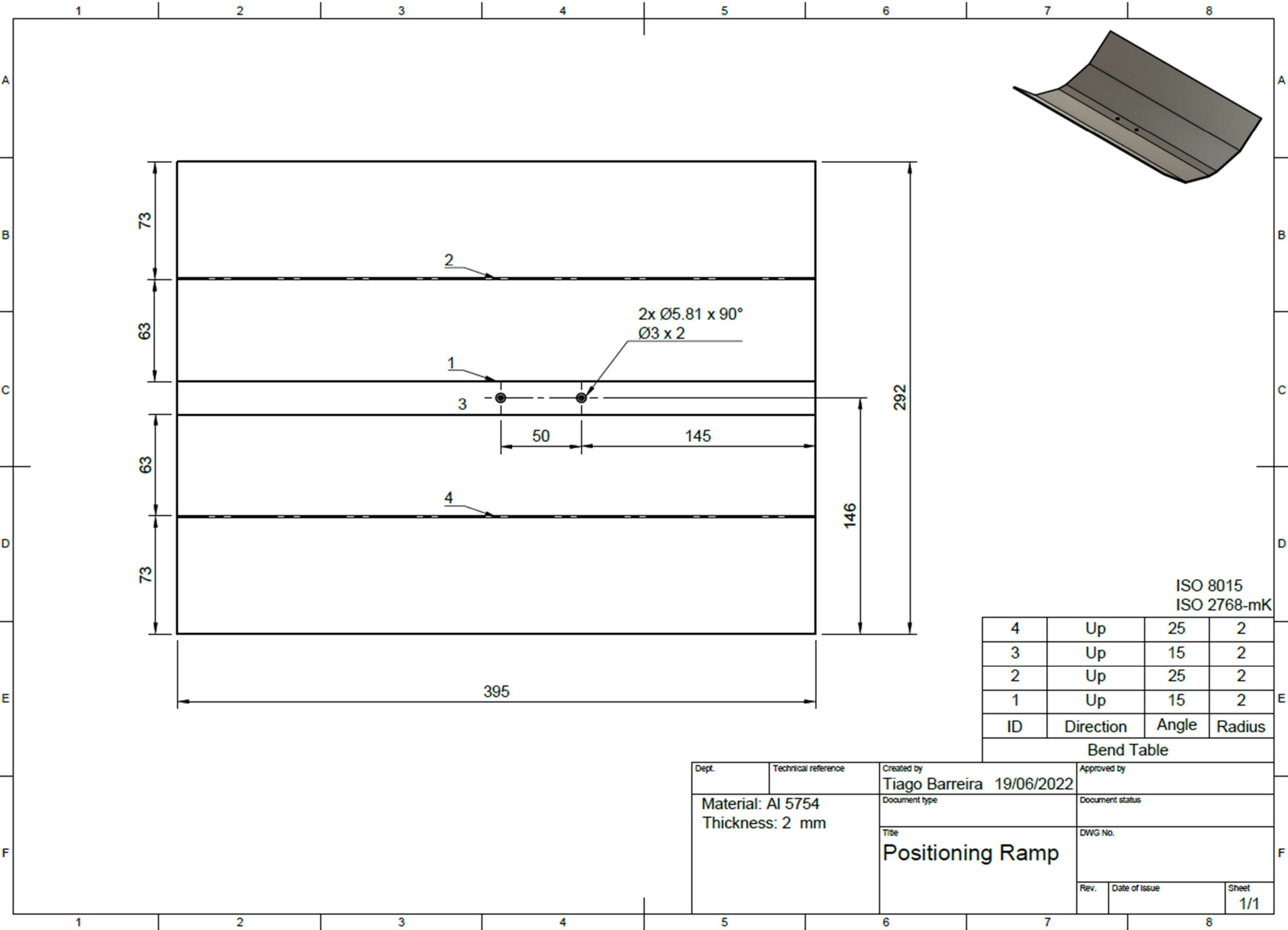


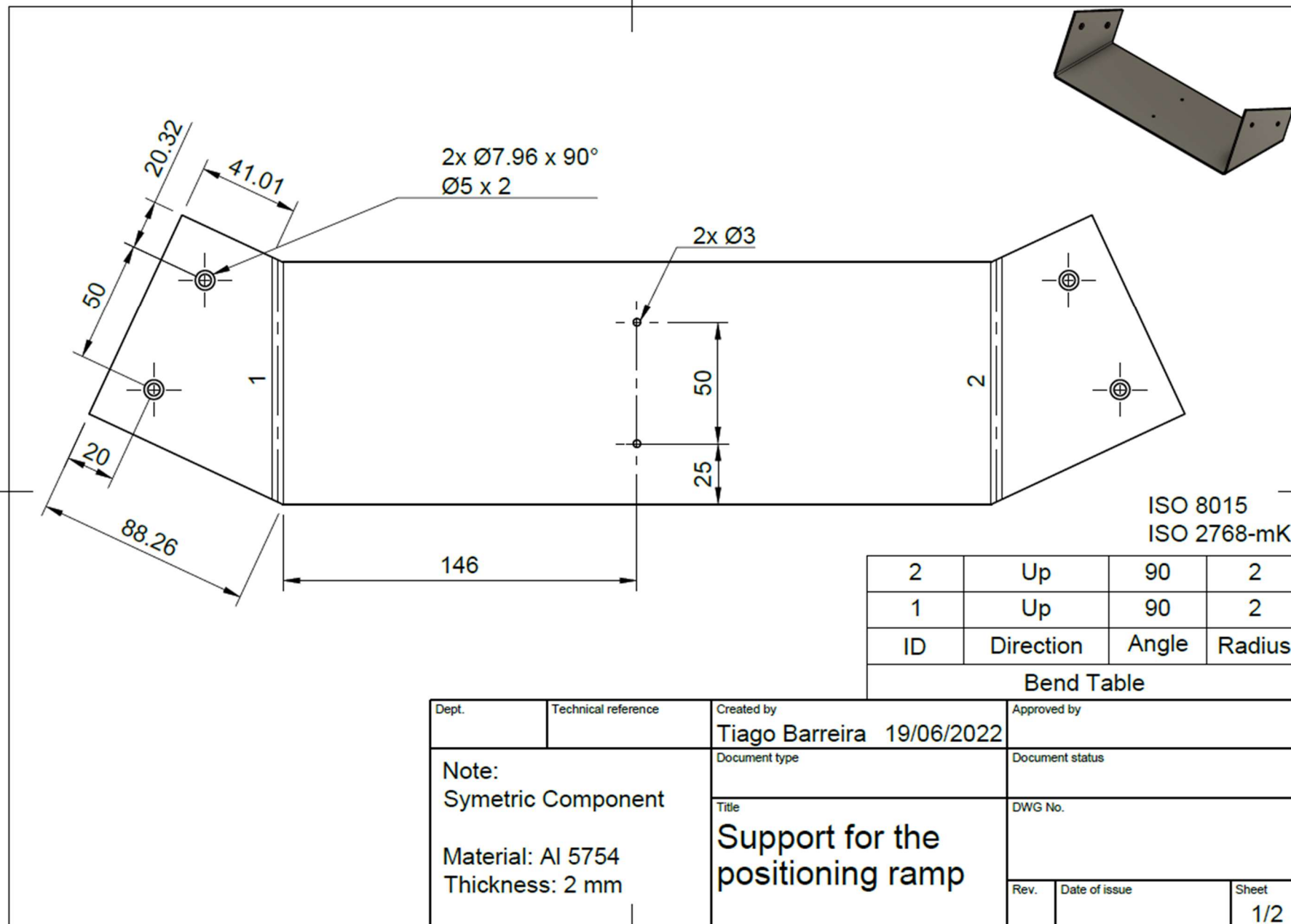
ISO 8015  
ISO 2768-mK

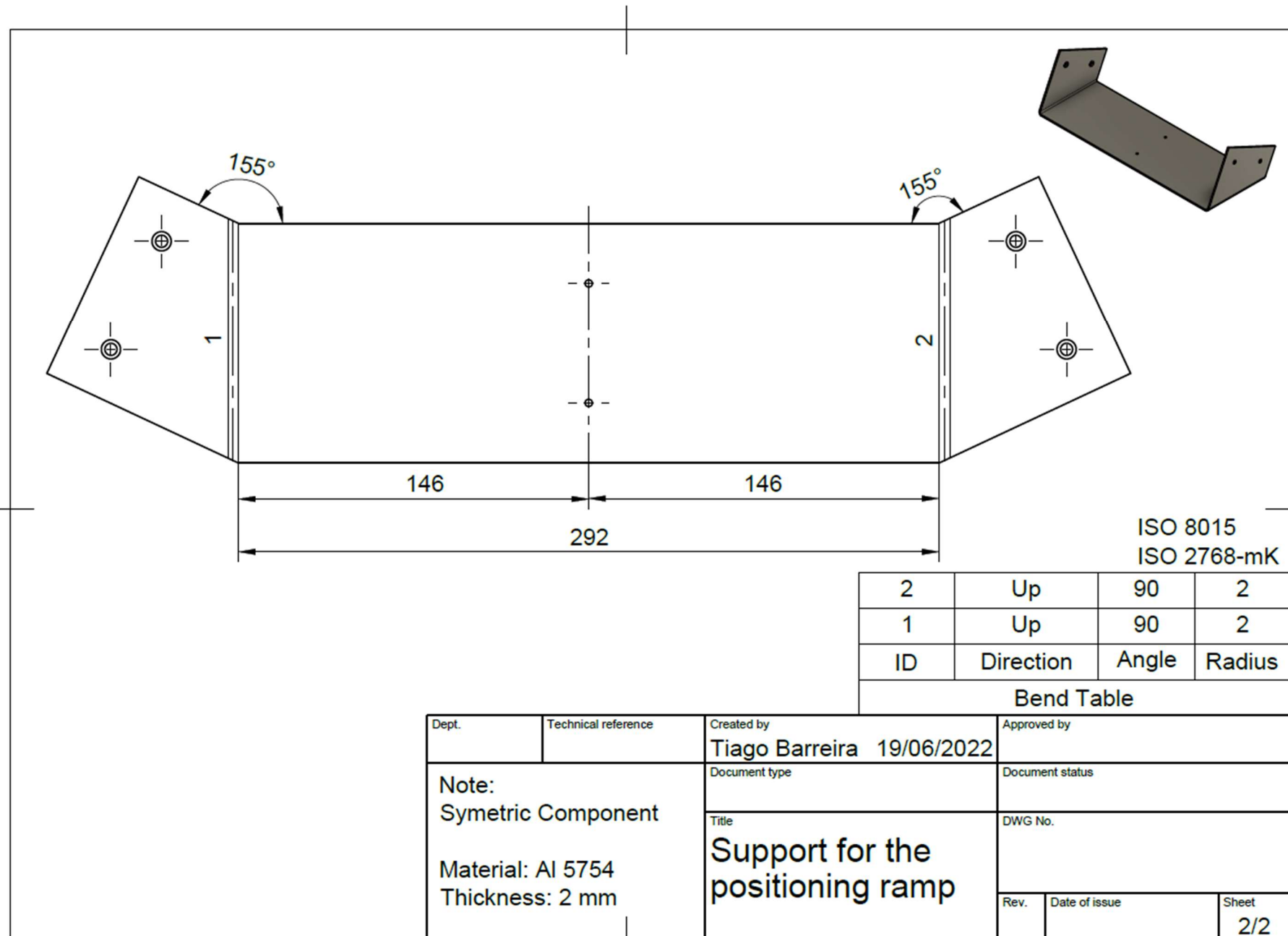
3	Up	30	2
2	Down	120	2
1	Up	90	2
ID	Direction	Angle	Radius

Bend Table

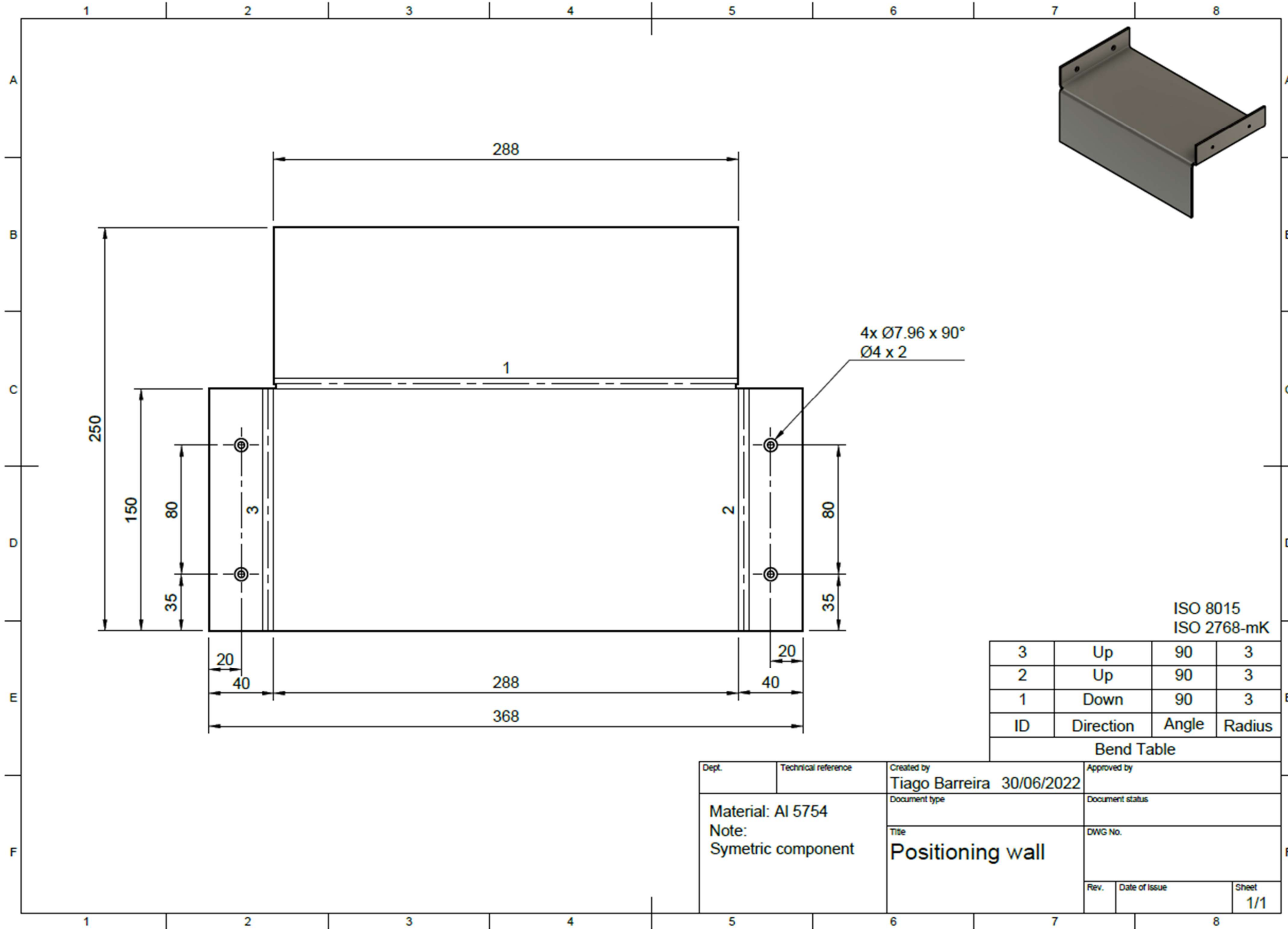
Dept.	Technical reference	Created by <b>Tiago Barreira</b> 15/06/2022	Approved by
Material: Al 5754 Thickness: 2 mm		Document type	Document status
		Title <b>Chicane</b>	DWG No.
		Rev.	Date of issue
		Sheet <b>1/1</b>	













# Appendix B - Products Datasheets

**Front view and mounting**

**Side view**

**Rear view**

**Y view**

\* Temperature on marked area must not exceed 80°C.  
From 50°C to 80°C follow derating curve.

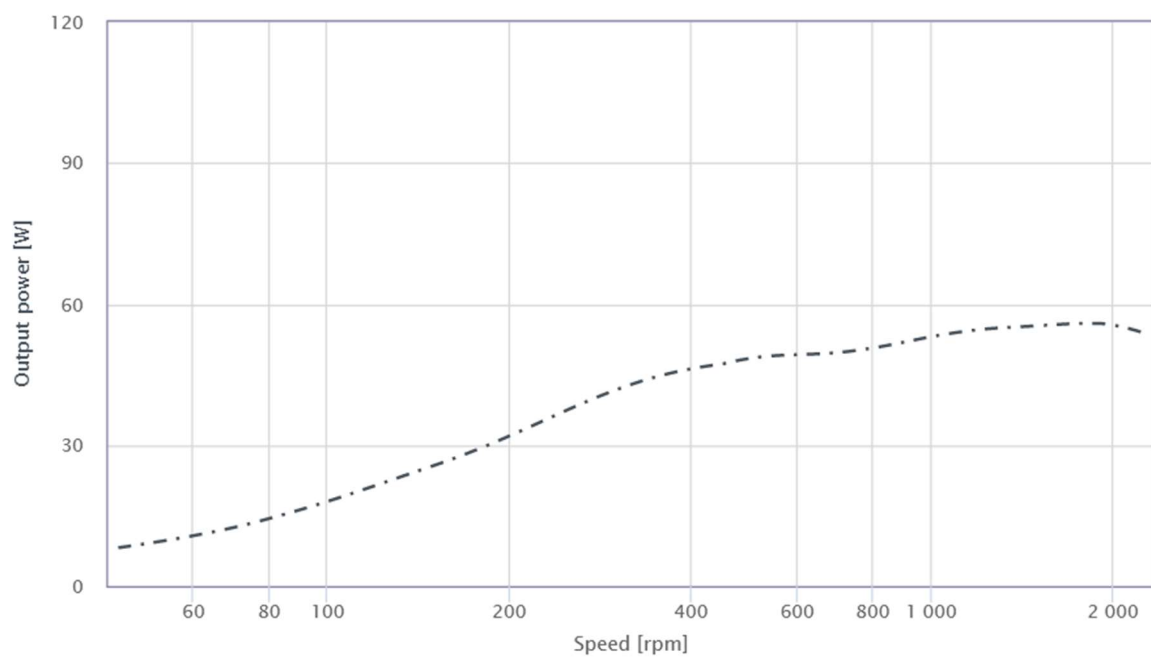
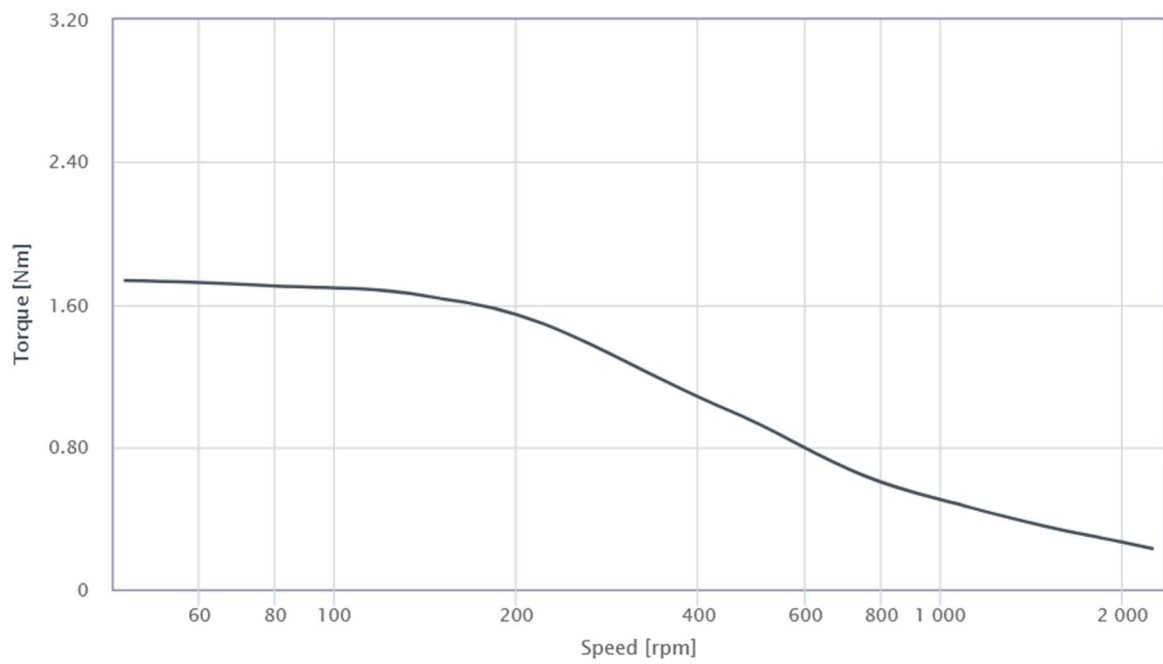
SPECIFICATION	CONNECTION	BIPOLAR PARALLEL	FULL STEP 2 PHASE-EX., WHEN FACING MOUNTING END (X)	PERMISSIBLE RADIAL+AXIAL FORCE	AXIAL-FORCE F <sub>a</sub> (N)	F <sub>0</sub> =15
VOLTAGE (VDC)		2.4	STEP A B A' B'	ROTOR SPRING-MOUNTED IN AXIAL DIRECTION	DISTANCE a (mm)	5 10 15 20
AMPS/PHASE		4.2 *	1 + + - -	BEARING	RADIAL-FORCE F <sub>r</sub> (N)	130 90 70 52
RESISTANCE/PHASE (Ohms)@25°C		0.58±15%	2 - + + - -	SPRING WASHER	AXIAL	RADIAL
INDUCTANCE/PHASE (mH) @1KHz		1.9±20%	3 - - + + -		SHAFT PLAY (mm)	0.08 0.02
HOLDING TORQUE (Nm) [lb-in]		1.87 [16.55]	4 + + - - +		AT LOAD MAX: (N)	4.5 4.5
STEP ANGLE (°)		1.8				
STEP ACCURACY (NON-ACCUM)		±5%				
ROTOR INERTIA (Kg-m²) [lb-in²]		4.8x10 <sup>-5</sup> [0.164]				
WEIGHT (kg) [lb]		1.14 [2.51]				
TEMPERATURE RISE: MAX.80°C (MOTOR STANDSTILL; FOR 2 PHASE ENERGIZED) * △						
AMBIENT TEMPERATURE -10~50°C [14°F ~ 122°F] * △						
INSULATION RESISTANCE 100 Mohm (UNDER NORMAL TEMPERATURE AND HUMIDITY)						
INSULATION CLASS B 130° [266°F]						
DIELECTRIC STRENGTH 500VAC FOR 1 MIN. (BETWEEN THE MOTOR COILS AND THE MOTOR CASE)						
AMBIENT HUMIDITY MAX. 85% (NO CONDENSATION)						
7 updt. resist./volt./tol.; del. det. torq		13.07.17	A.S.	APVD	S.R.	12.12.08
6 change holding torque		17.08.16	A.S.	CHKD		
5 warning notice/ rework draw		05.04.16	A.S.	DRN	J.W.	12.12.08
REV DESCRIPTION		DATE	DRN	SIGNATURE	DATE	

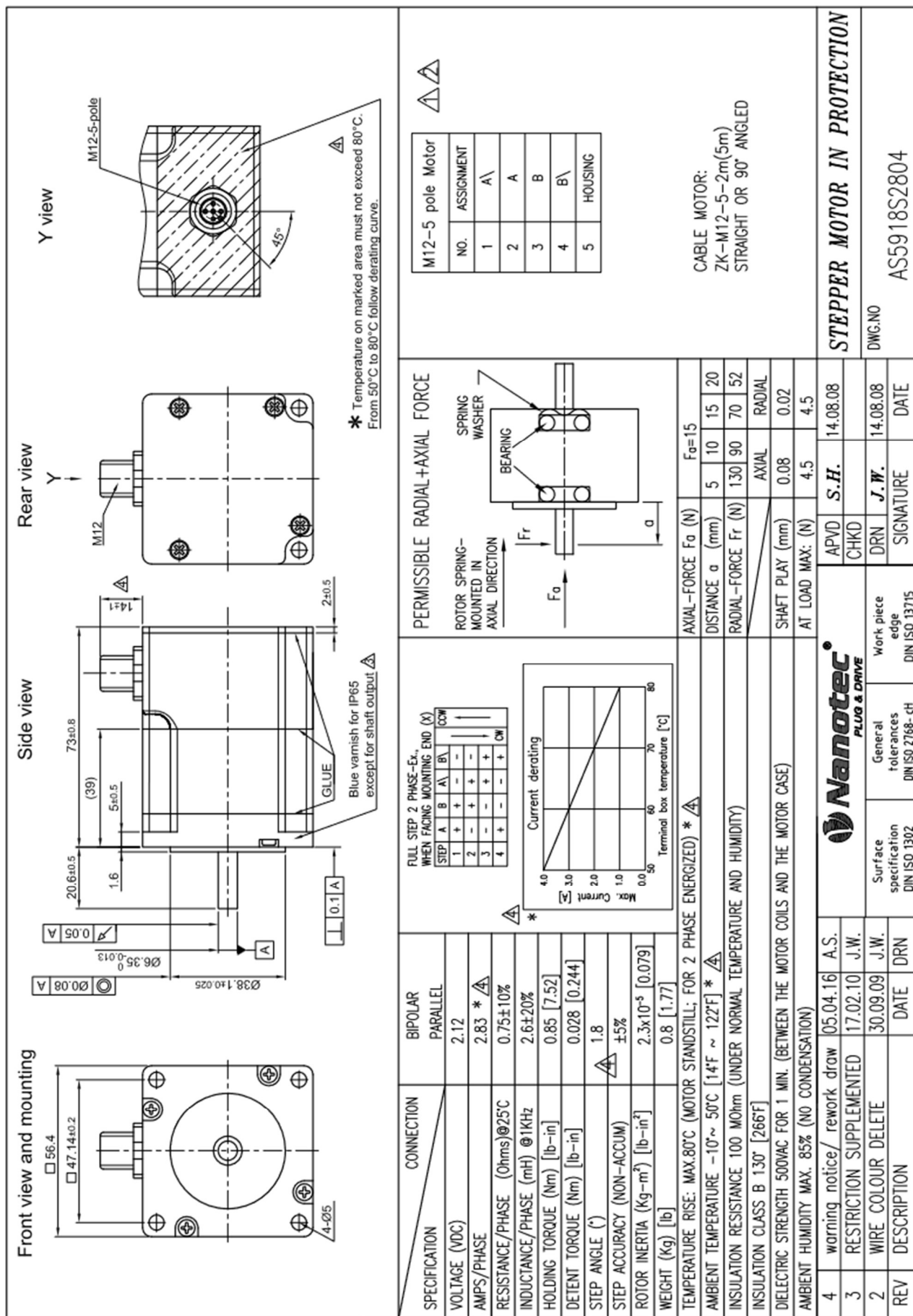
CABLE MOTOR:  
ZK-M12-5-2m(5m)  
STRAIGHT OR 90° ANGLED

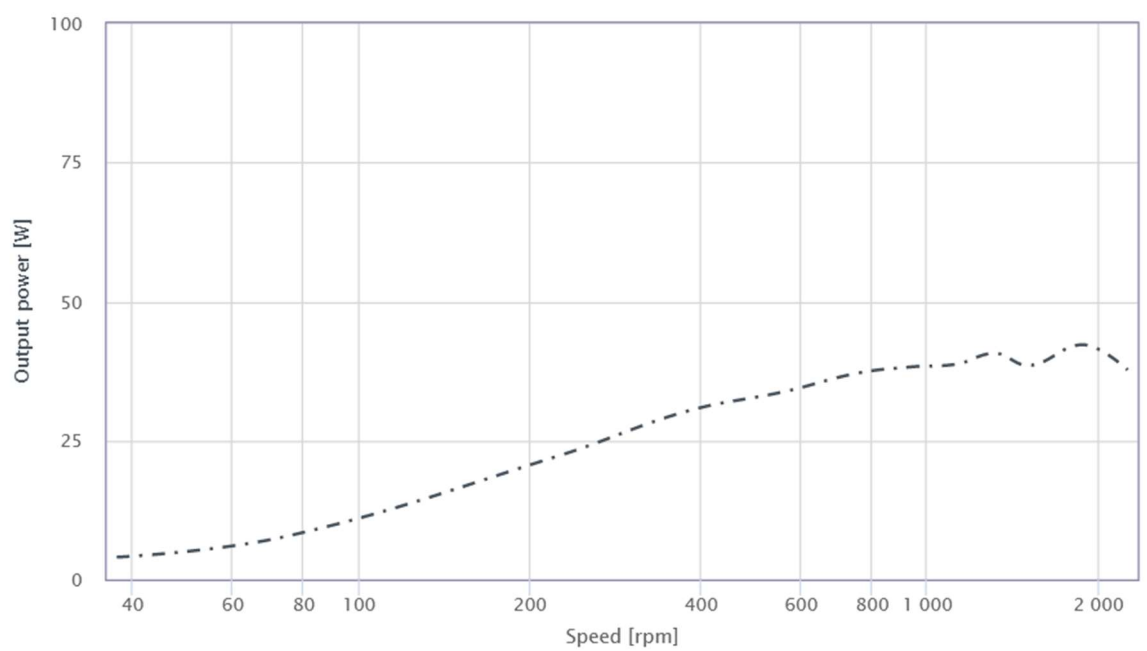
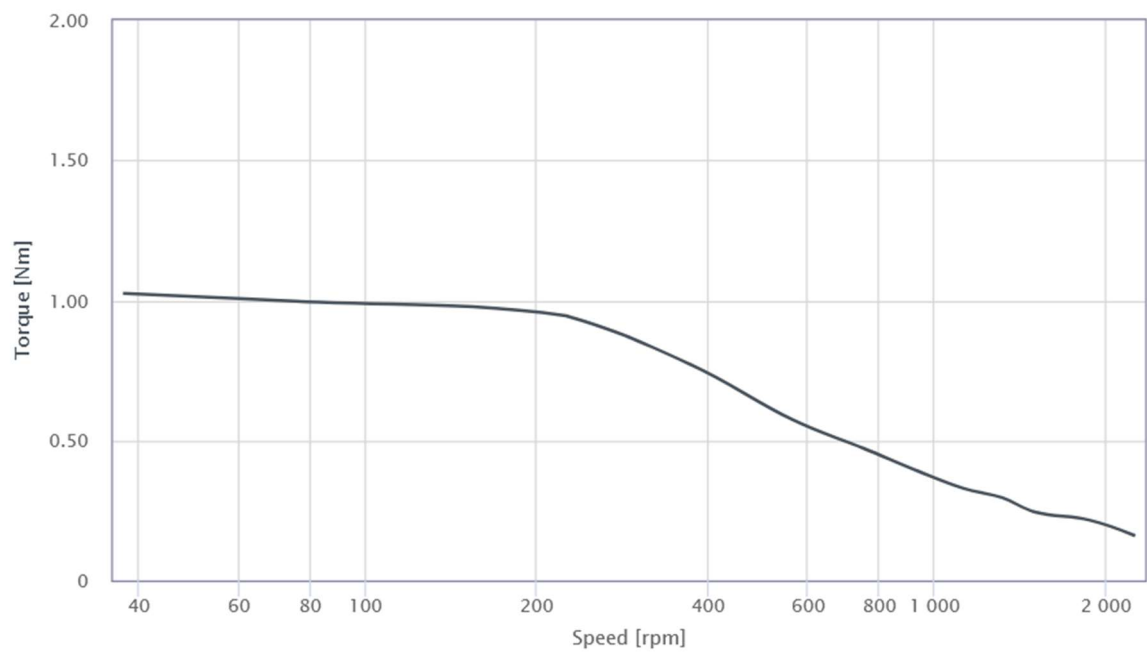
M12-5 pole Motor  
NO. ASSIGNMENT  
1 A\ A  
2 A  
3 B  
4 B\ B  
5 HOUSING

STEPPER MOTOR IN PROTECTION  
AS5918L4204  
DWG.NO

General tolerances DIN ISO 2768-ch  
Surface specification DIN ISO 1302  
Work piece edge DIN ISO 13715

**Characteristic motor curves – AS5918L4204**



**Characteristic motor curves – AS5918S2804**



# MEGADYNE MEGA CONVEY DATA SHEET



P9/Z

PUCON 2LR/6 W15 U0/Z AS FA

KD2WH1501

## TECHNICAL INFORMATION

	IMPERIAL	METRIC
Max Production Width	125.98in	3200mm
Total Thickness	0.06in	1.52mm
Mass	0.29lb/ft <sup>2</sup>	1.42kg/m <sup>2</sup>
Pull Per 1%	34lb/in	6N/mm
Working Temp.	-22/+212F°	-30/+100C°
Flexion (A)	0.24in 6mm	
Counter Flexion (B)	0.31in 8mm	

## BEST USED FOR

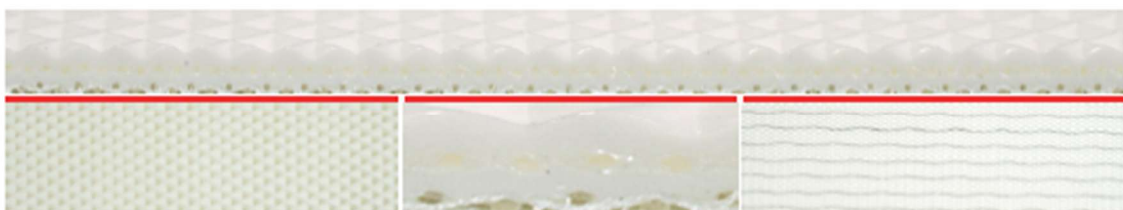
### GENERAL CHARACTERISTICS

2 ply white PU, inverted pyramid cover, knife edge rated. FDA and antistatic

## SPECIAL CHARACTERISTICS

Antistatic	YES	High Conductive	NO	Abrasion Resistant	NO
Food Approved	YES	Flame Retardant	NO	Tear Resistant	NO
ATEX Certified	NO	Pyrolysis Resistant	NO	Hydrolysis Resistant	NO
Antimicrobial Protection	NO	Low Noise	NO	Oil & Fat Resistant	YES

## BELT CONSTRUCTION INFORMATION



TOP SIDE (Carrying)		CARCASS	BOTTOM SIDE (Pulley)		
Material	PU	Interply	PU	Material	Fabric
Color	White (W)	Fabric	Light Rigid (LR)	Color	Fabric (FA)
Thickness	0.01in 0.25mm	Plies	2	Thickness	0in 0mm
Hardness	92 Shore A	Weft	Rigid (R)	Hardness	-
Surface	Inverted Pyramid (Z)			Surface	PU Impregnated (U0)



# MEGACONVEY DATA SHEET



P9/Z

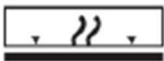




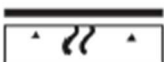
PUCON 2LR/6 W15 U0/Z AS FA

KD2WH1501

## SPLICE INSTRUCTIONS (Preferred)



## STRAIGHT FINGERS (SF)

	WATER COOL	AIR COOL
	<b>Temperature:</b> 160 C° 320 F° <b>Pressure:</b> 29 PSI 2 Bars	<b>Temperature:</b> 160 C° 320 F° <b>Pressure:</b> 7.3 PSI 0.5 Bars
	Silicone Matrix	
	Foil	
	Belt (Conveying Side Up)	
	Release Paper	
	<b>Temperature:</b> 160 C° 320 F° <b>Pressure:</b> 29 PSI 2 Bars <b>Dwell Time:</b> 0 Min	<b>Temperature:</b> 160 C° 320 F° <b>Pressure:</b> 7.3 PSI 0.5 Bars <b>Dwell Time:</b> 2 Min













Note: Foil is optional for air cooled.

## MECHANICAL JOINING METHOD

	Recessed Lacing	NO
	Hidden Lacing	NO
	Staple Lacing	RS62
	Plastic Spiral Lacing	YES
	Spiral Finger	YES
	APF Fasteners	APF-100
	Alligator	00
	Clipper Lacing	25, UCM36SL XSP, UCM36 XSP, 30

## FRICTION COEFFICIENT (Bottom Side)

Stainless Steel, BA (Brilliant Surface)	0.25
Stainless Steel, 2B (Half-Brilliant Surface)	0.25
Stainless Steel, 2D (Hot-Laminated Surface)	0.29
Rolled Steel Plate	0.25
Plastic Sheet (Brilliant Surface)	0.25

											
●	●	○	○	○	●	●	○	○	●	●	●

● Applicable    ● Limited Use    ○ Not Applicable

info@megadynegroup.com

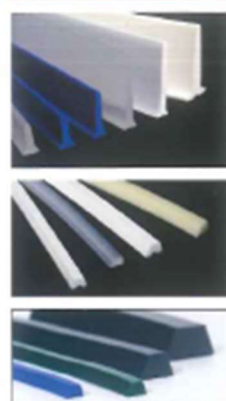
www.megadynegroup.com



© Megadyne 2018



## Perfiles



Sección	Tipo	Medidas			Material (1)	Peso g/m	Transversales		Longitudinales		Posible disposición (3)	
		b mm	h mm	a mm			Peso mínimo mm	Ø mínimo (2) mm	Ø mínimo mm (2)	cara interna		cara portante
	NE.008	8	8		PVC	75	28	100	60	110	T - G - L - V	
	NE.012	12	12		PVC	175	32	100	80	120	T - V	
	PE.008	8	8		PO	56	28	100				
	PE.012	12	12		PO	133	32	100				
	NE.015	20	15		PVC	330			200	250	G - L	
	NA.X04-62	6	4	4,0	PVC	23			25	30	G - L	
	NE.Y05-62	8	5	4,4		40	28	50	50	60		
	NE.Z06-62	10	6	5,6		60	30	70	70	80		
	NE.A08-62	13	8	7,2	PVC	100	33	90	90	100	T - G - L - V	
	NE.B11-62	17	11	9,0		180	37	100	100	120		
	NE.C14-62	22	14	11,8		300	42	150	150	180		
	NE.K16-70	30	16	18,4		470	50	250	250	250		
	UE.Y05	8	5	4,4		40	28	50	50	60		
	UE.Z06	10	6	5,6	PU	59	30	70	70	80	T - G - L - V	
	UE.A08	13	8	7,2		98	33	90	90	100		
	UE.B11	17	11	9,0		170	37	100	100	120		
	PE.Z06	10	6	5,6		46	30	100				
	PE.A08	13	8	7,2	PO	75	33	110			T - V	
	PE.B11	17	11	9,0		130	37	120				
	EE.Z06	10	6	5,6		56	30	80		80		
	EE.A08	13	8	7,2	TPE	95	33	90		100	T - G - L - V	
	EE.B11	17	11	9,0		167	37	100		120		
	DA.X04-62	6	3,5	4,25	PVC	18			15		G - L	
	DE.Y05-62	8	4,5	4,7		30			35			
	DE.Z06-70	10	5,5	6,0		45			50			
	DE.A08-62	13	7,5	7,5	PVC	75			70		G - L	
	DE.B11-62	17	10,5	10,3		140			80			
	DE.C14-62	22	13,5	12,2		245			125			
	DE.K16-70	30	15,5	18,4		370			170			
		DUE.Z06	10	5,5	6,0		45			50		
DUE.A08		13	7,5	7,5	PU	74			70		G - L	
DUE.B11		17	10,5	9,0		130			80			
NV.020-70		25	20			285		120				
NV.030-70		25	30		PVC	370		120				
NV.040-70		25	40			450	45	120			T	
NV.050-70		25	50			600		120				
NV.060-70		25	60			700		150				
NL.030-70		25	30			430	50	120				
NL.040-70		25	40		PVC	550	50	120				
NL.050-70		25	50			700	50	120			T	
NL.060-70		25	60			780	50	150				
	NL.070-70	40	70			1240	130	170				
	NL.080-70	40	80			1400	130	170				
	UV.020	10	20			140		40				
	UV.030	10	30		PU	180	30	45			T	
	UV.050	10	50			300		50				
	PV.020	10	20			95						
	PV.030	10	30		PO	135	30	100			T	
	PV.050	10	50			235						
	EV.020	10	20			130						
	EV.030	10	30		TPE	170	30	80			T	
	EV.050	10	50			300						
		UL.030	10	30		PU	215	40	45			T
UL.050		10	50			320		50				
PL.030		10	30		PO	155	40	100			T	
PL.050		10	50			225						
EL.030		10	30		TPE	210	40	80			T	
EL.050		10	50			310						
		NEM.040-62	45	40		PVC	640		120			T
		NEM.060-62	55	60		blando	1050		150			
		NEQ.040-62	42	40		PVC	635		120			
		NEQ.060-62	60	60		blando	1150		150			T
		NEQ.070-62	60	70			1400		170			

(2) Los diámetros mínimos indicados son los recomendados para condiciones normales de trabajo, a 20°C. Temperaturas inferiores exigen diámetros superiores.

(3) Disposición de los perfiles:  
T - Transversal, G - Guía interna, L - Lateral de contención, V - Forma de "V".

Ángulo del perfil sin soldar.



Una vez soldado, la variación del ángulo es mínima.







## MEGA CONVEY DATA SHEET



P9/A

PUCON 2LR/6 W13 U0/U03A AS FA

KD2WH1301

### TECHNICAL INFORMATION

	IMPERIAL	METRIC
<b>Max Production Width</b>	125.98in	3200mm
<b>Total Thickness</b>	0.05in	1.27mm
<b>Mass</b>	0.27lb/ft <sup>2</sup>	1.32kg/m <sup>2</sup>
<b>Pull Per 1%</b>	48lb/in	8N/mm
<b>Working Temp.</b>	-22/+212F°	-30/+100C°
<b>Flexion (A)</b>	0.24in 6mm	
<b>Counter Flexion (B)</b>	0.31in 8mm	

### BEST USED FOR

### GENERAL CHARACTERISTICS

2 ply white PU, knife edge rated, FDA and antistatic

### SPECIAL CHARACTERISTICS

Antistatic	YES	High Conductive	NO	Abrasion Resistant	NO
Food Approved	YES	Flame Retardant	NO	Tear Resistant	NO
ATEX Certified	NO	Pyrolysis Resistant	NO	Hydrolysis Resistant	NO
Antimicrobial Protection	NO	Low Noise	NO	Oil & Fat Resistant	YES

### BELT CONSTRUCTION INFORMATION

TOP SIDE (Carrying)			CARCASS		BOTTOM SIDE (Pulley)	
<b>Material</b>	PU		<b>Interply</b>	PU	<b>Material</b>	Fabric
<b>Color</b>	White (W)		<b>Fabric</b>	Light Rigid (LR)	<b>Color</b>	Fabric (FA)
<b>Thickness</b>	0.01in 0.25mm		<b>Plies</b>	2	<b>Thickness</b>	0in 0mm
<b>Hardness</b>	92 Shore A		<b>Weft</b>	Rigid (R)	<b>Hardness</b>	-
<b>Surface</b>	Smooth - Matte (A)				<b>Surface</b>	PU Impregnated (U0)



# MEGA CONVEY DATA SHEET



P9/A

PUCON 2LR/6 W13 U0/U03A AS FA

KD2WH1301

## SPLICE INSTRUCTIONS (Preferred)



## STRAIGHT FINGERS (SF)

	WATER COOL	AIR COOL
	<b>Temperature:</b> 160 C° 320 F° <b>Pressure:</b> 29 PSI 2 Bars	<b>Temperature:</b> 160 C° 320 F° <b>Pressure:</b> 7.3 PSI 0.5 Bars
Release Paper Foil Belt (Conveying Side Up) Release Paper		
	<b>Temperature:</b> 160 C° 320 F° <b>Pressure:</b> 29 PSI 2 Bars	<b>Temperature:</b> 160 C° 320 F° <b>Pressure:</b> 7.3 PSI 0.5 Bars
<b>Dwell Time:</b>	0 Min	2 Min

Note: Foil is optional for air cooled.

## MECHANICAL JOINING METHOD

	Recessed Lacing	NO
	Hidden Lacing	NO
	Staple Lacing	-
	Plastic Spiral Lacing	YES
	Spiral Finger	YES
	APF Fasteners	APF-100
	Alligator	00
	Clipper Lacing	25, UCM36SL XSP, UCM36 XSP, 30

## FRICTION COEFFICIENT (Bottom Side)

Stainless Steel, BA (Brilliant Surface)	0.25
Stainless Steel, 2B (Half-Brilliant Surface)	0.25
Stainless Steel, 2D (Hot-Laminated Surface)	0.29
Rolled Steel Plate	0.25
Plastic Sheet (Brilliant Surface)	0.25

●	●	○	○	○	○	○	○	●	●	●	●

● Applicable    ● Limited Use    ○ Not Applicable

info@megadynegroup.com

www.megadynegroup.com



© Megadyne 2018

# Appendix C - Bill of Materials

## - First Conveyor Bill of Materials (BoM)

Qty	Name	ISO / DIN	Supplier	Supplier Reference	Material	Price/Unit
1	Back Cover Conv. 1	-	-	-	Al 5754	180.41
2	Barrier	-	-	-	Al 5754	79.66
2	Barrier Spacer	-	-	-	PLA	1.43
2	Bearing Box with hole	-	-	-	Al 7075	68.28
1	Bearing Box without hole	-	-	-	Al 7075	52.99
1	Bearing Special Screw	-	MISUMI	BGPW4-7-L25-S5-F4	-	17.66
2	Belt Support	-	-	-	Al 5754	236.99
1	Big Pulley	-	MISUMI	GPA48GT3060-A-NK10	-	29.41
2	Circular Pipe D12 x 440	-	Leroy Merlim	80108616	-	1.41
1	Conveyor Belt	-	MEGADYNE	P9/Z	-	-
3	Cover with hole	-	-	-	Al 7075	40.54
1	Cover without hole	-	-	-	Al 7075	45.68
2	Driving Roller	-	MISUMI	RWBMG48-N10-230-X10-Y8-Z6	-	101.28
12	Hexagon Socket Set Screw	DIN 916 M4 x 8	FABORY	07840.040.008	-	0.016
1	Left Support Conv. 1	-	-	-	Al 5754	279.38
1	Motor	-	Nanotec	AS5918L4204	-	120
1	Motor Shaft Support	-	-	-	Al 7075	264.57
1	Motor Support	-	-	-	Al 7075	161.93
4	Nuts	DIN 934 M12	FABORY	01300.120.001	-	0.077
16	Nuts	DIN 934 M3	FABORY	01300.030.001	-	0.0055
2	Nuts	DIN 934 M4	FABORY	01300.040.001	-	0.0055
8	Nuts	DIN 934 M5	FABORY	01300.050.001	-	0.009
2	Profile 8 40x40x420	-	Item Portugal	7.0.000.09	-	-
4	Profile 8 40x40x960	-	Item Portugal	7.0.000.09	-	-
1	Pulley Key	DIN 6885 4x4x16	FABORY	39250.044.016	-	0.1938
1	Pulley Shaft	-	MISUMI	PSFGKR10-52-KA1-A16	-	10.51

Qty	Name	ISO / DIN	Supplier	Supplier Reference	Material	Price/Unit
1	Pulley Tensioner Bearing	-	MISUMI	634-H-ZZ	-	2.88
1	Right Support Conv. 1	-	-	-	Al 5754	294.58
4	Screw	DIN 10642 M3 x 20	FABORY	07400.030.020	-	0.0415
4	Screw	DIN 10642 M3 x 8	FABORY	07400.030.008	-	0.0355
8	Screw	ISO 7380 M6 x 12	FABORY	07151.060.012	-	0.0535
8	Screw	DIN 912 M2 x 10	FABORY	07000.020.010	-	0.0505
8	Screw	DIN 912 M5 x 30	FABORY	07000.050.030	-	0.0665
12	Screw	DIN 912 M2 x 6	FABORY	07000.020.006	-	0.0405
12	Screw	DIN 912 M3 x 20	FABORY	07000.020.020	-	0.057
4	Screw	DIN 912 M5 x 12	FABORY	07000.050.012	-	7.46
3	Shaft	-	MISUMI	PSFHR10-30	-	7.44
3	Shafts Bearings	-	MISUMI	6800-H-20ZZ	-	5.86
4	Sleeves with flange	-	IGUS	XFM-1416-17	-	12.94
1	Small Pulley	-	MISUMI	GPA16GT3060-A-H6.35	-	114.5
4	Spacer 450mm	-	-	-	Al 5083	81.39
2	Tensioner	-	-	-	Al 7075	0.165
2	Tensioner Endless Screw	-	Leroy Merlim	81972706	-	0.99
1	Transmission Belt	-	MISUMI	GBN2583GT-60	-	4.77
8	T-Slot Nut V 8 St M6	-	Item Portugal	0.0.480.50	-	-
4	Washers	DIN 125 M12	FABORY	38130.120.001	-	0.0695
16	Washers	DIN 125 M2	FABORY	38130.020.001	-	0.005
32	Washers	DIN 125 M3	FABORY	38130.030.001	-	0.003
2	Washers	DIN 125 M4	FABORY	38130.040.001	-	0.0065
4	Washers	DIN 125 M5	FABORY	38130.050.001	-	0.0065
16	Washers	DIN 9021 M5	FABORY	51530.050.001	-	0.0135

TOTAL = 3132.736 €

- Second and Third Conveyor Bill of Materials (BoM)

Qty	Name	ISO / DIN	Supplier	Supplier Reference	Material	Price / Unit
4	Bearing Box with hole	-	-	-	Al 7075	68.28
2	Bearing Box without hole	-	-	-	Al 7075	52.99
2	Bearing Special Screw	-	MISUMI	BGPW4-7-L25-S5-F4	-	17.66
2	Big Pulley	-	MISUMI	GPA16GT3060-A-H6.35	-	12.94
2	Chicanes	-	-	-	Al 5754	197.77
2	Circular Pipe D12 x 440	-	Leroy Merlim	80108616	-	1.405
2	Conveyor Belts	-	MEGADYNE	P9/A	-	-

Qty	Name	ISO / DIN	Supplier	Supplier Reference	Material	Price / Unit
4	Cover with hole	-	-	-	Al 7075	40.54
2	Cover without hole	-	-	-	Al 7075	45.68
8	Hexagon Socket Set Screw	DIN 916 M4 x 8	FABORY	07840.040.008	-	0.0135
4	Knife Edge Bearing	-	MISUMI	BACA6001DD	-	31.78
1	Left Support Conv. 2	-	-	-	Al 5754	247.23
2	Motor	-	Nanotec	AS5918L4204	-	120
2	Motor Shaft Support	-	-	-	Al 7075	264.57
2	Motor Support	-	-	-	Al 7075	161.93
4	Nuts	DIN 934 M3	FABORY	01300.030.001	-	0.0055
32	Nuts	DIN 934 M4	FABORY	01300.040.001	-	0.0055
8	Nuts	DIN 934 M5	FABORY	01300.050.001	-	0.009
2	Profile 8 40x40x420	-	Item Portugal	7.0.000.09	-	-
4	Profile 8 40x40x960	-	Item Portugal	7.0.000.09	-	-
2	Pulley Key	DIN 6885 4x4x16	FABORY	39250.044.016	-	0.1575
2	Pulley Shaft	-	MISUMI	PSFGKR10-52-KA1-A16	-	52.5
2	Pulley Tensioner Bearing	-	MISUMI	634-H-ZZ	-	2.88
1	Ramp Conv. 1-2	-	-	-	Al 5754	199.03
1	Right Support Conv. 2	-	-	-	Al 5754	268.28
2	Roller D 32 mm	-	MISUMI	ROFAWC30-10-L300	-	62.45
2	Roller D 48 mm	-	MISUMI	RWBMG48-10-280-X10-Y8-Z6	-	109.3
8	Screw	ISO 10642 M3 x 10	FABORY	07400.030.010	-	0.0355
8	Screw	ISO 7380 M6 x 12	FABORY	07151.060.012	-	0.0535
16	Screw	DIN 912 M2 x 10	FABORY	07000.020.010	-	0.0505
16	Screw	DIN 912 M2 x 6	FABORY	07000.020.006	-	0.0665
16	Screw	DIN 912 M3 x 20	FABORY	07000.020.020	-	0.0405
8	Screw	DIN 912 M4 x 20	FABORY	07000.050.012	-	0.057
8	Screw	DIN 912 M5 x 12	FABORY	07000.050.030	-	0.057
8	Screw	DIN 912 M5 x 30	FABORY	07000.050.030	-	0.034
4	Screw	ISO 10642 M3 x 10	FABORY	07400.030.010	-	7.46
6	Shaft	-	MISUMI	PSFHR10-30	-	6.6
6	Shafts Bearings	-	MISUMI	B6800ZZ	-	29.41
2	Small Pulley	-	MISUMI	GPA48GT3060-A-NK10	-	114.5
4	Spacer 250mm	-	-	-	Al 5083	81.39
4	Tensioner	-	-	-	Al 7075	0.165
4	Tensioner Endless Screw	-	Leroy Merlim	81972706	-	0.99
2	Transmission Belt	-	MISUMI	GBN2823GT-60	-	4.89
8	T-Slot Nut V 8 St M6	-	Item Portugal	0.0.480.50	-	-
32	Washers	DIN 125 M2	FABORY	38130.120.001	-	0.0695
16	Washers	DIN 125 M3	FABORY	38130.020.001	-	0.005

Qty	Name	ISO / DIN	Supplier	Supplier Reference	Material	Price / Unit
12	Washers	DIN 125 M4	FABORY	38130.030.001	-	0.003
8	Washers	DIN 125 M5	FABORY	38130.040.001	-	0.0065
12	Washers	DIN 9021 M3	FABORY	38130.050.001	-	0.0065
16	Washers	DIN 9021 M5	FABORY	51530.050.001	-	0.0135

TOTAL = 4303.75€

**- Positioning assembly Bill of Materials (BoM)**

Qty	Name	ISO / DIN	Supplier	Supplier Reference	Material	Price / Unit
2	Nuts	DIN 934 M3	FABORY	01300.030.001	-	0.005
1	Positioning ramp	-	-	-	Al 5754	180.50
1	Positioning ramp support	-	-	-	Al 5754	162.25
1	Positioning wall	-	-	-	Al 5754	196.50
5	Profile 8 40x40x300	-	Item Portugal	7.0.000.09	-	-
2	Profile 8 40x40x420	-	Item Portugal	7.0.000.09	-	-
2	Screw	ISO 10642 M3 x 8	FABORY	07470.030.008	-	0.0215
2	Washers	DIN 125 M3	FABORY	38130.030.001	-	0.003

TOTAL = 539.31€

**- Control system Bill of Materials (BoM)**

Qty	Name	ISO / DIN	Supplier	Supplier Reference	Material	Price / Unit
3	Stepper Terminal	-	Beckhoff	EL 7041	-	-
1	PLC	-	Beckhoff	CX 9020	-	-
7	Photoelectric sensors	-	Banner	VS 3	-	-
1	Power Unit	-	Mean Well	NDR – 480 – 48	-	-
1	Sensor Terminal	-	Beckhoff	EL 1014	-	-